SRI International

Final Technical Report • December 2007

Diffusion Coatings for Corrosion-Resistant Components in Coal Gasification Systems

Final Technical Report
Covering the period June 1, 2003 through May 31, 2007

SRI Project P13063

DOE Contract No. DE-FC26-03NT41616

Prepared by:

Gopala N. Krishnan, Ripudaman Malhotra, Jordi Perez, Marc Hornbostel, Kai-Hung Lau, and Angel Sanjurjo
SRI International
333 Ravenswood Avenue
Menlo Park, CA 94025

Prepared for:

U.S. Department of Energy
National Energy Technology Center
P. O. Box 10940
Pittsburgh, PA 15236

Attention: Dr. Richard Read

DISCLAIMER

ABSTRACT

Advanced electric power generation systems use a coal gasifier to convert coal to a gas rich in fuels such as H_2 and CO. The gas stream contains impurities such as H_2S and HCl, which attack metal components of the coal gas train, causing plant downtime and increasing the cost of power generation. Corrosion-resistant coatings would improve plant availability and decrease maintenance costs, thus allowing the environmentally superior integrated-gasification-combined-cycle (IGCC) plants to be more competitive with standard power-generation technologies.

Heat-exchangers, particle filters, turbines, and other components in the IGCC system must withstand the highly sulfiding conditions of the high-temperature coal gas over an extended period of time. The performance of components degrades significantly with time unless expensive high alloy materials are used. Deposition of a suitable coating on a low cost alloy will improve is resistance to such sulfidation attack and decrease capital and operating costs. The alloys used in the gasifier service include austenitic and ferritic stainless steels, nickel-chromium-iron alloys, and expensive nickel-cobalt alloys. The Fe- and Ni-based high-temperature alloys are susceptible to sulfidation attack unless they are fortified with high levels of Cr, Al, and Si. To impart corrosion resistance, these elements need not be in the bulk of the alloy and need only be present at the surface layers.

In this study, the use of corrosion-resistant coatings on low alloy steels was investigated for use as high-temperature components in IGCC systems. The coatings were deposited using SRI's fluidized-bed reactor chemical vapor deposition technique. Diffusion coatings of Cr and Al were deposited by this method on to dense and porous, low alloy stainless steel substrates. Bench-scale exposure tests at 900°C with a simulated coal gas stream containing 1.7% H_2S showed that the low alloy steels such SS405 and SS409 coated with ~20%Cr and Al each can be resistant to sulfidation attack for 500 h. However, exposure to an actual coal gasifier gas stream at the Wabash River gasifier facility for 1000 h in the temperature range 900° to 950°C indicated that Cr and Al present in the coating diffused further into the substrate decreasing the protective ability of these elements against attack by H_2S.

Similarly, adherent multilayer coatings containing Si, Ti, Al, and Nb were also deposited with subsequent nitridation of these elements to increase the corrosion resistance. Both dense and porous SS409 or SS 410 alloy substrates were coated by using this method. Multilayer coatings containing Ti-Al-Si nitrides along with a diffusion barrier of Nb were deposited on SS410 and they were found also to be resistant to sulfidation attack in the bench scale tests at

900°C. However, they were corroded during exposure to the actual coal gasifier stream at the Wabash River gasifier facility for 1000 h.

The Cr/Al coatings deposited inside a porous substrate was found to be resistant to sulfidation attack in the bench-scale simulated tests at 370°C. The long-term exposure test at the Wabash River gasifier facility at 370°C for 2100 h showed that only a minor sulfidation attack occurred inside the porous SS 409 alloy coupons that contained Cr and Al diffusion coatings. This attack can be prevented by improving the coating process to deposit uniform coatings at the interior of the porous structure.

It is recommended that additional studies be initiated to optimize the FBR-CVD process to deposit diffusion coatings of the corrosion resistant elements such as Cr, Al, and Ti inside porous metal filters to increase their corrosion resistance. Long-term exposure tests using an actual gas stream from an operating gasifier need to be conducted to determine the suitability of the coatings for use in the gasifier environment.

CONTENTS

LIST OF TABLES

LIST OF ILLUSTRATIONS

EXECUTIVE SUMMARY

Advanced coal gasification systems such as integrated coal gasification combined cycle (IGCC) processes offer many advantages over conventional pulverized coal combustors. Heat-exchangers, particulate ash filters, turbines, and other components in coal-fired power plants are often must withstand demanding conditions of high temperatures and pressure differentials. These components are exposed to corrosive gases and particulates that can erode the material and degrade their performance. In this study, the use of corrosion-resistant coatings was investigated for high-temperature components in IGCC systems. The coatings were deposited using SRI's fluidized-bed reactor chemical vapor deposition technique. The coated samples were exposed to a simulated coal gas stream containing 1.7% H_2S for periods up to 500 h at SRI. Coatings that survived these exposure tests were exposed to an operating gasifier gas stream at the Conoco/Phillips SG Solution's Wabash River Gasifier in Terra Haute, IN for ~2500 h. Successful coatings were developed that survived the gasifier exposure at 370°C and these coatings are useful for particulate filter material applications.

To help select the appropriate substrate and coating materials appropriate for a coal gasifier, a brief review was conducted of the different environments that the components may be exposed to, the alloy materials that are commonly used, and the coating technologies. Coal is a complex and heterogeneous substance that contains several impurities including sulfur, chlorine, nitrogen, and metal compounds. During gasification many of these impurities are converted to gaseous species such as H_2S, HCl, and NH_3. If coatings are to be used to provide corrosion resistance, their chemical composition must be chosen appropriately to protect the components under gasifier conditions. Although the actual gas composition depends on the gasifier design and the type of coal that is being used, it generally has a low $p(O_2)$ and a high $p(S_2)$, that is highly sulfiding in nature. Such a corrosive atmosphere at elevated pressures and temperatures require development of novel coating techniques to impart adequate corrosion resistance.

The selection of the substrate material is generally governed by the service temperature, stresses that the structures are likely to experience, erosion and corrosion resistance, and cost. For high-temperature applications, the components tend to be made of high-alloy steels that contain Fe, Cr, Ni, Co, and other elements that provide sufficient mechanical strength at the temperature of operation. The results described in the published literature indicate that many ferrous alloys suffered breakaway corrosion in coal gasification atmospheres. High nickel alloys are more susceptible to sulfidation attack due to formation of Ni-Ni_3S_2 eutectic that melts at 635°C. Increasing Cr content to levels greater than 25 wt% in Fe-Cr-Ni alloys is generally effective against sulfidation corrosion. Addition of Al and Co appears to improve the sulfidation

resistance. Other beneficial elements include Ti and Si. The formation of a stable barrier containing Al_2O_3, Cr_2O_3, SiO_2, or TiO_2 is partly responsible for increased corrosion resistance. However, such high alloy steels are hard to fabricate and expensive. To impart sulfidation corrosion resistance, these elements need not be in the bulk of the alloy and need only be present at the surface layers.

The need for corrosion resistant coatings exists in many areas of the gasifier train. Examples of the components where the coatings are useful are: (1) the tube sheet of a heat exchanger at ~900°C that is immediately downstream of the gasifier and (2) porous metal particulate filters at 370°C, which is downstream of the heat exchanger. These components operate at gas streams containing about 2% H_2S. Although the specifications of the material components used in the gasifier system are proprietary, alloys used in the gasifier service include nickel-based alloys such as Incoloy 800, and nickel-cobalt alloys such as HR160. A protective metal or ceramic coating on a low alloy steel that can resist sulfidation corrosion will reduce the capital cost of the components, extend the lifetime and reduce maintenance costs.

A fluidized-bed chemical vapor deposition (FBR-CVD) technique was developed at SRI to coat several metal and ceramic compositions on powders, tubes, and sheets. This technique is more rapid than pack cementation used for chromizing and aluminizing metal parts. It is relatively low in cost in comparison with conventional chemical vapor deposition technique as the precursors are generated in the fluidized bed reactor. Because of excellent mass and heat transfer characteristics of the fluidized bed, the rate of coating is rapid. The technique can be used to coat complex shapes because the chemical vapor deposition technique is not limited to line-of-sight.

A test reactor was designed and installed to expose about 20 different coupons to simulated gasifier environment at high temperatures. In this reactor about 20 coated and uncoated coupons can be exposed at 900°C to a simulated coal gas mixture containing 26% H_2, 39% CO, 17% CO_2, 17% H_2O, and 1.7% H_2S at 900°C for extended periods of time, as long as a month. After the exposure period, the external and fractured internal surfaces of the samples were examined by scanning electron microscopy. Electron-induced X-ray analysis was used to determine the elemental composition of these surfaces.

Initially, several pure metals and some common alloys were exposed to the simulated coal gas stream at 900°C for about 112 h. The results of this test indicated that noble metals such as Au and Pt did not suffer any observable degradation. Highly reactive metals such as Ti, Zr, Cr, and V were converted mainly to their oxides. Similarly, Ta and Nb are mainly converted to their oxides, although a small amount of oxysulfides may have formed. The surface of the

base metals such as Co, Fe, Ni, and Mo were converted mainly to their sulfides. Under the test conditions, uncoated austenitic (SS304, SS316 and IN800 alloys), and ferritic stainless steel alloy (SS405, SS409, and SS410) coupons were badly corroded. The alloy Kanthal containing Cr and Al had negligibly small weight change and very low sulfur levels, indicating that Cr_2O_3 and Al_2O_3 form protective layers. At high levels of H_2S (8% v/v) in the simulated coal gas, even high alloys steels such as HR 160 were attacked. These results are in general agreement with the thermodynamic equilibrium analysis.

Several ferritic and austenitic stainless steel coupons were coated with Cr and Al by the FBR-CVD technique. Surface Cr levels as high as 60 wt% were achieved in these coatings on ferritic alloy substrates such as 405 steel. Similarly, Al levels as high as of 22 wt% were deposited. Although these high levels of both Cr and Al were not present simultaneously, a limited number of SS409 alloy coupons were coated with 20 wt% Cr and Al each. Many coupons coated with different compositions of Cr and Al were exposed to the simulated coal gas stream at 900°C for periods up to 500 h. Some of the coupons that had diffusion coatings of ~22% Cr and Al each showed less than 0.05 wt% mass change during the exposure tests indicating very little sulfidation.

In addition to the Cr and Al diffusion coatings, coatings containing Ti, Ta, Si Nb, or W were deposited on the SS405 and SS409 alloy coupons by the FBR-CVD technique. After deposition of some of these metals, the surface of the coatings was converted to their corresponding nitrides. The presence of nitrides was expected to increase the sulfidation resistance and it was confirmed by the simulated coal exposure test at 900°C for 300 h.

To simulate the particulate filters used in a gasifier, porous stainless steel coupons made from SS409 alloy powder were fabricated and coated with Cr/Al or Ti-Ta-Si nitride coatings. These porous coupons were exposed to the simulated coal gas composition at 370°C. The coupons coated with Cr/Al were attacked by the H_2S present in the gas due to non-uniform coating of these protective metals at the interior of the porous coupons. However, porous coupons coated with nitrides of Ti and Al showed very little degradation after 300 h at 370°C indicating that protective coatings can be applied to the interior of the porous metal samples by the FBR-CVD technique.

Long-term exposure tests were conducted at the Wabash River Gasifier facility. Although coatings containing Cr/Al survived the simulated gasifier stream test at the laboratory for more than 300 h, the coupons exposed to the actual gasifier stream at 900° to 950°C for more than 1000 h suffered extensive degradation. The difference between tests with simulated and actual gasifier conditions may be due to (1) increased length of duration and (2) higher

temperature at the actual gasifier, and presence of other contaminants. Under these conditions, the Cr and Al surface coatings may have diffused into the bulk of the coupons thereby decreasing their enhancement at the surface. Such depletion would have reduced the resistance to attack by H_2S and allowed iron sulfide formation.

Exposure test at the Wabash River gasifier facility at 370°C for 2100 h showed that only a minor sulfidation attack occurred inside the porous SS 409 alloy coupons that contained Cr and Al diffusion coatings. This attack can be prevented by improving the coating process to deposit uniform coatings at the interior of the porous structure. The coupons coated with the multilayer nitride coatings were attacked by H_2S in this long-term test. These results indicate that the diffusion coatings of Cr/Al onto low cost substrates such as SS409 stainless steel can provide adequate sulfidation resistance at 370°C.

It is recommended that additional studies be initiated to optimize the FBR-CVD process to deposit diffusion coatings of the corrosion resistant elements such as Cr, Al, and Ti inside porous metal filters to increase their corrosion resistance. Long-term exposure tests using an actual gas stream from an operating gasifier need to be conducted to determine the suitability of the coatings for use in the gasifier environment.

INTRODUCTION

The objective of this program was to develop corrosion-resistant coatings for components that are exposed to gas streams at high temperatures and pressures typical of advanced coal gasifiers. Development of low-cost corrosion-resistant components will minimize maintenance and replacement costs and increase plant availability, which will in turn result in an overall decrease in the cost of power generation from coal in the environmentally superior gasification process, and in less reliance on foreign oil.

Advanced coal gasification systems such as integrated coal gasification combined cycle (IGCC) processes offer many advantages over conventional pulverized coal combustors. IGCC systems have high energy-conversion efficiencies, reduced pollutant emissions, modular construction, and potentially low capital and operating costs. The gasification process allows the contaminants to be removed in their reactive state. The volume of a coal gas stream is significantly less than that of a combustor flue gas stream in a plant of comparable size; hence, capital and operating costs for contaminant removal are low. Fixed-, fluidized-, and entrained-bed reactors have been developed and tested for coal gasification.

The current program is a collaborative effort between SRI International and SG Solutions, a subsidiary of ConocoPhillips. A significant aspect of the proposed program is to test the coatings, both at SRI in Menlo Park, CA, using simulated coal gas for determining the performance at various temperatures, and in an actual coal gas stream at SG Solutions' facility, the Wabash River Energy Laboratory (WREL), in Terre Haute, IN.

Heat-exchangers, filters, turbines, and other components in coal-fired power plants must withstand demanding conditions of high temperatures and pressure differentials. Furthermore, the components are exposed to corrosive gases and particulates that can erode the material and degrade their performance. As an example, corrosion occurs in the tube-sheet of the high-temperature heat recovery unit of a coal gasification power plant. This corrosion is the leading cause of unscheduled downtime in some plants, and development of corrosion-resistant coatings will directly impact the plant availability and its operating costs. Coatings that are successfully developed for this application may find use in similar situations in other areas of coal-fired power plants.

The Fe- and Ni-based high-temperature alloys that are used in gasifier trains are susceptible to sulfidation attack unless they are fortified with high levels of Cr, Al, and Si. To impart corrosion resistance, these elements need not be in the bulk of the alloy and need only be present at the surface layers. This study addressed development of coatings for two areas in the

gasifier train: (1) heat exchanger, which is a separate chamber immediately downstream of the gasifier, and (2) porous metal filter, which is downstream of the heat exchanger. The specific conditions of these areas are discussed below:

1. The heat recovery unit consists of single-pass tubes in shell design (Figure 1). The hot gases pass through the tubes, and the steam is in the shell. Hot gases enter the exchanger from top at 1800-1900°F (982° to 1038°C) and 400 psig and contain between 1.0 and 1.5% H_2S. Most of the gas is steam, CO, H_2, and CO_2. Ash and other particulate matter are also present. They exit from the bottom at 700°F (370°C), with no significant drop in pressure or change in composition. Condensate water is injected near the bottom, and steam at 1500 psig (saturated at about 600°F or 315°C) exits near the top. The tube sheets have to withstand about 1100 psi of pressure differential at about 1900°F (1000°C). The upper tube sheet is where most of the material problems occur.

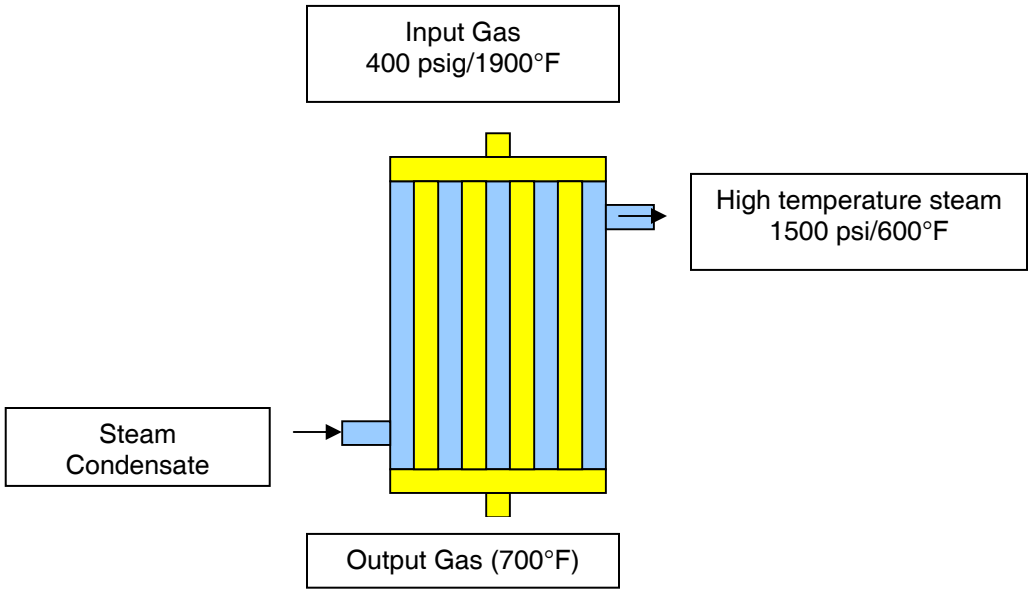

Figure 1. Schematic of high-temperature heat-recovery unit (HTHRU) at WREL.

2. A porous metal filter is used to trap the char and fly ash particulates in the coal gas stream. The metal is exposed to the gas stream exiting from the heat exchanger at 700°F (370°C). No significant pressure differential exists between the inlet and the outlet of the filter, but the material must stand up to the corrosion caused by H_2S. A protective metal or ceramic coating on the porous metal surfaces that can resist sulfidation corrosion without blocking the pores will extend the lifetime of the metal filters.

Although the specifications of the material components used in the gasifier system are proprietary, alloys used in the gasifier service include austenitic stainless steels such as 304 alloy, ferritic stainless steels such as 405 and 410 alloys, nickel-based alloys such as Incoloy 800, and nickel-cobalt alloys such as HR160.

In this study, we performed several tasks. First, we reviewed available information and selected several coating compositions that are suitable for service in the coal gasifier environment. Selected formulations were coated on steel coupons using a fluidized-bed reactor chemical vapor deposition (FBR-CVD) approach. Coated and uncoated specimens were exposed to a simulated coal gas stream containing about 1.7% H2S at 370° and 900°C for several hundred hours. Samples coated with several suitable compositions were also exposed for several thousand hours to a gas stream in an operating coal gasifier. Upon completion of the test period, the specimens were examined using a variety of techniques including optical and scanning electron microscopy, X-ray fluorescence, and X-ray diffraction to identify composition, phase, and morphological changes.

The FBR-CVD approach developed at SRI is a technique to coat several metal and ceramic compositions on powders, tubes, and sheets. This technique is more rapid than pack cementation used for chromizing and aluminizing metal parts. It is relatively low in cost compared with the conventional CVD technique because the precursors are generated in the fluidized bed reactor. Because of excellent mass and heat transfer characteristics of the fluidized bed, the rate of coating can be rapid. The technique is not limited to line-of-sight. The technique allows (1) both internal and external surfaces to be coated, (2) diffusion bonding to the substrate, (3) formation of a dense layer on the surface and increased corrosion protection of the substrate, and (4) requires a relatively low temperature (500° to 800°C) during the coating process and a short period of time (< 2 h), resulting in minimal changes in mechanical and physical properties. A significant advantage of the FBR-CVD technology is the ability to deposit more than one element or their compounds simultaneously or sequentially on metal surfaces. This feature allows the composition to vary across the coating thickness, if necessary, to maximize the desired functional characteristics.

LITERATURE REVIEW

DEGRADATION OF MATERIALS IN COAL GASIFICATION SYSTEMS

Coal is a complex and heterogeneous substance that contains several impurities including sulfur, chlorine, nitrogen, and metal compounds. During gasification many of these impurities are converted to gaseous species such as H_2S, HCl, and NH_3. The gas streams from fixed-, fluidized-, and entrained-bed coal gasifiers have different compositions and temperatures (Table 1).

Table 1. Characteristics of gas streams from various coal gasifiers

System Characteristics	Fixed-Bed Gasification	Fluidized-Bed Gasification	Entrained-Bed Gasification
Typical Process	Lurgi	KRW	Texaco
Exit Temperature (°C)	450-600	700-1000	1300
Pressure (psig)	300	300	450
Gas Composition(%)			
CH_4	4.28	4.5	0.3
C_2H_4	0.13	<0.01	<0.01
C_2H_6	0.20	<0.01	<0.01
H_2	20.92	30.0	29.8
CO	7.49	45.0	41.0
CO_2	15.28	9.0	10.2
H_2S	0.6-1.1	1.1	1.0
COS	0.03-0.06	0.1	0.1
N_2/Ar	0.18	0.8	0.8
NH_3	0.4	0.2	0.2
H_2O	50.5	9.5	17.1
Particulate Loading (ppm)	1000-2000	1000-10,000	4000

The extent to which the materials undergo corrosion is influenced by the prevailing chemistry, temperature, and other parameters. In coal gasification systems, the coal is gasified at high temperatures by reaction of controlled levels of oxygen and steam with coal, and the resulting gaseous environment is reducing in nature. In contrast, the gaseous environment in coal combustors is oxidizing in nature. For example, the sulfur in coal is converted to SO_2 in a coal combustor and to H_2S in a coal gasifier. In general, H_2S is more reactive than SO_2. When H_2S is present at high levels under reducing conditions, the exposed metal surfaces can be converted into corresponding sulfides. The sulfides do not form protective coatings and the metal underneath the sulfide layer continues to be attacked.

Coating compositions must therefore be chosen appropriately to provide proper protection. Although the actual gas composition depends on the gasifier design and the type of coal that is being used, it generally has a low partial pressure of oxygen, $p(O_2)$, and a high partial pressure of sulfur, $p(S_2)$. The gas, using a typical coal from an O_2-blown gasifier such as the one operating at WREL, may contain 28% H_2, 36% CO, 13% CO_2, 15% H_2O, 1% CH_4, 2% Ar and N_2 and up to about 2% H_2S. The $p(O_2)$ and $p(S_2)$ in this gas are about 10^{-15} atm and up to 10^{-4} atm, respectively at 870°C. These conditions are highly sulfiding in nature and require development of novel coating techniques to impart adequate corrosion resistance.

Other components of the gas stream from the coal gasifier may contribute to corrosion. The gas stream from an entrained-bed, slagging gasifier contains relatively few hydrocarbons and has a high level of CO. Such a gas composition may promote carburization. The gas stream from a fixed-bed gasifier is at a relatively low temperature of about 550°C and contains a significant fraction of hydrocarbons (including tars) and a low level of CO. The partial pressure of NH_3 is higher in the gas stream from a fixed-bed gasifier than that from fluidized- and entrained-bed gasifiers. The particulate matter is low in the fixed-bed design compared to that in the other two types of gasifiers.

The hot reducing gas leaving a slagging gasifier is typically at temperatures exceeding 900°C, and heat exchangers or syngas coolers are used to recover most of the sensible heat in the coal gas. The reducing environment also leads to the presence of alkali vapors in the gas stream, which are also very corrosive due to interaction with the protective oxide layers present in a heat exchanger surface.

In addition to the direct chemical attack by the gaseous components, the particulate matter present in the gas stream of a coal gasifier can also attack ceramic components or protective oxide surfaces of alloy steels. A fraction of the mineral matter in coal escapes the gasifier or combustor in the form of fly ash. The composition of fly ash depends on the type of coal, the combustion or gasification conditions, and the particle size of the ash. A sub-pilot scale test conducted by Westinghouse Science and Technology Center with cross-flow filters at the Texaco pilot-scale gasifier facility at Montebello, CA, showed a particulate loading to the filter varied from 250 to 2000 ppm [Lippert et al., 1991]. A similar test at the PFBC facility of New York University indicated that the cross-flow filter was able to reduce to ash dust loading from an inlet level of 250 to 1050 ppm to about 3 to 30 ppm [Lippert et al., 1989]. Thus, although the high-temperature barrier filters are able to remove nearly 99% of the fly ash, a small amount of these particles (likely to be submicron fume) escape the filters and could be reactive because of their relatively high surface area and intimate contact with the alloy steel components. The constituents of these particles are silica, silicates, alumino-silicates, ferrous oxides, and alkali and

alkaline earth compounds. The alkali compounds especially are likely to react with system components, forming chemical phases that are weaker or otherwise corroded. Table 2 lists the predicted phases to be formed by the interaction of fly ash components with the surfaces of alloy steels.

Table 2: Thermodynamically projected solid phases formed between ash and alloy steel surfaces

	Oxide Layer on the Alloy Steel Surface			
Ash Component	**Fe_2O_3**	**NiO**	**Cr_2O_3**	**Al_2O_3**
SiO_2	Iron silicates	Nickel silicate	Mixed oxides	Aluminosilicates
Al_2O_3	Iron aluminate	Nickel aluminate	No interaction	-
CaO	No interaction	No interaction	Calcium chromate	Calcium aluminate
MgO	No interaction	No interaction	Magnesium chromate	Magnesium aluminate
Na_2O	Sodium ferrite	No interaction	Sodium chromate	Sodium aluminate
K_2O	Potassium ferrite	No interaction	Potassium chromate	Potassium aluminate
Fe_2O_3	-	No interaction	Iron chromate	Iron aluminate

The composition of the submicron fume that is most likely to escape the barrier filters differs significantly from that of the coarser particles retained by cyclones and barrier filters [Quann et al., 1990]. Oxides of Si, Al, Mg, Fe, and Ca are generally the major constituents of the fume. Several other compounds of Na, P, Mn, V, Cr, As, Sb, Zn, Co, and Ba can also be present. The compounds of Na, P, As, and Co are significantly enriched in the fume fraction in comparison to the coarser particles. The major oxides and alkali compounds pose a significant threat to the stability of protective oxides present in alloy steels used in a gasifier system.

By depositing on the heat exchanger tubes, particulate matter in the gas stream degrades tube performance. However, at high flow velocities they can also have a detrimental effect by eroding the protective coating. Natesan (1993) has reviewed the temperature and chemical environments experienced by heat exchangers and turbines under various coal-utilizing technologies. He has also reported on the mechanisms and failure modes experienced in these components (Tables 3 and 4).

Liquid water also causes corrosion. Although under most operating conditions, water will be in the vapor phase, during shutdown and startup periods the steam can condense and form pools in contact with the component materials. Liquid water can dissolve certain salts, and contact of metal surfaces with this salt solution can lead to pitting corrosion.

Table 3. Service conditions and modes of degradation for component materials in coal-fired systems						
Component System	Gas Environment	Gas Temp. Range (°C)	Metal Temp Range (°C)	Deposit Type	Particulate and/or Particle Velocity	Mode of Degradation
Heat Exchangers						
PC boilers	Oxidizing	1300-1600	400-700	Alkali Sulfates Ash	Fly ash, < 20 m/s	Alkali corrosion Fouling
FBC	Oxidizing, locally reducing	850	400-850	$CaSO_4$, CaO Carbon, Fly ash Fly ash	Sorbent bed, fly ash 3-? m/s	Oxidation/sulfidation Erosion
IGCC	Reducing, moderate to high H_2S	900-1100	400-650	Fly ash Alkalis Chlorides	Fly ash, < 20 m/s	Sulfidation/erosion Fouling
HIPPS	Oxidizing	1300-1600	400-1300	Fly ash, Slag Alkali sulfates	Fly ash	Ceramic fracture Alkali corrosion Fouling
LEBS	Reducing, Sulfidizing	1300-1600	400-600	Sulfides Slag	Fly ash	Sulfidation Deposit corrosion Fouling
Turbines						
IGCC	Oxidizing	850-900	850-950	Fly ash/slag Alkali	Slag, 200-500 m/s	Hot corrosion/erosion
FBC Effluent	Oxidizing	850-900	600-900	Alkali sulfates Silicates Sorbent	Fly ash, sorbent, 200-500 m/s	Hot corrosion/erosion
HIPPS	Oxidizing	1300	1000	Alkalis	200-500 m/s	Oxidation/erosion

Source: Natesan, 2001

Table 4. Materials degradation in coal-fired systems		
Phenomenon	**Key Variables**	**Possible Rate-Limiting Step**
Boiler tube corrosion	Alkali and chlorine contents Fly ash, temperature	Alkali condensation Oxide-sulfate reaction
Substoichiometric combustion (also gasification)	O and S partial pressures, temperature Downtime condensate Alkali/slag deposit	Fracture of oxide scale Oxidation/sulfidation Pitting and crevice corrosion
FBC in-bed corrosion	Bed chemistry Local particle velocity Particle size and loading	Oxidation/sulfidation Arrival rate of particles Fracture of surface scales
Low-temperature hot corrosion	Temperature, temperature gradient salt-film thickness, S and alkali level	Sulfidation of transient oxides Transport of base metal (e.g., Ni and Co)
Hot corrosion/erosion	Alkali level Temperature Particle size, loading, and velocity	Fracture of scale Sulfidation of transient oxides Transport of base metals

Source: Natesan, 2001

COMPONENT MATERIALS

The selection of the substrate material is generally governed by several factors including (1) the service temperature, (2) stresses (pressure differentials) that the structures are likely to experience, (3) erosion and corrosion resistance, and (4) cost. For high-temperature applications, the substrates tend to be high-alloy steels that contain Fe, Cr, Ni, Co, and other elements to provide mechanical strength at the temperature of operation. Even the ability of alloy steels to withstand high stresses decreases sharply at elevated temperatures. Figures 2 and 3 present the data on the ranges of conditions under which different alloys are useful as substrate materials [Viswanathan, et al., 2003]. It shows that the strength of the ferritic materials declines rapidly above 600°C.

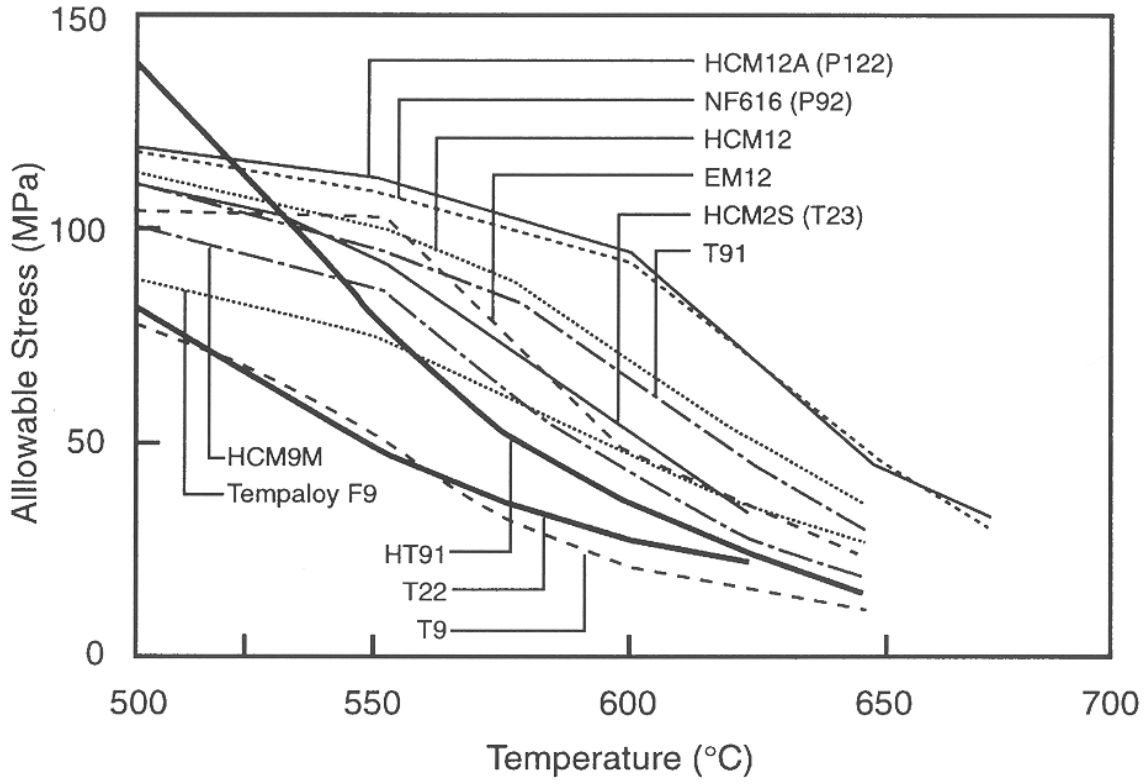

Figure 2. Allowable stress of various alloys as a function of temperature.

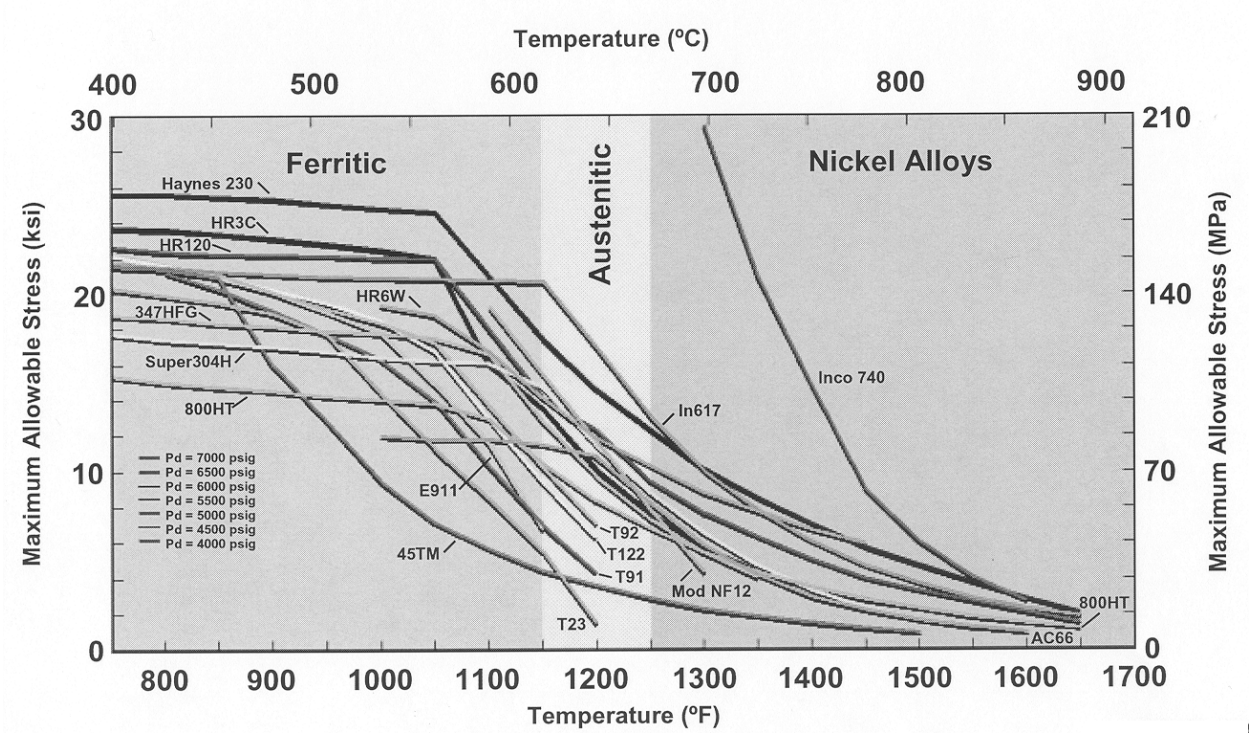

Figure 3. Maximum allowable stress of alloys as a function of temperature.

A second selection criterion of a component material is its ability to resist corrosion or oxidation during service. In general, alloy steels depend on the formation of a protective oxide layer such as Cr_2O_3 for protection against sulfidation or further oxidation. Although Cr_2O_3 scale is generally protective against sulfidation, high levels of H_2S may cause sulfidation of Cr_2O_3 in gasifiers operating in O_2-blown mode with moderate to high sulfur coals.

Many studies have been conducted on the degradation of metal alloys in coal gasification atmospheres [Humphreys and Schafer, 1983]. Several alloys suffered breakaway corrosion under such conditions. High-nickel alloys are more susceptible to sulfidation attack due to formation of Ni-Ni_3S_2 eutectic that melts at 635°C. Increasing Cr content to levels greater than 25 wt% in Fe-Cr-Ni alloys is generally effective against sulfidation corrosion. Co-containing alloys are also more resistant to sulfidation than Ni-based alloys. Verma suggested that Cr_2O_3 scale doped with Co improves sulfidation resistance.[Verma, 1982] Addition of Al also improves the sulfidation resistance [Bradshaw, 1977]. Recently, iron aluminides have been tested in coal gas environments and are found to be superior to high-Cr alloys [Natesan, 2001]. Other beneficial elements include Ti and Si. A Ni-Co-based alloy (HR-160) developed by Haynes International containing high Cr and Si is claimed to have exceptional sulfidation resistance [Lai, 1990]. We

postulate that in the above cases, the formation of a stable barrier containing Al_2O_3, SiO_2, or TiO_2 are partly responsible for increased corrosion resistance.

Even under conditions where the Cr_2O_3 is stable, sulfidation attack is feasible. The alloying element that forms a stable sulfide can diffuse through the oxide scale and eventually form sulfide on the surface of the oxide scale, leading to breakaway corrosion. Alloying elements such as Mn, Fe, Co, and Ni may diffuse through the Cr_2O_3 scale and react with H_2S on top of the oxide scale to form an external sulfide scale [Perkins et al., 1982]. Mn is the fastest diffusing element, followed by Fe, Co, Ni, and Cr. Alternatively, the corrosion mechanism may involve penetration of S atoms through the oxide layer to form discrete particles of sulfides in the base alloy matrix. A diffusion barrier layer may be needed to prevent this type of corrosion.

Both iron-based and nickel-based alloys are used in the heat exchanger and metal filter applications. Because of the proprietary nature, the exact composition of the alloys cannot be disclosed publicly. However, Table 5 describes the composition of typical alloys used in these high-temperature applications.

Table 5. Composition of alloy steels used in coal gasifier systems

Alloy[1]/Element	HR160, N12160	Incoloy800, N0880	SS304, S30400	SS405, S40500	SS410, S41000, Tempered	SS410, S41000, Annealed
Aluminum		0.15-0.6		0.2		0.2
Carbon	0.05	<0.1	0.015	<0.08	<0.15	<0.08
Chromium	28	19-23	19	13		13
Cobalt	30					
Copper		<0.75				
Iron	<3.5	>39.5	69	85		85
Manganese	0.5	<1.5	1	<1	<1	<1
Molybdenum	<1					
Nickel	37	30-35	10			
Niobium	<1					
Phosphorus			0.23		<0.04	<0.04
Silicon	2.75	<1	0.5	<1		<1
Sulfur		<0.015	0.015		<0.03	<0.03
Titanium	0.5	0.15-0.6				
Tungsten	<1					

1 The composition of the elements is in weight percent. Alloys are designated both in common nomenclature and unified numbering system

As seen from Table 5, significant composition differences exist between the alloys. The HR160 nickel-based super alloy contains significant fractions of Cr, Co, and Si. The cost of HR-160 is significantly more than that of the 304 stainless steel. The Incoloy 800 is also a nickel-based alloy used as a heat exchanger material in nuclear reactors. It contains about equal fractions of Fe and Ni and about 20% Cr. Its mechanical properties at high temperatures are not as good as HR-160. SS 304 is the well-known austenitic stainless steel containing 18% Cr and 10% Ni. Its corrosion resistance at moderate temperature is good, but at high temperatures it is prone to both oxidation and sulfidation. The SS 400 series is less expensive than other alloys listed, and they benefit more from corrosion-resistant coatings. The fraction of carbon in these alloys is very low. High levels of carbon lead to the formation of chromium carbides.

COATINGS

Natesan (1993) reviewed the suitability of Al, Cr, and Si coatings made by pack cementation, electrospark deposition, plasma spray, and CVD for coal gasification and combustion applications. A minimum Cr concentration of 25 wt% or an Al concentration of 15 wt% is required to achieve adequate sulfidation resistance at about 650°C. Addition of V to the Cr layer minimized the formation of chromium carbides at the grain boundaries. These studies indicated that increasing Cr and/or Al levels in the alloy is beneficial in resisting sulfidation attack, but the integrity of the coating is strongly dictated by the adhesion of the coating to the substrate. Thin layers of Si or SiO_2 deposited on an Fe-Cr alloy improved corrosion resistance against sulfidation at about 700°C, due to the presence of a SiO_2 layer at the alloy surface that acts a barrier to the migration of sulfur inward and cation transport outward.

In summary, the environment present in the coal gas stream at high temperatures is very aggressive to the metal components of coal gasifiers. Alloys containing high levels of Cr, Al, and other elements are being used to minimize sulfidation attack. Coatings with similar compositions have been attempted to impart sulfidation resistance. Development of coatings with improved resistance will provide options to the selection of suitable components for the gasifier service.

EXPERIMENTAL METHODS

COATING COMPOSITION

Based on the literature review, a minimum Cr concentration of 25 wt% or an Al concentration of 15 wt% may be required to achieve adequate sulfidation resistance at about 650°C. Addition of V to the Cr layer minimized the formation of chromium carbides at the grain boundaries. Increasing both Cr and Al levels in the alloy is beneficial in resisting sulfidation attack, but the benefit of the coating strongly depends on the adhesion of the coating to the substrate. Thin layers of Si or SiO_2 deposited on an Fe-Cr alloy improved corrosion resistance against sulfidation at about 700°C, due to the presence of a SiO_2 layer at the alloy surface that acts a barrier to the migration of sulfur inward and cation transport outward.

We selected the following coating compositions:

- Chromium – diffusion coating with surface concentration of about 50 wt%
- Aluminum – diffusion coating with surface concentration of about 15 wt%
- Silicon – diffusion coating with surface concentration of about 10 wt%
- Titanium – coating

In addition to the above components, we also deposited coating of other elements such as tantalum, vanadium, and tungsten, which has been shown to be beneficial in some cases. Furthermore, the metal coatings may be nitrided to prevent inter-diffusion between different coating layers. Titanium nitride is used as a diffusion barrier in the manufacture of integrated circuits.

COATING TECHNIQUE

SRI International's FBR-CVD technique has been used to coat fibers, particles, powders, and fabricated parts. Briefly, in this technique, a source metal powder bed is fluidized with a carrier gas (e.g., Ar) and reacted with HCl and H_2. When the reactor is operated at an appropriate temperature and conditions for the coating metal, volatile metal halides are formed *in situ* that decompose on the substrate (e.g., steel) to form a metallic coating. The substrates act as a sink because the activity of coating metal in them is typically very low (<1%) while the gas is saturated. In many cases, such coatings are deposited on substrate materials at much lower temperatures than are possible with other coating techniques. In the initial stages, deposition and diffusion are very fast for steel substrates above 550°C. Because the CVD process is not a line-of-sight coating technique, it can be applied uniformly on complex geometric shapes. The technique may also be used to coat porous materials such as metal particulate filters.

Fluidized-Bed Reactor Chemical Vapor Deposition System

Figure 4 is a schematic diagram of the FBR-CVD system. The system consists of a cylindrical quartz reactor (4.7 cm ID and 50 cm long) with a porous fused quartz plate to support the powder bed and serve as a gas distributor, and a gas-metering and gas-mixing unit. Fused Al_2O_3 powder with particle size in the range 150-175 μm was loaded in the reactor to form a bed of 4 to 6 cm high. The powder bed was fluidized by an upward flow of Ar + H_2 mixture and they were metered independently at atmospheric pressure. A combined flow rate between 6-8 l/min (about 6-8 cm/s linear flow velocity) was required to maintain fluidization of the bed. The metal coupons immersed in the powder bath were loosely hung from the top and were about 1.5 cm above the porous fused quartz plate. For Cr-Al coating experiment, as shown in Figure 4, the reactor was heated using either an electric resistance furnace or a RF induction coil. The system was heated rapidly to coating temperature, and the volatile and reactive precursors were then added from the top and through the bottom of the reactor at the coating temperature.

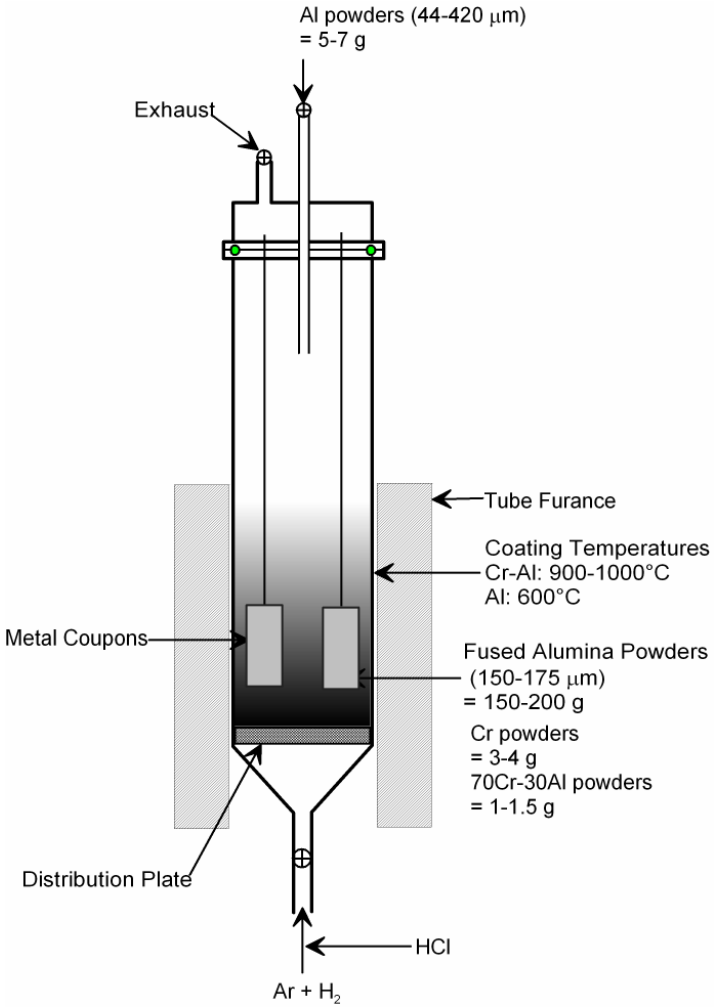

Figure 4. Schematic diagram of the fluidized bed reactor for Cr-Al and Al coatings of metal coupons.

Procedure

For depositing Cr-Al coating, the specimens were immersed in a fluidized bed containing a mixture of alumina powder, chromium powder, and Cr-Al alloy powder. During heating, the bed was fluidized with a stream of Ar(g) and H_2(g). When the bed reached a temperature in the range 960° to 1000°C, HCl(g) (1 to 2% v/v) was also admitted to generate volatile chromium ($CrCl_2$) and aluminum chloride (AlCl) species, which then decomposed or reduced on the specimen. The reactive precursors are reduced by the presence of H_2 forming Cr-Al on the metal coupon. After the Cr-Al at high temperature, the reactor temperature was lowered to 600°C, and then a small amount of Al powder was added to the reactor for additional Al coating on the metal substrates. Some of the Cr-Al and Al-coated coupons were heat-treated in Ar + H_2O mixture at 900-950°C, forming a thin Al_2O_3 layer on the coupons. Deposition durations were typically about 3 h each.

For TiN or (TiTa)N coating, a small amount of TiH_2 powder was added to the powder bed to promote the formation of $TiCl_3$ and $TiCl_2$ reactive gaseous precursors. A gaseous mixture of Ar + $TiCl_4$ was supplied from a $TiCl_4$ (l) bubbler heated between 26-40°C using pure Ar at atmospheric pressure as carrier gas. The Ar + $TiCl_4$ mixture was added together with the Ar + H_2 fluidizing gas mixture through the bottom of the reactor. At coating temperature between 900° and 1100°C, $TiCl_4$ gas will react rapidly with Ti powders, forming reactive $TiCl_3$ and $TiCl_2$ gaseous precursors, and Ti metal will be deposited on the coupon surface by H_2 reduction. Ta deposition was done by reduction of $TaCl_5$ powders by H_2 when the powders were slowly added to the powder bed. After the metal coating experiment, the reactor temperature was lowered and the coating was nitrided by admitting NH_3 gas from the top of the reactor.

For (TiAl)N coating experiments, $AlCl_3$ gas was supplied to the bottom of the reactor by vaporization of $AlCl_3$ powders from a heated reactor using Ar as carrier gas. For Ti-Al coating, 1-2 g of Al powders were added to the fused alumina powder bed to promote the formation of reactive $TiCl_3$ and AlCl gaseous precursors at the desired temperature. The nitridation was performed at lower temperature after the Ti-Al coating experiment.

For (TiSi)N coating, $SiHCl_3$ from the bubbler using Ar as carrier gas was admitted together with TiCl4 gas through the bottom of the reactor. The $SiHCl_3$ bubbler was kept at ice temperature during the coating experiments. As in other cases, nitridation was conducted at lower temperature.

FABRICATION OF POROUS COUPONS WITH SS 409 ALLOY

In view of the fact that no porous metal filters were commercially available, we procured a batch of SS409 powder (300 mesh, 0.04 mm) and fabricated our own coupons. The alloy steel powder was sintered under hydrogen at 1300°C for 12 h. Flat and mechanically strong samples were obtained by this procedure. The porosity of the coupons was determined to be about 55%.

SIMULATED COAL GAS STREAM TEST EQUIPMENT

We assembled a test facility to expose coupons to simulated gasifier environments for 300 h or longer. The test facility consists of a 9.0-cm OD by 90-cm long quartz tube heated by a 3-zone electrical resistance furnace. The furnace is long enough to easily accommodate over 20 coupons. The ends of the quartz tube are capped with steel flanges with ports to admit and/or vent gases.

The gas stream at the WREL plant consists mostly of H_2, CO, and CO_2 in roughly 30:36:15%. The balance is steam and about 2% H_2S. To achieve some degree of flexibility in metering in different amounts of H_2, CO and CO_2, and H_2S, we opted in favor of using two mixed-gas cylinders. One cylinder contained H_2, CO, and CO_2 in a 19:57:24 ratio. The other cylinder contained 10% H_2S in H_2. Mass flow controllers metered these mixtures to blend a simulated coal gas stream of desired composition. A heated evaporator was used to produce steam with a controlled rate of injection of liquid water by a syringe pump. The tube carrying steam and other gases was heated to prevent further condensation. H_2S/H_2 was added near the inlet of the reactor to prevent corrosion of the metal tubing. The final gas composition was 25.7% H_2, 38.9% CO, 17.3% CO_2, 1.7% H_2S, and the remainder steam. The total flow rate of the gas stream was about 120 standard cubic centimeters per minute (SCCM). A schematic diagram of the test system is shown in Figure 5.

The furnace has three heating zones, each of which can be independently controlled. After a few adjustments to the power supply, we were able to achieve a uniform temperature profile across most of the central portion of the furnace. For example, the temperature inside the furnace was 900°± 5°C through the central 50 cm length (Figure 6). About 20 sample coupons can be placed inside the furnace using a notched sample holder made of quartz. This arrangement allowed all samples to be exposed to the coal gas uniformly. Both coated and uncoated specimen coupons were tested for their resistance to sulfidation.

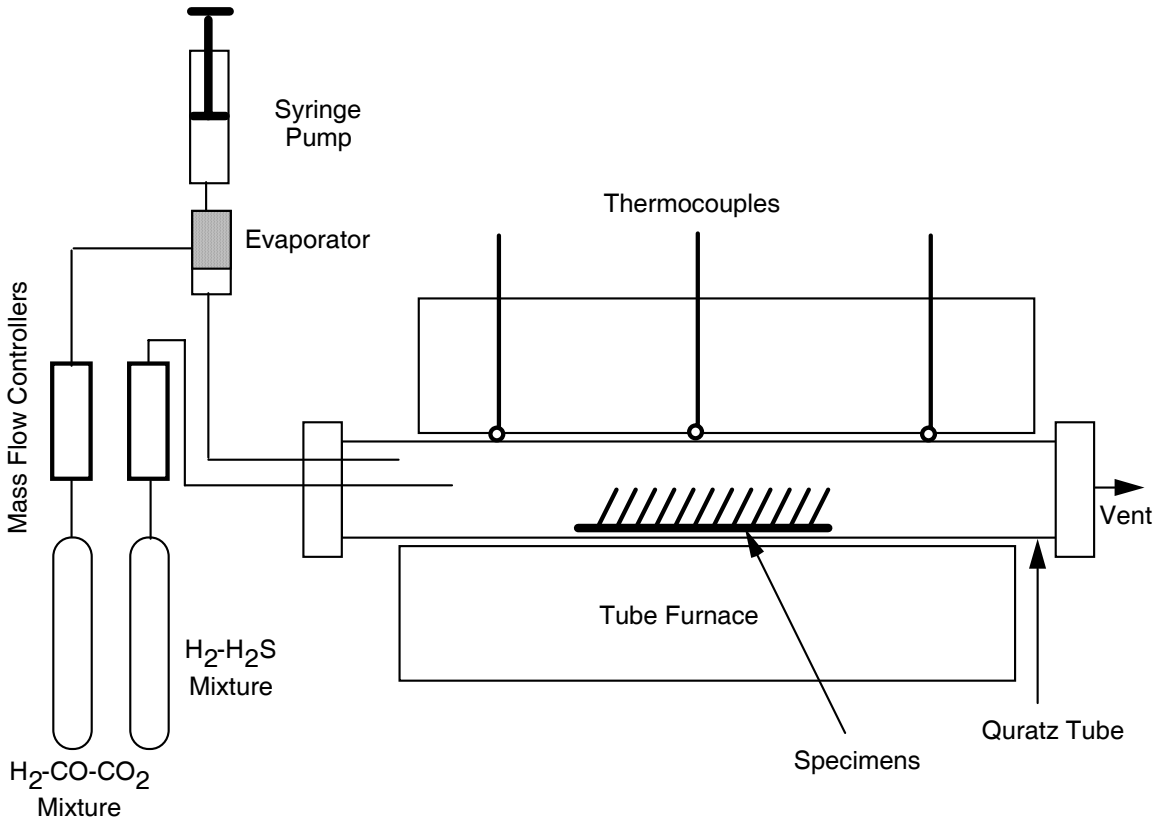

Figure 5. Schematic diagram of the bench-scale exposure test system.

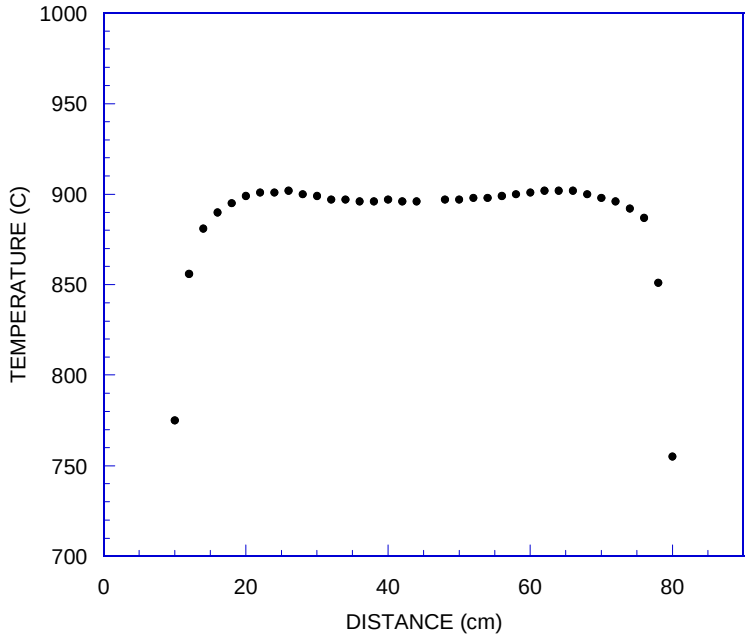

Figure 6. Temperature profile across the length of the furnace.

RESULTS AND DISCUSSION

DEPOSITION OF COATINGS ON ALLOY SUBSTRATES

The composition of the uncoated alloy coupons, as determined by the X-ray fluorescence (XRF) elemental analyses is summarized in Table 6.

Table 6. XRF analysis of various metal alloy coupons used as substrates

Element	SS405	SS409	SS410	SS316	HR160
Fe	86.7	87.1	87.4	66.8	
Cr	12.4	11.1	11.7	18.0	28.2
Al		0.3	0.22	0.4	
Mo				2.3	
Ni	0.18		0.18	11.0	38.2
Si	0.53	0.5	0.41	1.5	2.6
Co					30.5
Ti					0.5

Coatings on Dense Substrates

Chromium diffusion coatings were deposited on various substrates using the fluidized bed reactor. Table 7 lists the coating depth and the surface chromium levels of the coatings. Generally, the chromium levels in the ferritic SS alloys 405 and 410 were higher than in the austenitic SS alloys such as 304 and 316. Note that the surface concentration in the nickel-based alloys IN 800 is also low. We believe that nickel present in the austenitic alloy hinders the deposition of Cr on the surface.

Table 7. Summary of initial coating runs

Run. No	Substrate	No. of Coupons	Coating	Coating depth	Surface Cr Concentration
39	SS 410	1	Cr	10	76.8
40	SS 410	1	Cr	5	60
41	SS 316L	3	Cr		32.3[1]
42	SS 304	1	Cr	5	62
42	SS 410	1	Cr	10	62
43	SS 304	1	Cr	5	33.5
43	SS 405	1	Cr	20	16
43	SS 410	1	Cr	3 to 5	28
43	IN-800	1	Cr	4 to 5	18
46	SS 405	3	Cr		20
48	SS 410	1	Cr	20 (plateau)	70

[1] Porous substrate.

The coated samples were examined by various techniques such as scanning electron microscope (SEM), energy-dispersive X-ray analysis (EDX), and X-ray fluorescence (XRF). The surface composition of Cr-Al-coated coupons is shown in Table 8. The data show that the surface is enriched in Cr-Al, except in the case of IN 800 alloy, which is a nickel-rich alloy.

Table 8. Surface composition of Cr-Al coated specimens

		Surface Composition (Wt%)			
Alloy	**Run No.**	**Al**	**Cr**	**Fe**	**Ni**
SS304	42	5.2	61.6	24.2	8.9
SS316	41	5.4	32.3	52.1	8.1
SS405	44	2.9	68.4	28.7	0
SS410	42	2.8	61.8	35.4	0
IN 800	44	12.0	18.0	42.4	17.5

We also measured the distribution of Cr and Al diffused into the samples. The depth profiles of SS 316 and SS 410 after coating with Cr-Al coated are shown in Figure 7. The data indicate that the surface concentration of Cr was high, but the diffusion depth was limited.

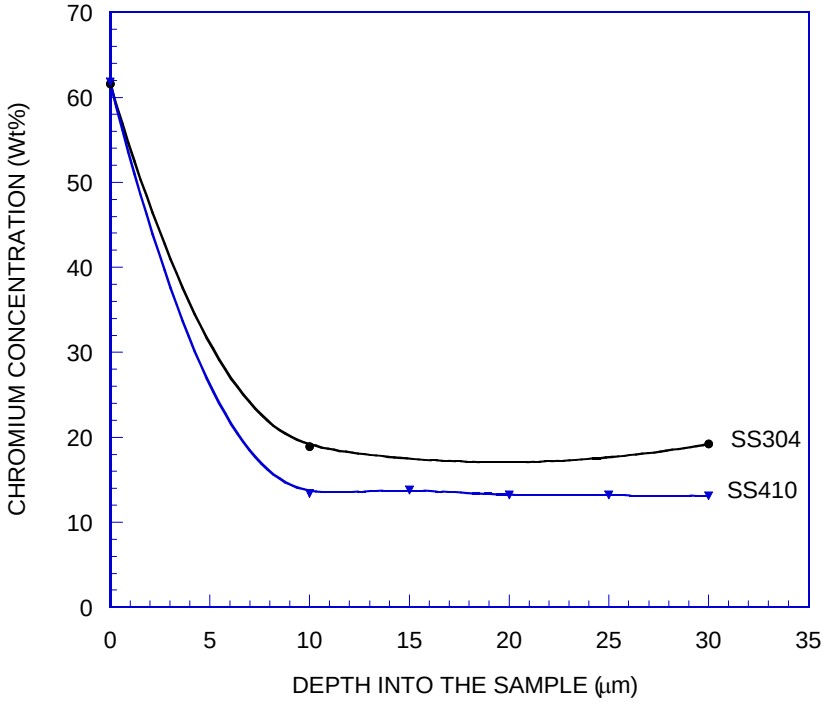

Figure 7. The depth profiles of SS304 and SS310 after Cr-Al coating.

Experimental conditions used in the coating runs and the XRF analyses of metal or alloy coatings on various stainless steel coupons are summarized in Table 9. Many of the metal or alloy coatings showed very good adherence on the metal substrate surface, as checked by

rubbing, high-pressure air blowing and scotch tape testing. The results show that the compositions and thickness of Cr-Al, Ti-Al, Ti-Ta, and TiSi coatings can be controlled by the coating temperature and time, and relative amount of precursors admitted to the reactor. From Runs #77-90, each coating experiment was performed over two days. The first was for the Ti-Al coating and followed by (TiAl)N or (TiSi)N nitride coating on the second day. A typical elemental line scan of the cross section from Run # 77, (TiAl)N/SS409 and from Run #86, (TiSi)N/SS410, is shown in Figures 8 and 9. The line scan clearly shows two distinct coating regions: the Ti and Al diffusion coating for both runs and (TiAl)N or (TiSi)N coating on the top surfaces. It is clear that Al enhances the Ti inward diffusion and the coating temperature controlled the depth of Ti layer.

Table 9. Summary of various metal alloy coatings on stainless steel coupons

Run No	SS Coupon	Coated Materials	Coating Conditions Temperature; Time	XRF Analysis of the Surface
56 56A (3/7/05)	304 409	TiN coating (TiTa)N coating TiN coating (TiTa)N coating	1045°C: 3.5 hrs 1045°C: 1.5 hrs 1045°C; 2.5 hrs 1045°C; 3.0 hrs	**304 alloy: Ti: 23.9; Ta: 9.4;** Fe: 38.1; Cr: 20.5**;** Ni: 7.7 **409 alloy: Ti: 24.5; Ta: 3.8;** Fe: 60.1; Cr: 11.3
57	409-07 409-08 409-09 409-10	Cr, Al coating	1000°C; 3 hrs 750-800°C; 5 hrs	**409-07: Al: 17.6; Cr: 13.1;** Fe: 68.3 **409-09: Al: 17.2; Cr: 14.3;** Fe: 67.9
57A (from 57)	409-07 409-09	Al coating	600°C: 2 hrs	**409-07: Al: 21.3; Cr: 13.6;** Fe: 64.1 **409-09: Al: 17.2; Cr: 13.8;** Fe: 67.9
58	409-11 409-12	Cr, Al Coating	1000°C: 3 hrs	**409-11: Al: 22.2; Cr: 21.3;** Fe: 55.7
59	**From #57** 409-08 409-10 **From #58** 409-11 409-12	Forming thin Al_2O_3 coating by controlled oxidation in Ar + H_2O mixture	950°C; 1 hr	
60 (3/21/05)	HR160-09 HR160-10	TiN coating (TiTa)N coating	1100°C; 3.2 hrs 1100°C; 2.5 hrs	**HR160-09: Ti: 38.7; Ta: 0.7;** Cr: 18.7; Co: 17.6 Ni: 23.9
61	Two 316 porous coupons	Cr, Al coating	1000°C; 2.5 hrs	**Al: 21.5; Cr: 24.6** Fe: 44.2; Ni: 6.5
62 (4/7/05)	Three 316 porous coupon	TiN coating (TiTa)N coating TiN coating	950-1120°C; 3 hrs 950-1000°C; 2 hrs 950-1080°C; 3 hrs	**Ti: 40.5; Ta: 1.6** Fe: 38.6; Cr: 10.7 Ni: 6.8

Run No	SS Coupon	Coated Materials	Coating Conditions Temperature; Time	XRF Analysis of the Surface
63 (4/14/05)	409-13 409-14 409-15	TiN coating	1080-1140°C; 5.5 hrs	**409-13** **Ti: 13.7; Al: 0.3** Fe: 70.4; Cr: 14 **409-14** **Ti: 13.6; Al: 0.3** Fe: 69.7; Cr: 14.1
64	HR160-06 HR160-07 HR160-08	Ti coating TiN coating	1180°C; 3 hrs 1120°C; 3 hrs	**Ti: 22.9; Al: 0.5** Cr: 22.4; Co: 22.5 Ni 28.8
65 (4/21/05)	410-05 410-06 410-07	Ti coating TiN coating	1160°C; 3.3 hrs 1120°C; 2.1 hrs	**Ti: 11.9; Al: 0.6** Fe: 75.0; Cr: 11.1
66	405-15 405-16 405-17	Ti coating TiN coating	1180°C; 4.0 hrs 1120°C; 2.0 hrs	**Ti: 14.4: Al: 0.4** Fe: 71.6; Cr: 12.0
67	409-16 409-17	Cr, Al coating Al coating	955-981°C; 1.5 hrs 600°C; 1.5 hrs	**Al: 35.2; Cr: 9.4** Fe: 54.5
68 (4/27/05)	409-18 409-19 409-20	Ti coating TiN coating	1180°C; 5.5 hrs 950-1020°C; 2.5 hrs	**Ti: 26.4; Ai: 0.9** Fe: 63.9; Cr: 8.0
69	Three 405	Ti coating TiN coating	1180°C; 6.5 hrs 920°C; 2.8 hrs	**Not analyzed**
70 (4/27/05)	409-16 409-17 (from 67)	Forming thin Al_2O_3 coating by controlled oxidation in Ar + H_2O mixture	950°C; 1 hrs (Ar + H_2O)	**Not analyzed**
71 (6/8/05)	409-01 (sand blasted) 409-02 (as received)	Cr, Al coating Al coating	975-996°C; 3 hr 600°C; 1 hr	**409-01** **Al: 12.0; Cr: 22.5** Fe: 63.7 **409-02** **Al: 18.9; Cr: 19.5** Fe: 60.6
72 (6/10/05)	405-01 (sand blasted) 405-02 (as received)	Cr, Al coating Al coating	890-933°C; 2 hrs 600°C; 1 hr	**405-1** **Al: 3.3; Cr: 24.7** Fe: 69.7 **405-02** **Al: 2.3; Cr: 21.1** Fe: 75.4
73	410-01 (sand blasted) 410-02 (as received)	Cr, Al coating Al coating	928-1000°C; 2.5 hrs 600°C; 1 hr	**410-1** **Al: 4.8; Cr: 25.4** Fe: 67.5 **410-02** **Al: 5.6; Cr: 23.1** Fe: 70.6
74	409-01 409-02	Cr, Al coating Al coating	1000°C; 1 hr 600°C; 1 hr	**409-1: Al: 31.8; Cr: 20.7;** Fe: 46.7 **409-02: Al: 30.1; Cr: 20.2;** Fe: 49.0
75	All coated coupon from 72, 73, 74	Forming thin Al_2O_3 coating by controlled oxidation in Ar + H_2O mixture	909-920°C; 1 hr (Ar + H_2O)	
76 (6/27/05)	409-14 (sand Blasted) 409-15 (as received)	Cr, Al coating Al coating	839-872°C; 2 hrs 600°C; 1 hr	**409-14: Al: 18.4; Cr: 11.0;** Fe: 70.0 **409-15** **Al: 16.9; Cr: 12.4**

Run No	SS Coupon	Coated Materials	Coating Conditions Temperature; Time	XRF Analysis of the Surface
				Fe: 70.1
77 (7/14/05)	409-06 409-07 409-10	Ti, Al coating (TiAl)N nitridation	920°C; 3 hrs 750-800°C; 5 hrs	**Ti: 55.5; Al: 4.8** Fe: 21.7; Cr: 2.7
78	Three 316 porous	Ti, Al coating (TiAl)N nitridation	1000-1100°C; 5 hrs 750-800°C; 5 hrs	**Ti: 27.1; Al: 2.2** Fe: 37.3; Cr; 19.15 Ni: 26.3; Si: 0.8
79	410-03 410-04 410-05	Ti, Al coating (TiAl)N nitridation	920-1000°C: 5.5 hrs 750-800°C; 5 hrs	**Ti: 5.9; Al: 47.7** Fe: 38.1; Cr; 7.0
80 (8/105)	405-03 405-04 405-05	Ti, Al coating (TiAl)N nitridation	920°C: 8 hrs 750-800°C: 5 hrs	**Ti:4.2 ; Al: 54.4** Fe: 32.9.1; Cr; 6.35
81	409-05 409-11 409-13	Ti, Al coating Ti, Ta Coating NH_3 nitridation	850-920°C: 4 hrs 850-920°C: 4 hrs 920°C: 0.5 hr	**Ti: 7.5; Al: 3.0;** **Ta: 0.13** Fe: 75.8; Cr: 10.9
82 (9/13/05)	409-08 409-09 409-18	Ti, Al coating Ti, Ta Coating (TiAlTa)N nitridation	850-920°C: 4.2 hrs 920-1000°C: 2.5 hrs 750-800°C: 5 hrs	**Ti: 5.8; Al: 49.6;** **Ta: 0.1** Fe: 35.9; Cr: 6.9
84	410-07 410-08 410-10	Ti,Al coating (TiSi)N nitridation	800-850°C: 5.5 hrs 750-850°C: 4 hrs	**Ti: 3.1; Al: 0.9;** **Si: 3.9** Fe: 78.6; Cr: 13.5
85	409-17 409-19 409-20	Ti,Al coating (TiAl)N nitridation	800-850°C: 6 hrs 750-800°C: 1 hr	**Ti: 4.0; Al: 48.4** Fe: 38.9; Cr: 6.7
86	410-15 410-16 410-17	Ti,Al coating (TiAl)N nitridation	850-900°C: 6 hrs 750-800°C: 2 hrs	**Ti: 13.5; Al: 0.95;** **Si: 13.1** Fe: 61.7; Cr: 10.1
87	405-10 409-16 410-12	Ti,Al coating (TiSi)N nitridation	850-980°C: 7.5 hrs 750-800°C: 5.1 hrs	**405-10: Ti: 82.3; Al: 0.15;Si: 3.1** **410-12: Ti: 86.5; Al: 0.1;Si: 3.1** Fe: 8.75; Cr: 0.8
89 (10/18/05)	405-13 410-18 410-19	Ti,Al coating (TiSi)N nitridation	870-1010°C: 8.0 hrs 750-800°C: 6.0 hrs	**405-13: Ti: 31.45; Al: 0.3;Si: 5.3** Fe: 53.8; Cr: 8.9 **410-19: Ti: 80.5; Al: 0.15;Si: 2.0** Fe: 15.6; Cr: 1.9
90 (10/25/05)	Three 410	Ti,Al coating (TiAl)N nitridation	870-1010°C: 8.2 hrs 750-800°C: 5 hrs	**Ti: 88.4; Al: 0.1;** Fe: 10.3; Cr: 1.2

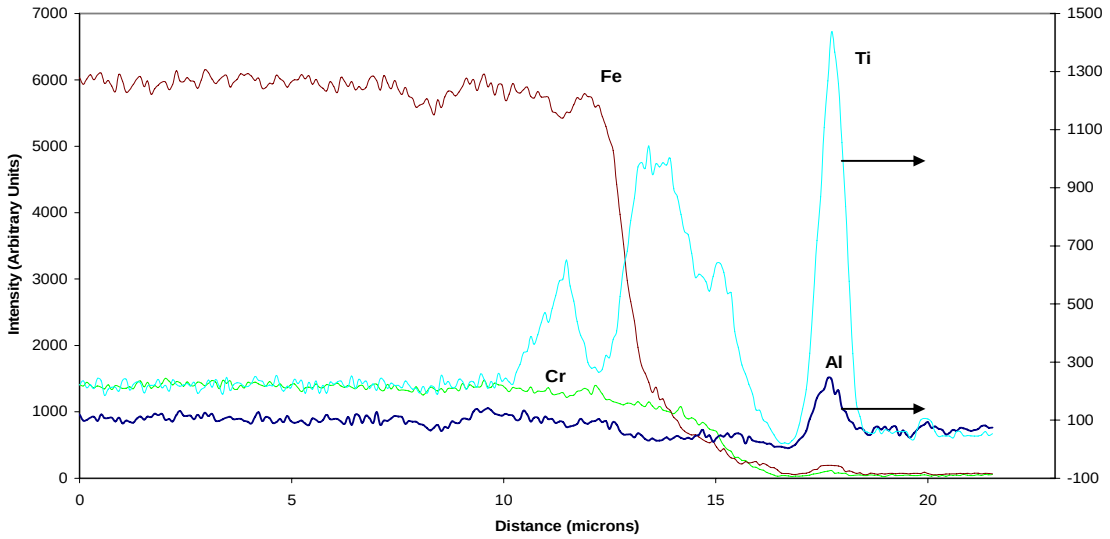

Figure 8. Line profile of the cross section TiAl and (TiAl)N-coated SS409 coupon from Run #77.

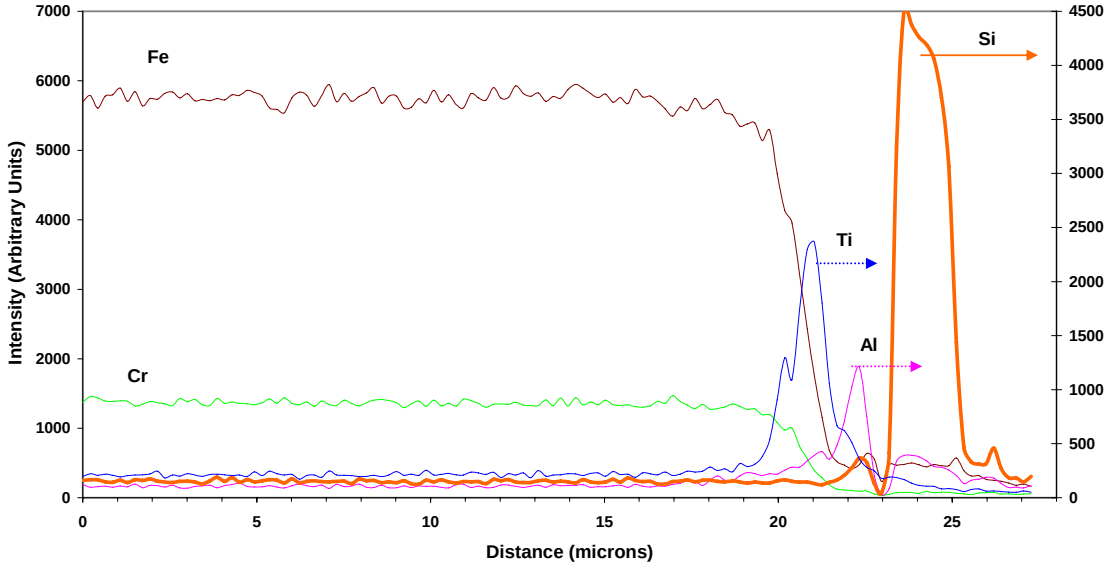

Figure 9. Line profile of the cross section TiAl and (TiSi)N-coated SS409 coupon from Run #86.

Coatings on Porous Substrates

The porous SS 409 alloy samples were coated with silicon and titanium and were nitrided. The Ti-Al-Si-coated sample was also examined by SEM. The distributions of Si and Ti inside the specimen were determined by the energy-dispersive X-ray analysis. Figure 10 illustrates the SEM image along with Fe, Si, and Ti maps in these samples.

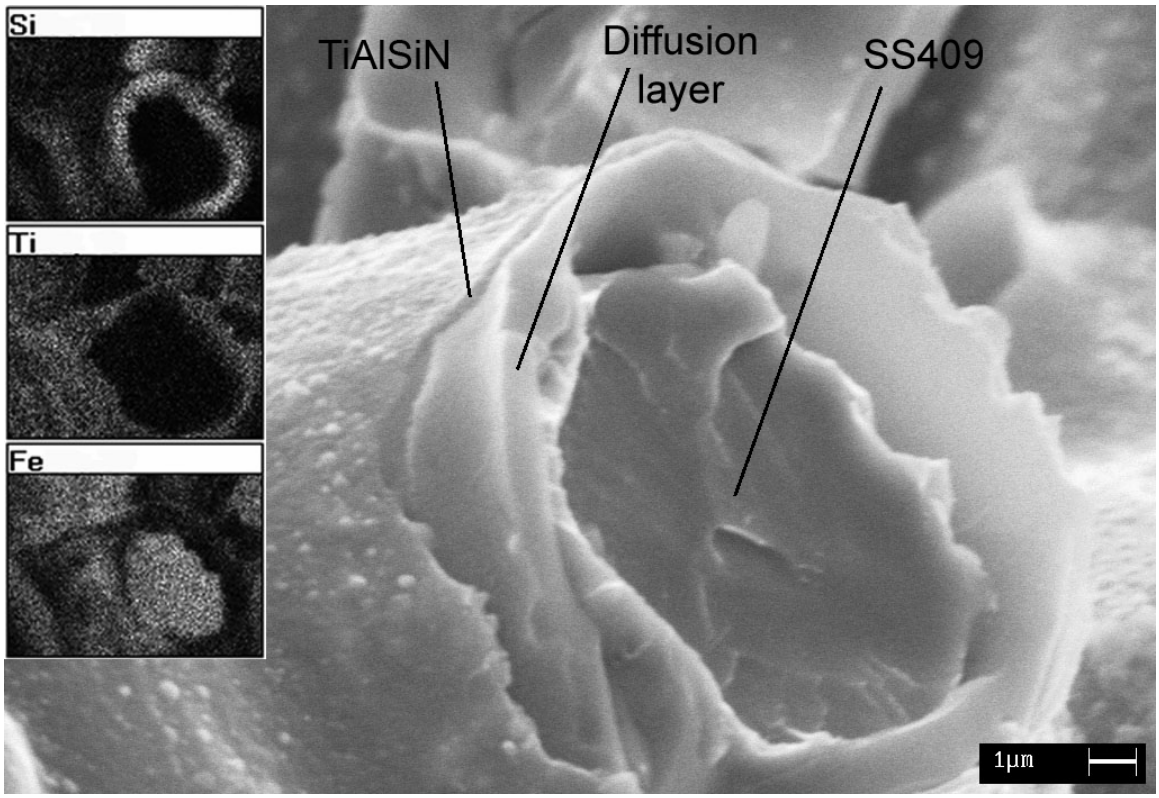

Figure 10. SEM image of Ti-Al-Si-coated along with the distribution of Fe, Si, and Ti inside the sample.

In this map, the brightness of the image is proportional to the concentration of the element at that point. As expected, the elemental maps show that the surface was enriched in Ti, which is consistent with the fact that Ti or TiN cannot diffuse into the stainless steel. The TiN coating appears to be dense and has a thickness of about 2 μm.

Figure 11 and Table 10 show the SEM image of the porous SS316 frit and the elemental composition inside the frit. They indicate that Si- and Ti-based coatings are present even in the interior of the porous frit, confirming that the fluidized bed chemical vapor deposition is capable of coating inside a porous material.

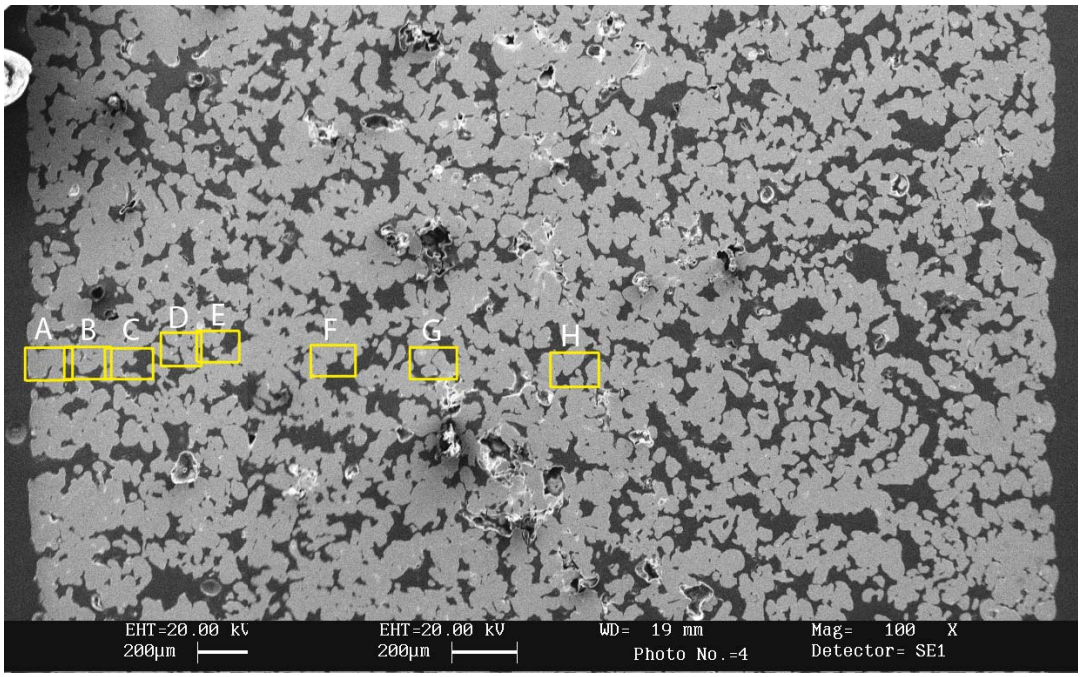

Figure 11. SEM image of the porous SS 316 frit.

Table 10. Elemental composition inside the porous SS316 frit

	Location							
Element	**A**	**B**	**C**	**D**	**E**	**F**	**G**	**H**
Ti	3.99	3.14	1.07	1.97	0.74	0.05*	0.02*	--
Si	2.89	2.73	1.72	2.18	2.06	2.17	1.95	2.12
Fe	61.50	61.19	66.49	63.29	64.79	68.09	67.89	67.37
Cr	18.57	20.12	18.69	20.57	20.42	17.95	17.32	17.99
Ni	10.58	11.02	10.37	10.91	10.78	10.56	12.05	10.93
Mo	1.21	1.19	1.21	1.08	1.21	1.18	0.77	1.58
Cl	1.25	0.62	0.45	--	--	--	--	--

Figure 12a illustrates a magnified image of one of the particles at location B shown in Figure 11 inside the porous frit. As shown in Figure 12c, titanium is present mainly on the outer edge of each of the metal particles. The level of Si is too low to show its distribution precisely in this map. We believe that Si is also coated only at the outer edges of the particles.

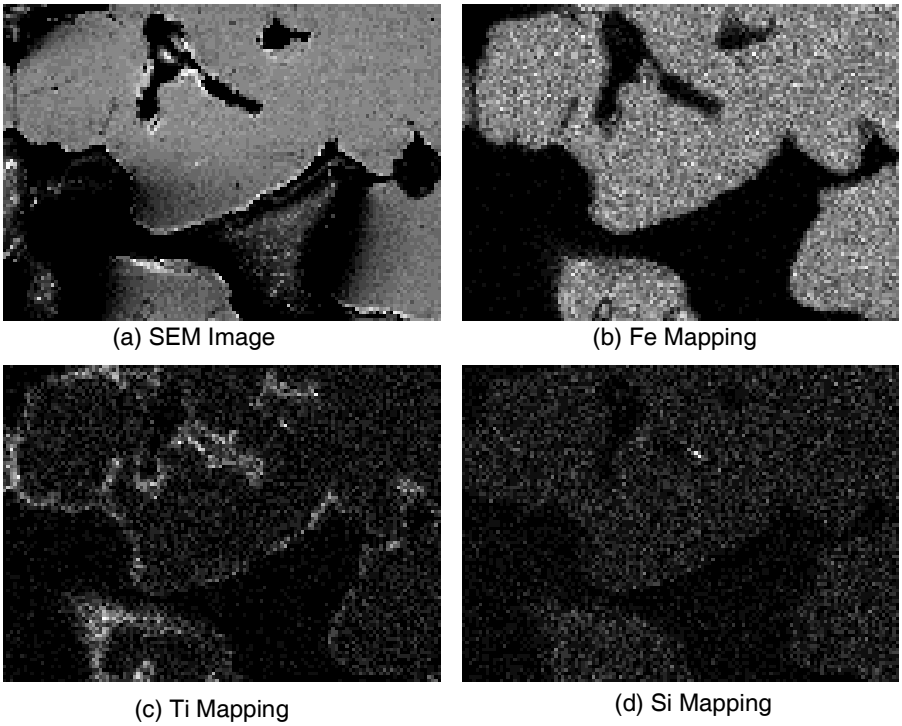

Figure 12. A magnified image of porous SS frit and the distribution of Ti inside the frit. (Note: The data is taken at location B shown in Figure 11).

EXPOSURE TO A SIMULATED COAL GAS ENVIRONMENT AT HIGH TEMPERATURES

Exposure of Uncoated Metals and Alloys

We exposed a range of pure metals and some common alloys to the reactive gases of a coal gasifier (Exposure Test #5). These alloys included Kanthal (a Fe, Cr, Al alloy steel), Ti6Al4V, and commercial steel drill bits coated with TiN and ZrN. The purpose of this test was to identify those metals that were particularly resistant and hence would make good ingredients for the coatings. The samples were exposed to a simulated gasifier environment for 112 h, after which they were retrieved for examination and analysis using XRF. Table 11 lists the samples used in this test, as well as the levels of sulfur detected by XRF following exposure and the phases predicted by thermodynamics. Figures 13 and 14 are photographs showing the state of the samples before and after the exposure. Two observations that are immediately apparent are: (1) the Ta sample had completely disintegrated into flakes, and (2) the Co sample had apparently melted and flowed out through the pores of the alumina support.

These results are in general agreement with the thermodynamic equilibrium analysis. The noble metals such as Au and Pt did not have a significant weight change as they remain in their metallic state. The highly reactive metals such as Ti, Zr, Cr, and V were converted mainly to

their oxides. The small level of sulfur measured with Cr may indicate the formation of a chromium oxysulfide. Thermodynamic data for chromium oxysulfide are not readily available. Similarly, Ta and Nb are mainly converted to their oxides, although a small amount of oxysulfides may have formed.

Table 11. Substrates and coatings used in Test #5 and the results of exposure

Sample No.	Material	%Wt. Change	Weight Gain/SA (g/cm^2)[1]	Wt% S[2]	Predicted Phase[3]
1	Au	-7.06E-04	-3.08E-05	0	Au
2	Ti	6.64E-01	2.01E-02	0	TiO_2
3	Zr	3.51E-01		0	ZrO_2
4	Pt	-1.81E-03	-3.85E-02	0	Pt
5	Ta		Disintegrated into a powder	N.M.	Ta_2O_5
6	Nb	3.13E-01	7.29E-02	0.67	Nb_2O_5
7	Mo	2.37E-02	1.33E-03	12.6	MoS_2
8	W	-1.03E-04	-5.48E-06	0.66	WS_2
9	Cr	2.40E-03	2.99E-03	0.52	Cr_2O_3
10	V	2.75E-02	1.58E-02	0.04	V_2O_3
11	Ti6Al4V	-6.36E-01		N.M.	TiO_2, Al_2O_3
12	Co	1.27E-01	Melted	21.1	CoS
13	Fe	5.83E-01	2.09E-01	13.9	FeS
14	Ni	3.37E-01	1.08E-02	18.6	Ni_3S_2
15	Cu	2.52E-01	3.18E-02		CuS
16	Kanthal	-2.15E-03	-1.70E-02	0.27	Cr_2O_3, Al_2O_3
17	Ti /Steel	2.35E-01	7.04E-03	7.4	FeS
18	Zr /Steel	2.37E-01	-3.08E-05	13.5	FeS

Notes:

1. Based on measured surface area.
2. Measured by XRF analysis of the surface of the sample.
3. Predicted by thermodynamic equilibrium analysis at 900°C for the gas composition used. The equivalent partial pressures of O_2 and S_2 are 3.6×10^{-4} and 1.8×10^{-15} atm, respectively.

The surface of the base metals such as Co, Fe, Ni, and Mo have been converted mainly to their sulfides as indicated by a significant amount of sulfur measured on the surface. The 0.3 atomic fraction of S found on Co, Ni, and Mo surfaces indicates that the compounds are likely to be of Co_2S, Ni_2S, and Mo_2S, respectively. Again, thermodynamic data for these compounds are not available, so the calculations predicted higher sulfides than found experimentally. The phase diagrams of Co-S and Ni-S predict that a sulfur level of 25 wt% will melt at about 900°C. Although the weight gain observed with Fe sample is higher than those observed with Ni and Co, the measured S level on the surface was relatively low. This anomaly may be due to the formation of an iron oxide layer.

The alloy Kanthal containing Cr and Al had negligibly small weight change and very low sulfur levels, indicating that Cr_2O_3 and Al_2O_3 form a protective layer. Similarly, the alloy Ti5Al4V also showed only a small weight change. Hence, our approach to apply coatings containing Cr, Al, and/or Ti is in agreement with the above results.

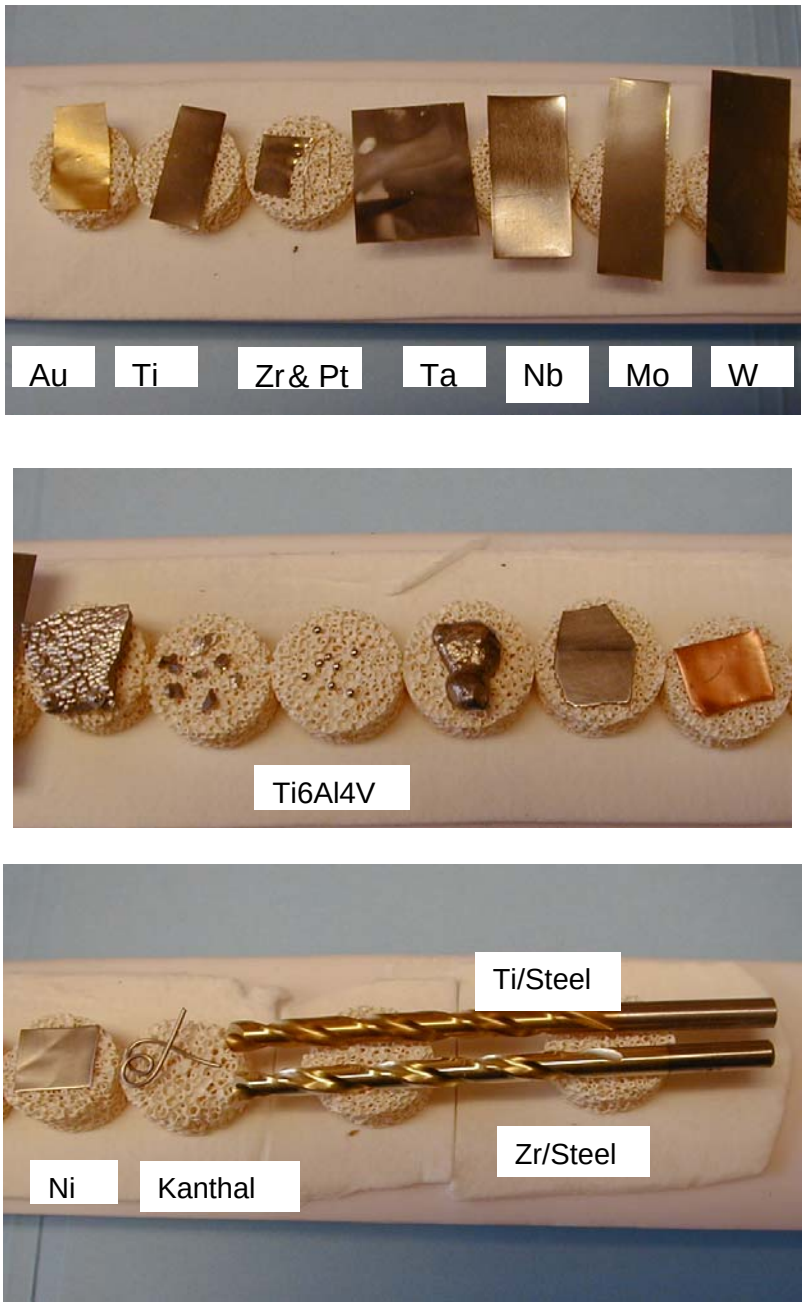

Figure 13. Samples before exposure to a simulated coal gas at 900°C in Test #5.

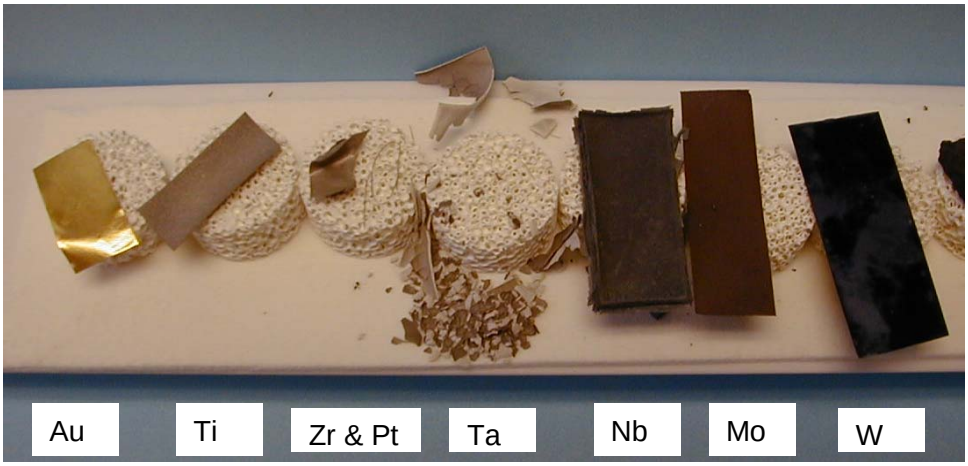

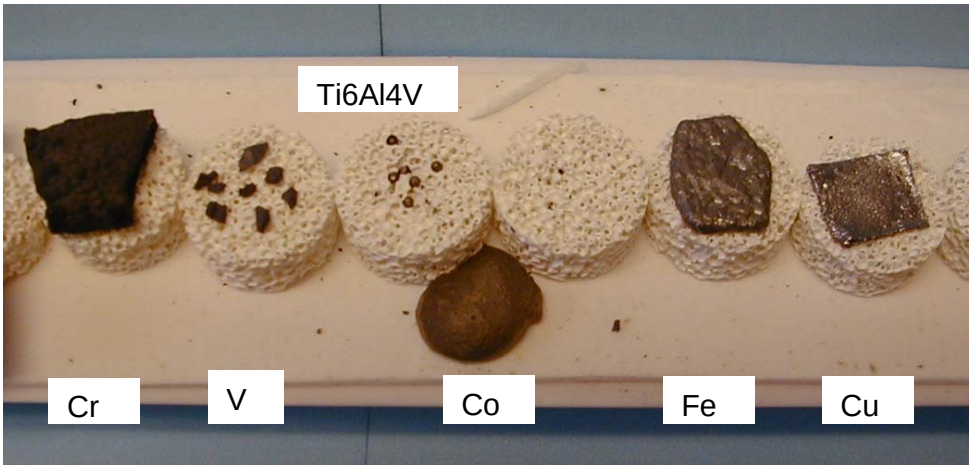

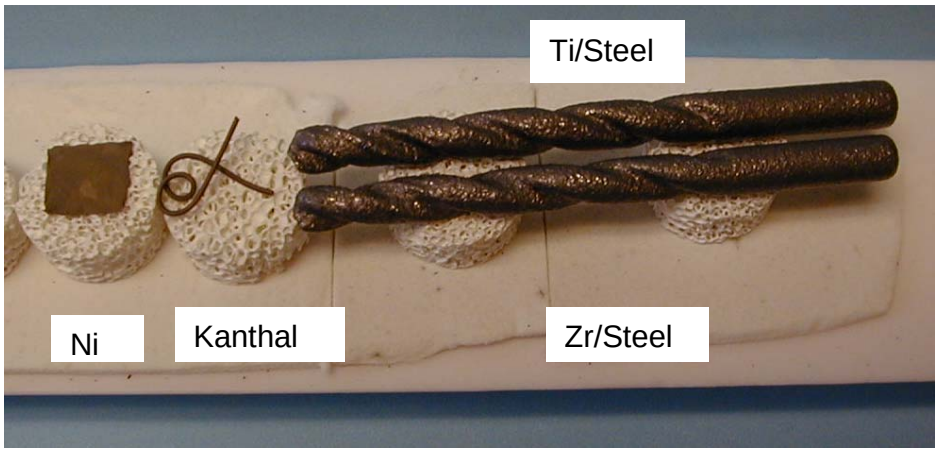

Figure 14. Samples after exposure to simulated coal gas at 900°C in Test #5.

EXPOSURE OF COATED ALLOYS TO A SIMULATED COAL GAS AT 900°C

Chromium-Aluminum Coatings

Exposure Test #1: We exposed 11 coated and uncoated samples as listed in Table 12 to a simulated coal gas stream at 900°C (Test #1). After loading the samples, the air inside the quartz tube was removed by purging with nitrogen. The furnace was heated in N_2 for about 2 h, and after the temperature reached 700°C, the reactive gases were turned on and the temperature was increased to 900°C. The gas composition was set at 30.8% H_2, 46.7% CO, 20.8% CO_2, 1.7% H_2S and the balance (20%) steam. The total gas flow was set at 120 standard cm^3 per min (SCCM). The run proceeded smoothly for 117 h, at which point it was terminated. After cooling the samples were retrieved and examined.

Table 12 also includes the weight changes in the samples before and after exposure as well as comments on the appearance of the samples at the end of the test. Figure 15 is a picture of the samples after the 117-h exposure.

Table 12. Substrates and coatings used in Test #1 and the results of exposure

Slot No.	Material	Coating Run	Coating Comp.	%Wt. Change(g)	
1	IN800	Uncoated	-	0.28	Adherent deposit on the surface
2	SS410	Uncoated	-	1.95	Adherent deposit on the surface
3	SS409	Uncoated	-	0.72	Adherent deposit on the surface
4	SS304L	Uncoated	-	24.56	Extensive attack. Sample crumpled
5	SS405	R46	Cr	0.16	Minimal adherent deposit on the surface
6	SS405	R47	Ti/Ta	0.58	Minimal adherent deposit on the surface
7	SS410	R39	Cr	0.10	Minimal adherent deposit on the surface
8	SS410	R40	Cr	0.04	Minimal adherent deposit on the surface
9	SS316	R41	Cr[1]	35.93	Extensive attack
10	SS405	R46	Cr	0.06	Minimal adherent deposit on the surface
11	SS316	uncoated	Note 1	28.61	Extensive attack. Sample crumpled

[1] Porous sample.

The weight gain data shown in Table 13 should be viewed with caution. At 900°C, in the presence of H_2S and steam, sulfides of Fe and Ni are formed along the oxides of Cr, resulting in a weight gain. However, if the reaction products do not adhere well to the substrate, they can fall out, resulting in a weight loss. In some cases, the attack by H_2S was so severe (for example: sample #4, Figure 15), liquid metal sulfide dripped out the surface of the coupon. We attempted to determine the weight change as precisely as possible. The uncoated SS316 porous metal filter coupon (sample #11, Figure 15) crumpled when a slight pressure was applied.

As expected, after the exposure to a simulated coal gas containing 1.7% H_2S at 900°C, many of the uncoated samples (Samples #1 through #4, and #11) were corroded extensively. Only the IN800 alloy showed minor signs of corrosion, resulting in an adherent deposit. However, the deposit was not uniform, but had relative large sulfide particles embedded in the deposit.

The coated coupons (Samples #5 through #10) showed various levels of attack by H_2S. A minimum level of attack was observed on Sample #6, which is a SS405 alloy coated with Ti/Ta. Other coupons that were coated with chromium also had minimum weight gain, but there were visible signs of varying degrees of corrosion. Cr-coating did not prevent corrosion of the porous SS316 alloy sample, although Cr was found to have penetrated the porous interior of the sample.

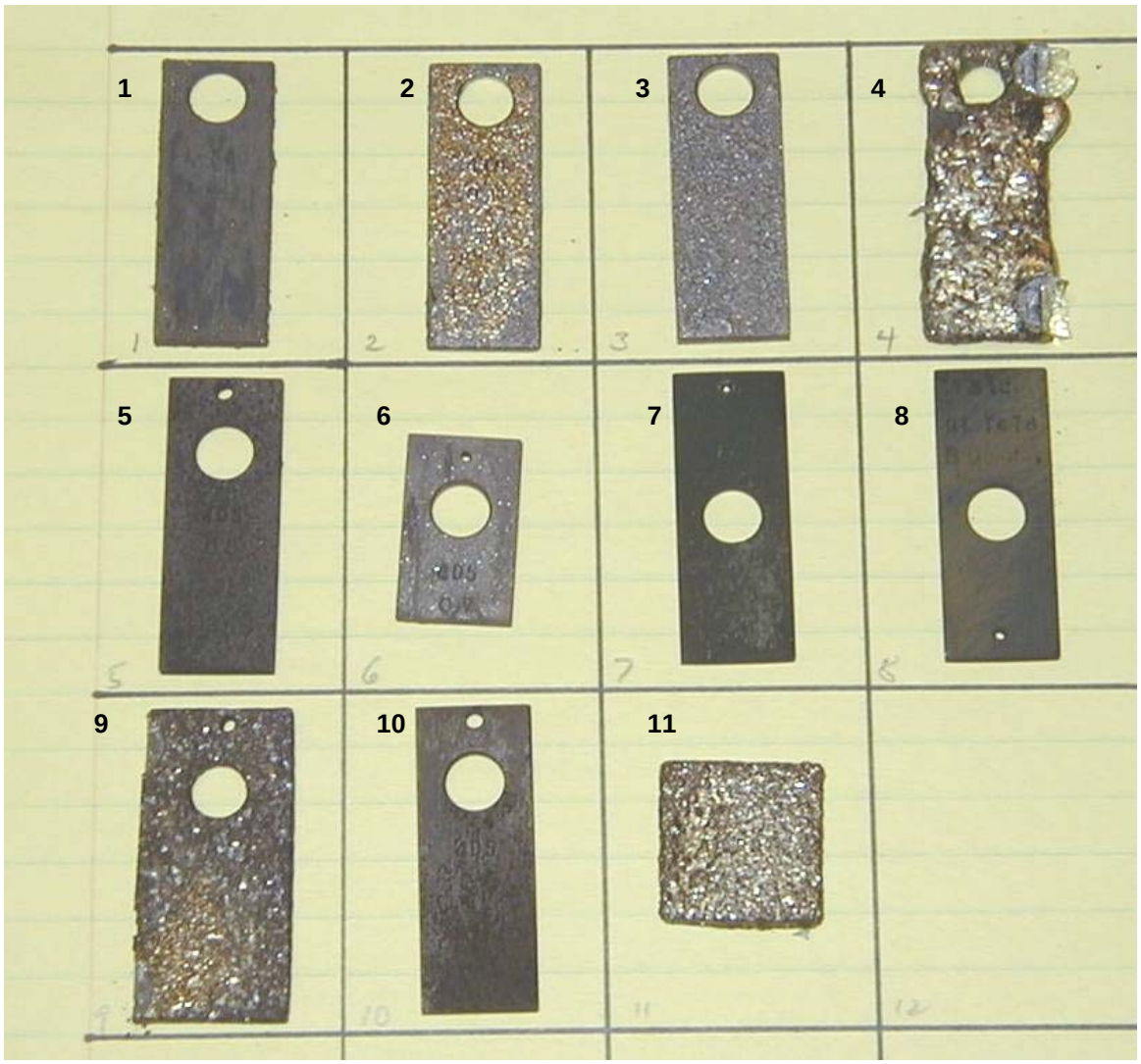

Figure 15. Samples after exposure to a simulated gasifier environment at 900°C for 117 h in Test #1.

Exposure Test #2: We conducted a second test with additional coated coupons. The samples used and the results of the exposure are listed in Table 13. This test was aborted after 20 h because of a leak in the pressure regulator of a $CO/CO_2/H_2$ mixture gas cylinder. Overnight, this cylinder emptied and the samples were exposed to a much higher concentration of H_2S (8.6%) because only steam and the gas mixture from the H_2S /H_2 gas cylinder were flowing. Some of the uncoated samples were badly corroded, and the sulfide layer buildup was severe enough to cause the quartz sample holder to break. Figure 16 is a photograph of the samples as retrieved from the aborted run. It is noteworthy that during the brief exposure to an H_2S concentration of 8.6%, even specialty alloys such as HR160 and I800 were badly corroded, yet the sample of SS 405 steel coated with Ti/Ta nitrides showed no signs of corrosion. Incidentally, this was the same sample that was previously exposed for 100 hours in the simulated gasifier stream.

Table 13. Substrates and coatings used in Test #2 and the results of exposure

Sample No.	Material	Coating Run	Coating (Surface Conc.)
1	I800; tie rod	Uncoated	-
2	HR160, tie rod	Uncoated	-
3	HR160	Uncoated	-
4	SS405	Uncoated	-
5	I800	Uncoated	-
6	SS410	R40	Cr (60%)
7	SS405	R46	Cr (20%)
8	SS410	R39	Cr (77%)
9	I800	R44	Cr-Al
10	SS405	R47	Ti-Ta

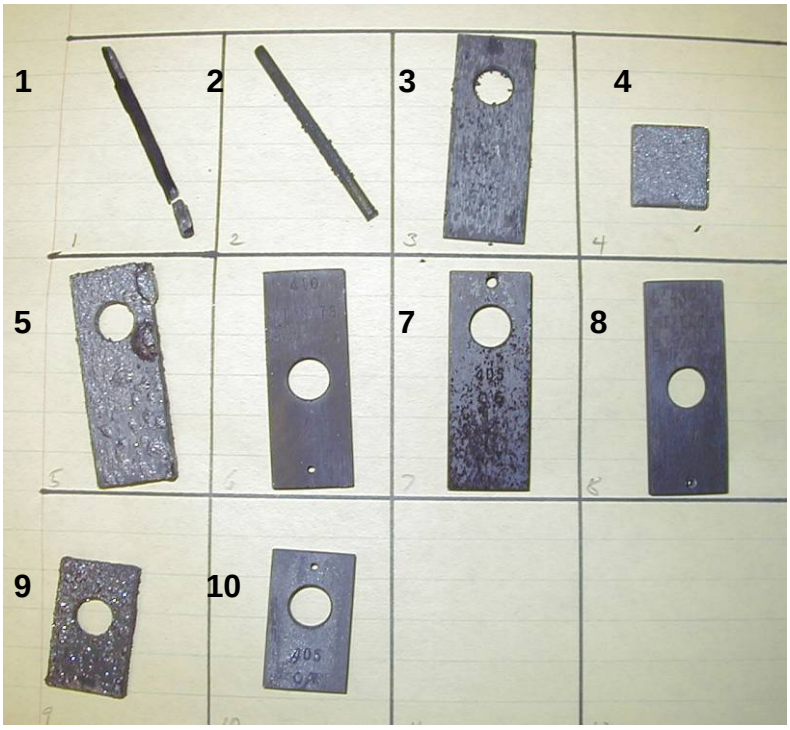

Figure 16. Samples after brief exposure to gasifier environment with 8.6%H_2S at 900°C in Test #2.

Exposure Test #3: The SS 405 and 410 alloy coupons were coated with Cr at various surface concentrations and exposed to the simulated coal gas at 900°C for 100 h. Table 14 lists the samples and the results of the test, and Figures 17 and 18 are photographs of the samples after exposure. The Ti-Ta-coated sample of SS 405 steel from the previous run (Test #2) was also included in this test. The exposure temperature and gas composition were the same as for Test #1. Sample #4, the uncoated SS405 coupon, developed a thick sulfide layer and broke the quartz sample holder from the resulting expansion. This sample, along with the other steel samples used in this run, is shown in Figure 17. Samples #6 and #8 are both SS410 coupons coated with Cr. They developed a black coating and show a small weight gain (~ 1%). Sample #7, SS405, had a lower surface concentration of Cr. It developed some scales and had a slightly larger weight gain of 1.6%. The Ti-Ta coated SS405 sample was unaffected.

Table 14. Substrates and coatings used in Test #3 and the results of exposure

Slot No.	Material	Coating Run	Coating (Surface Conc.)	Appearance	Weight Change (%)
1	I800 tie rod	Uncoated	-	Corroded	N.D.[1]
2	HR160 tie rod	Uncoated	-	Corroded	N.D.
3	HR160	Uncoated	-	Some beads	N.D.
4	SS405	Uncoated	-	Thick scale	N.D.
5	I800	Uncoated	-	Badly corroded	N.D.
6	SS410	R40	Cr (60%)	Black coating	0.91
7	SS405	R46	Cr (20%)	Minor scaling	1.63
8	SS410	R39	Cr (77%)	Black coating	1.20
9	I800	R44	Cr-Al	Pyrite beads	-4.78
10	SS405	R47	Ti-Ta	Unaffected	0.03

N.D.: Not determined due to severe corrosion of the samples and loss of corroded layers.

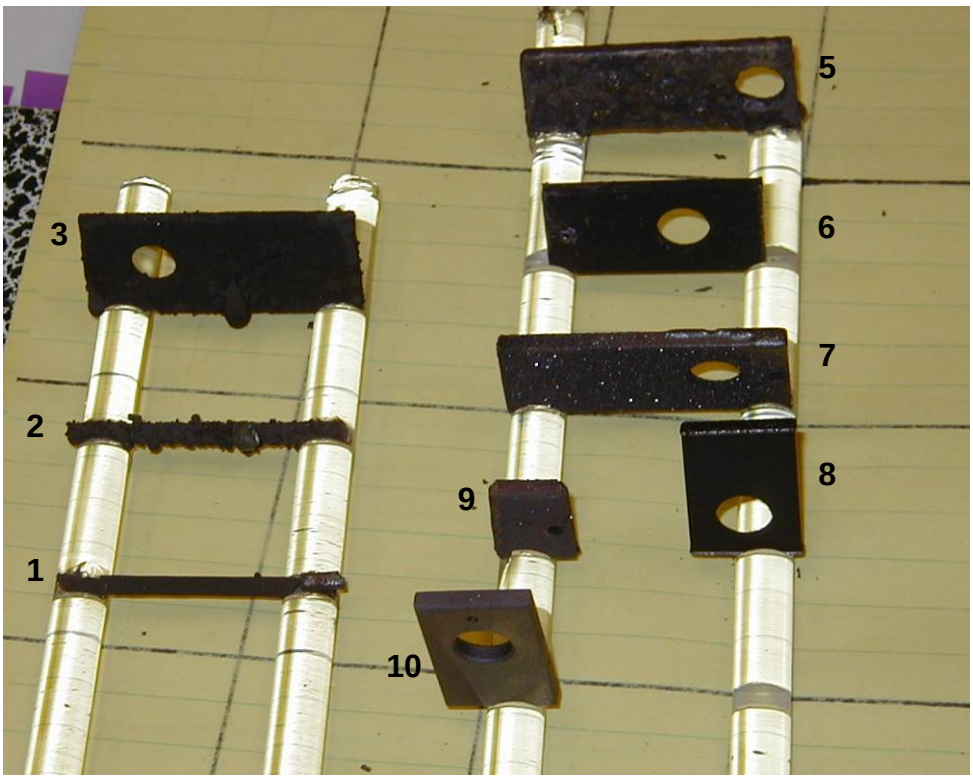

Figure 17. Steel samples after exposure to a simulated coal gas at 900°C in Test #3.
(Note: Sample 4 fell off the quartz holder)

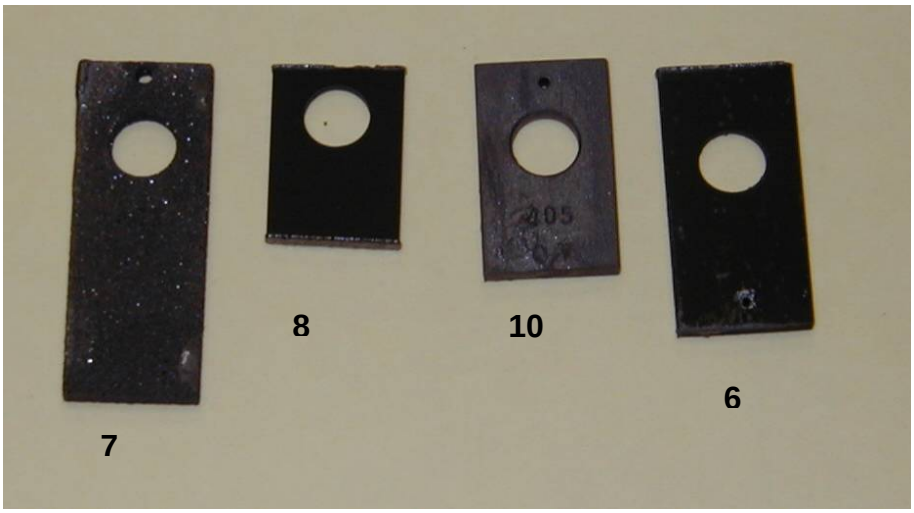

Figure 18. The face view of steel samples after exposure to simulated coal gas at 900°C in Test #3.

Titanium-Tantalum Nitride Coated Specimens

A review of the literature showed that addition of Ti and Si to the alloy steels can be beneficial in improving their sulfidation resistance. Formation of a compact, protective oxide layer that resists the ingress of S into the alloy is likely to be the cause of the improved sulfidation resistance. The Ni-Co-based alloy HR-160 contains Si as an additive and it has high sulfidation resistance. TiN coatings are used in the semiconductor resistance as diffusion barrier coatings. Based on these factors, we decided to investigate the use of TiN coatings.

Exposure Test #4: The samples used in Test #4 and the results of exposure are listed in Table 15. Several samples were coated with Ti/Ta nitride coatings in deposition Runs 51 and 52. We also included samples of conical ferrules (316 steel) used during the coating procedure as they too got coated. In both runs, several coupons were suspended in the fluidized bed simultaneously. Figure 19 shows a picture of the coated samples before they were exposed to simulated gasifier conditions at 900°C. The test was conducted for 316 h, after which the reactive gases were turned off and the furnace cooled to retrieve the samples for examination. Figure 20 is a photograph of the samples after exposure.

In each of the two coating runs used to prepare the samples, between four and six coupons were simultaneously suspended into the fluidized bed. We suspect that this procedure led to inhomogeneous coatings. The non-uniformity was visible even before exposure to reactive gases. It is instructive to note that the areas that show a high degree of nitride coating (gold color) are also the areas most resistant to corrosion.

Table 15. Substrates and coatings used in Test #4 and the results of exposure

Sample No.	Material	Coating Run	Appearance
1	HR160	51	No visible degradation
2	I 800	51	Pools of molten product
3	SS410	51	Part of the surface is corroded; rest of the surface is normal
4	I 625	51	No apparent degradation
5	I 82	51	Badly corroded; beads of molten product
6	SS405	52	Part of the surface is corroded; rest of the surface is normal
7	SS316 (porous)	52	Thick film of corroded product
8	HR160	52	No apparent degradation
9	Ferrules (SS316)	51	Corroded
10	Ferrules (SS316)	52	No visible degradation

These results indicate that the Ti/Ta nitride coatings are generally satisfactory on alloys such as HR160 and I625 (samples #1, #4, and #8). The results with steels containing Cr (samples #3 and #6) indicate that the coatings are not uniform. As indicated earlier, some of the areas in these samples may not have had uniform coatings and may have been degraded, while the coated areas were protected. The Ni-containing steel samples (#2, #5, and #7) were badly corroded, indicating that the presence of Ni in the alloy may hinder the diffusion of Ti into the sample. However, the results with sample #10 that appeared to have no visible degradation indicate that, under some conditions, the Ni-containing steels may be coated with a protective coating.

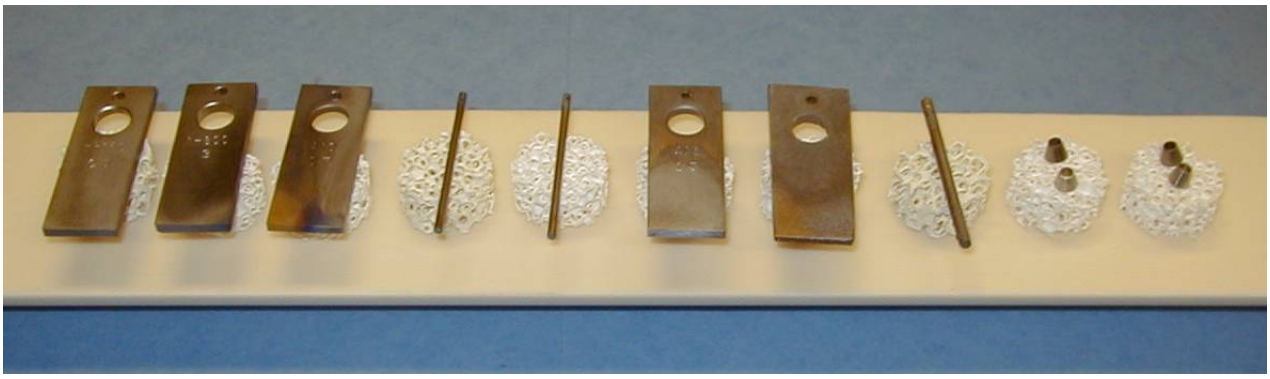

Figure 19. Samples used in Test #4 prior to exposure.

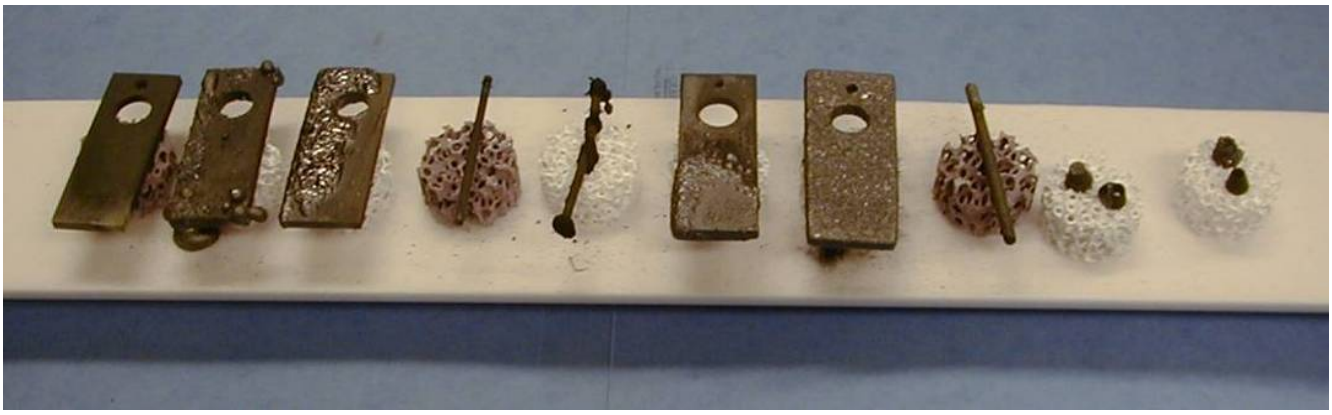

Figure 20.Samples after exposure to a simulated coal gas stream for 316 h at 900°C in Test #4.

Exposure Test #5: The results from this series are described in a section titled "Exposure of Uncoated Metals and Alloys to a Simulated Coal Gas Environment."

Exposure Test #6: The objective of this test was to determine the effect of long time (500 h) exposure to steel samples coated with either Ti/Ta nitride or Cr/Al coatings. The test was designed to examine coupons after exposure for about 100 h, and to then continue exposing those that showed good performance for an additional 400 h.

The samples used are listed in Table 16. In an earlier run (Test #5), we had observed that a Co metal sample had melted and flowed down. We wanted to make sure that the sample had not simply fallen off the alumina support during the loading, and so we included it again in this run. This time we ensured that after the samples were loaded in the oven, the Co slug was still on its alumina perch.

Figure 21 shows photographs of these samples before exposure. The inhomogeneity of the coating on samples #5 (SS304, TiTa-N), #7 (SS409/CrAl-Al), #8 (SS409/CrAl-oxAl), and #10 (HR160/TiTa-N) can be seen in the photograph. Figure 22 shows the results after exposure for 122 h. As is evident, the Co sample (Sample #1) was again found to have melted and flowed through the support. The TiN-coated SS409 steel tube (Sample #2) showed evidence of corrosion at the cut ends, but not on the tube sides. The 409 steel coated with Cr-Al (Sample #3) showed no signs of corrosion, but the similarly coated samples of SS 410 alloy and porous SS 316 alloy, which were also coated with Cr-Al, were badly corroded. These samples were removed, and the remaining samples were reloaded into the oven and exposed for an additional 360 h, bringing the total exposure to 482 h. Figure 23 is a photograph of the samples after exposure to 482 h.

The difference between samples #3 and #4 (SS409 and SS410), both of which were coated in the same run, is remarkable. Sample #3 showed only a few beads that may have resulted from pinhole imperfections in the coating, whereas sample #4 is completely corroded.

This difference can be ascribed to the presence of carbon in SS410. Evidently, carbon binds to the Cr and interferes with the formation of a diffusion coating. Similarly, Ni (which is present in 300-series steels) also interferes with our coating procedures.

The HR160 and SS409 alloys coated with either a Cr/Al composition or Ti/Ta nitride suffered minimal degradation. However, only sample #8, which was coated with Cr/Al-oxAl composition, showed no degradation after 482 h exposure.

Table 16. Substrates and coatings used in Test #6 and the results of exposure

Sample No.	Material	ID 1	Coating (Run)	Salient Observation
1	Cobalt	lump	none	Melted and flowed
2	SS409	tube	TiN (53)	Corrosion at tube edge
3	SS409	03	Cr-Al (54)	Some beads
4	SS410	03	Cr-Al (54)	Corroded
5	SS304	01	Ti/TaN (56)	In homogeneous coating; corrosion where coating was poor
6	SS409	04	Ti/TaN (56)	Same as #5
7	SS409	07	Cr-Al-Al (57)	Badly corroded
8	SS409	12	Ox. CrAl-Al (59)	No corrosion
9	SS316	Porous	Cr-Al-Al (61)	Badly corroded in 122 h
10	HR160	09	(Ti/Ta)N (60)	Some flakes, otherwise good

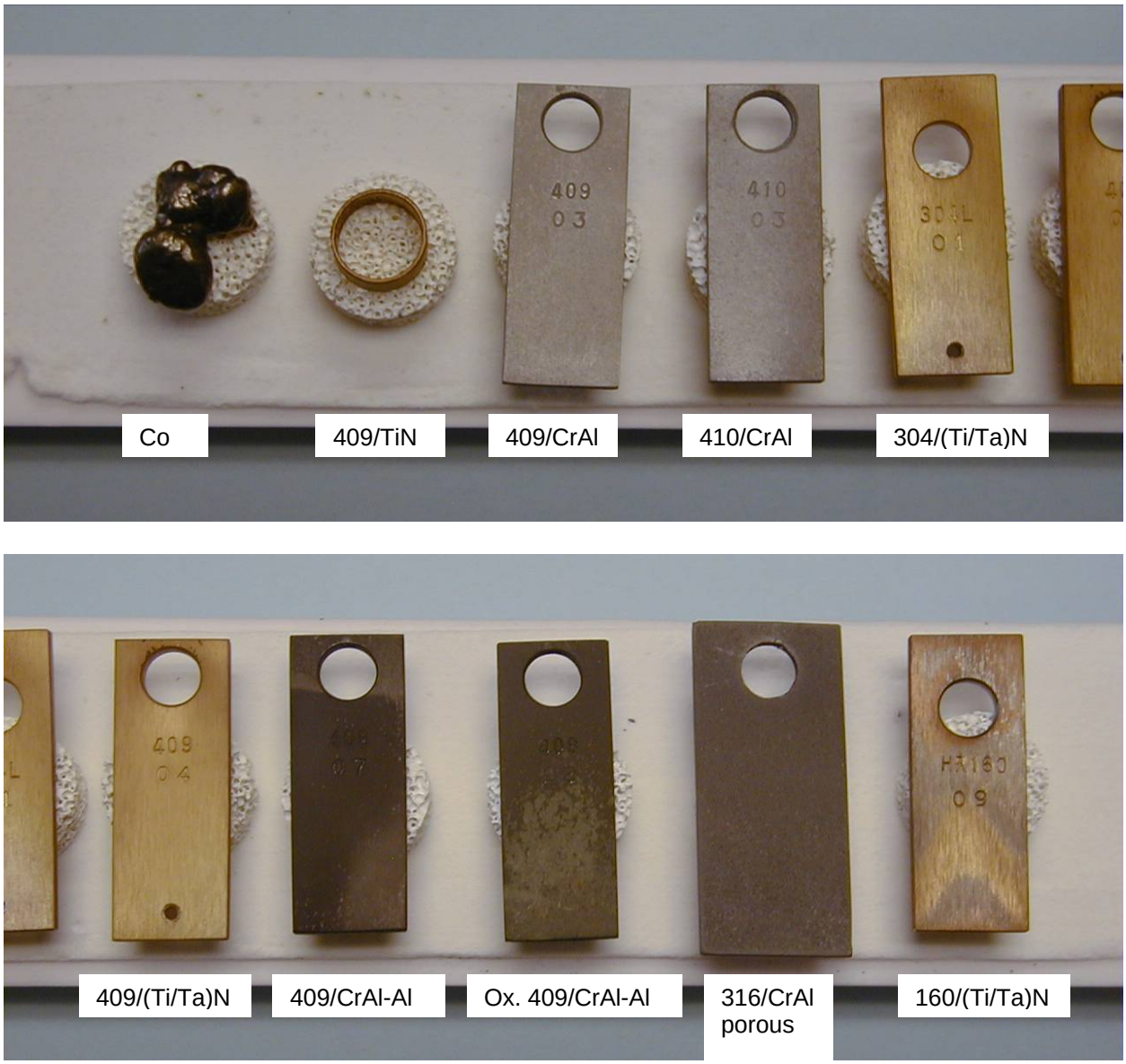

Figure 21. Samples used in Test #6 prior to exposure.

Figure 22. Samples after 122 h exposure to a simulated coal gas at 900°C in Test #6. (Note specs around the HR160 sample).

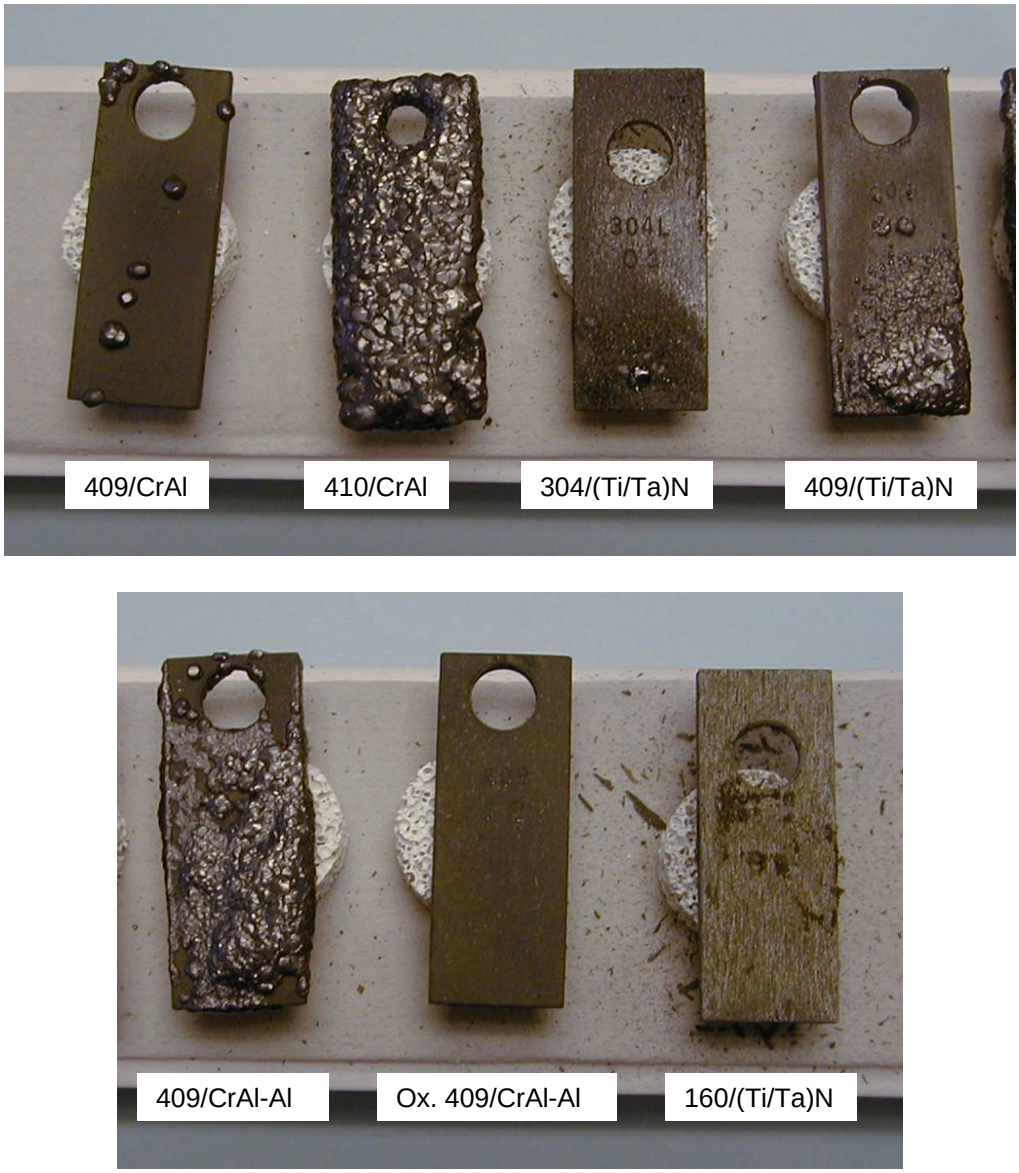

Figure 23. Samples after exposure to a simulated coal gas at 900°C for 482 h in Test #6. (Note beads on SS409/CrAl; CrAl coating on SS410 did not survive.)

Exposure Test #7: Although earlier tests showed that nitrided coatings offer significant protection against corrosion, they also revealed a lack of uniformity in the coatings. We improved the coatings procedure, as well as the fluidized bed reactor and its heater.

The samples used in Test #7 and the results of exposure are listed in Table 18. We focused on samples coated with Ti nitride from several deposition runs with an attempt to get uniform coatings. To see the effect of surface morphology, we sand-blasted a sample of SS409 coupon (#14) and coated it alongside another coupon that was not sand-blasted (#14). We also included a porous SS316 sample coated with (Ti/Ta) nitride to see if this coating would fare better than the previous attempts with Ti/T nitride (Exposure Test #4) or the oxidized Cr/Al-Al coating (Exposure Test #6). Figure 24 shows the picture of the coated samples before and after they were exposed to

simulated gasifier conditions at 900°C. The test was conducted for 96 h, after which the reactive gases were turned off and the furnace cooled to retrieve the samples for examination.

Table 17. Substrates and coatings used in Test #7a and the results of exposure

Sample No.	Material	Coating/ Run	Appearance
1	HR160 – 08	TiN/64	Some discoloration
2	Porous SS 360	(Ti/Ta)N/62	Badly corroded
3	SS410 – 06	TiN/65	Pinhole corrosion or bubbles from adjacent sample
4	SS409 – 12	Ox-Cr/Al-Al/ 59	No apparent degradation
5	SS409 – 13	TiN/63	Some corrosion, reverse side looks good
6	SS409 – 14	TiN/63	Some corrosion, reverse side looks good

Figure 24. Samples from Test #7a before and after exposure to simulated gasifier environment for 96 h.

We noticed that some of the samples in the run had different degrees of corrosion on the top and bottom surfaces, although most of them seemed to have survived well. We decided to continue exposing them to the gasification environment after flipping them over. Also, we removed the SS409-12 sample (coated with Cr/Al-Al, oxidized) that had survived over 500 h under the gasifier conditions with no signs of corrosion. We added a sample of TiN-coated SS405 that was recently prepared (run 66). Table 19 lists the samples that were exposed in the continuation of this run (Test #7b).

Table 18. Substrates and coatings used in Test #7b and the results of exposure

Sample No.	Material	Coating/ Run	Appearance
1	HR160 – 08	TiN/64	Survived. Minimal corrosion at edges.
2	SS409 – 13	TiN/63	Lots of signs of corrosion.
3	SS409 – 14	TiN/63	Only edges corroded.
4	SS410 – 06	TiN/65	Only edges show corrosion.
5	SS405 – 17	TiN/66	Badly corroded.

By and large, these samples seemed to have fared well (Figure 25). The HR160 sample had minimal corrosion. The pair of SS409 samples showed the effect of sand-blasting. There was less corrosion on the sand-blasted sample. This fact, together with the observation that corrosion is often limited to the edges, suggests that morphological stresses may be a contributing factor in corrosion. The SS405 alloy sample showed extensive signs of corrosion. We have previously noted that the presence of Ni in the alloys such as the 300 series stainless steels interferes with the formation of the diffusion barrier coating. The result with SS405 suggests that the presence of carbon in the alloy also interferes with the coating process. Only SS 409 alloy, which has extremely low carbon, appears to be amenable to protection by our coating process.

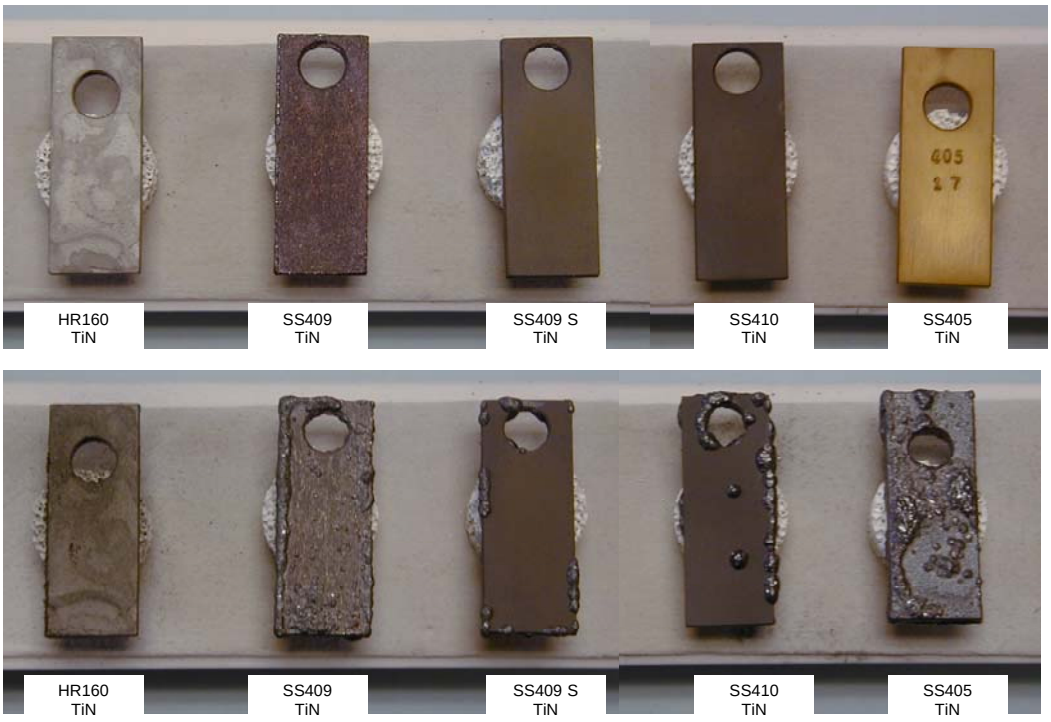

Figure 25. Samples from Test #7b before and after exposure to a simulated coal gas for 240 h.

Exposure Test #8: The results from this series are described in a section titled "Exposure to a Simulated Coal Gas at 370°C."

Exposure Test #9: We performed additional coating runs with Ti, Ta, Al, Si with subsequent nitridation. The top panel of Figure 26 shows the picture of the samples before they were exposed to simulated gasifier conditions at 900°C. The bottom panel is a photograph of the samples after exposure after 306 h. Table 20 lists the samples, the specific coatings, and some general observations.

Figure 26. Samples before and after exposure for 306 h at 900°C to a simulated coal gas in Test #9a.

Table 19. Substrates and coatings used in Test #9 and the results of exposure

Sample No.	Material	Coating	Run	Appearance	% Wt. Gain
1	HR160	(Ti/Ta)N,	64	No significant attack	-1.12%
2	HR160	TiN,	64	No significant attack	-0.31%
3	SS410	(Ti,Al)N,	79	Severe attack, sulfide deposit	34.05%
4	SS405	(Ti,Al)N,	80	Severe attack, sulfide deposit	30.12%
5	SS409	(Ti/Ta)N,	81	Severe attack, sulfide deposit	34.20%
6	SS409	(Ti,Al,Ta)N,	82	Severe attack, sulfide deposit	8.39%
7	SS410	(Ti,Si)N,	84	Severe attack, sulfide deposit	44.72%
8	SS410	(Ti,Si)N,	89	No significant attack	0.73%
9	SS410	TiN,	90	Severe attack at the edges	13.33%

As is evident from Figure 26, most of the samples gained in weight substantially and showed signs of significant sulfidation attack; only the two HR-160 coated samples, and a 410 steel that was coated with (TiSi)N appeared to survive well. These three samples were put back into the furnace and exposed to a simulated gasifier environment for an additional 100 h. Figure 27 shows their appearance before and after this second round of exposure. A significant amount of corrosion was evident on both HR160 alloy and the coated 410 alloy.

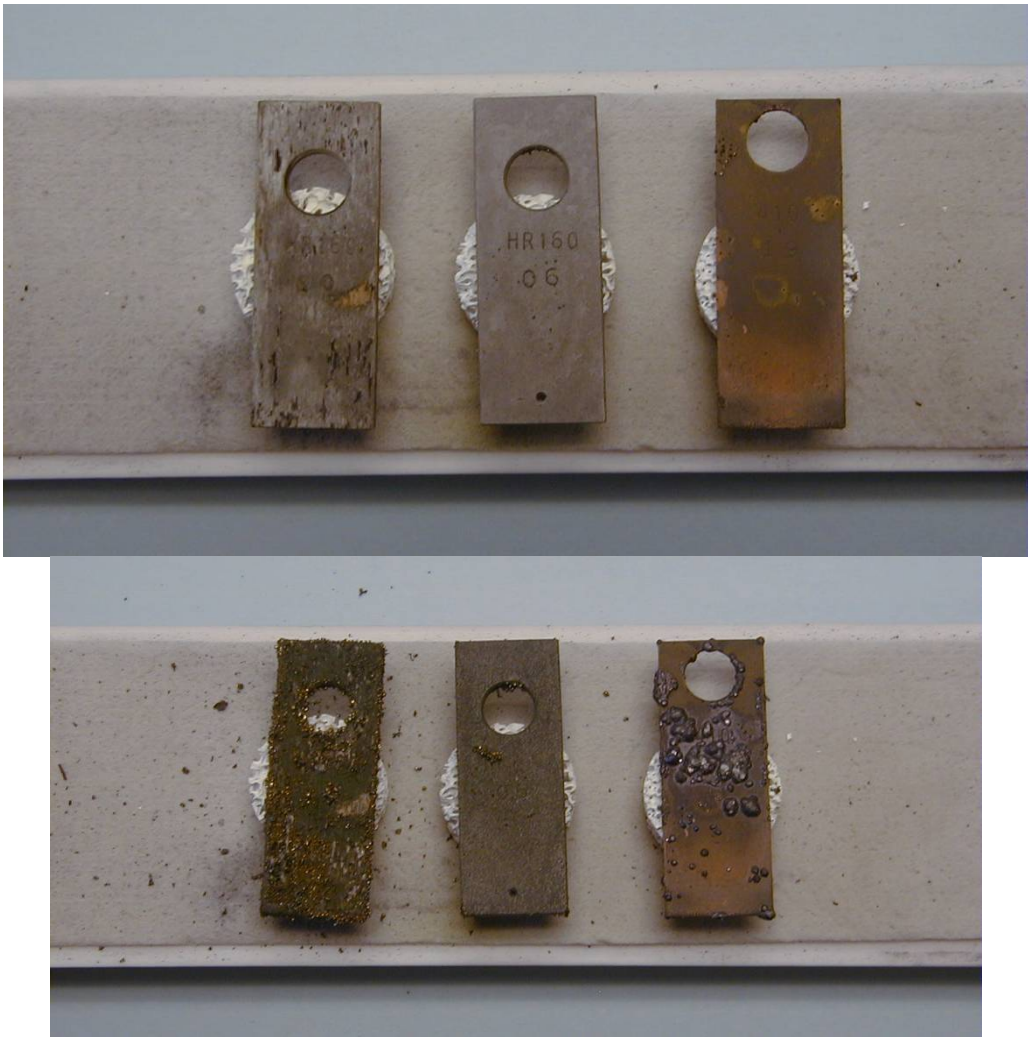

Figure 27. Samples before and after exposure for 100 h at 900°C to a simulated coal gas in Test #9b.

Exposure Test #10: In this test, we continued to test the effectiveness of nitrided coatings. The top panel of Figure 28 shows a picture of the samples before they were exposed to simulated gasifier conditions at 900°C. The bottom panel is a photograph of the samples after exposure after 308 h. Table 21 lists the samples, the specific coatings, and some general observations.

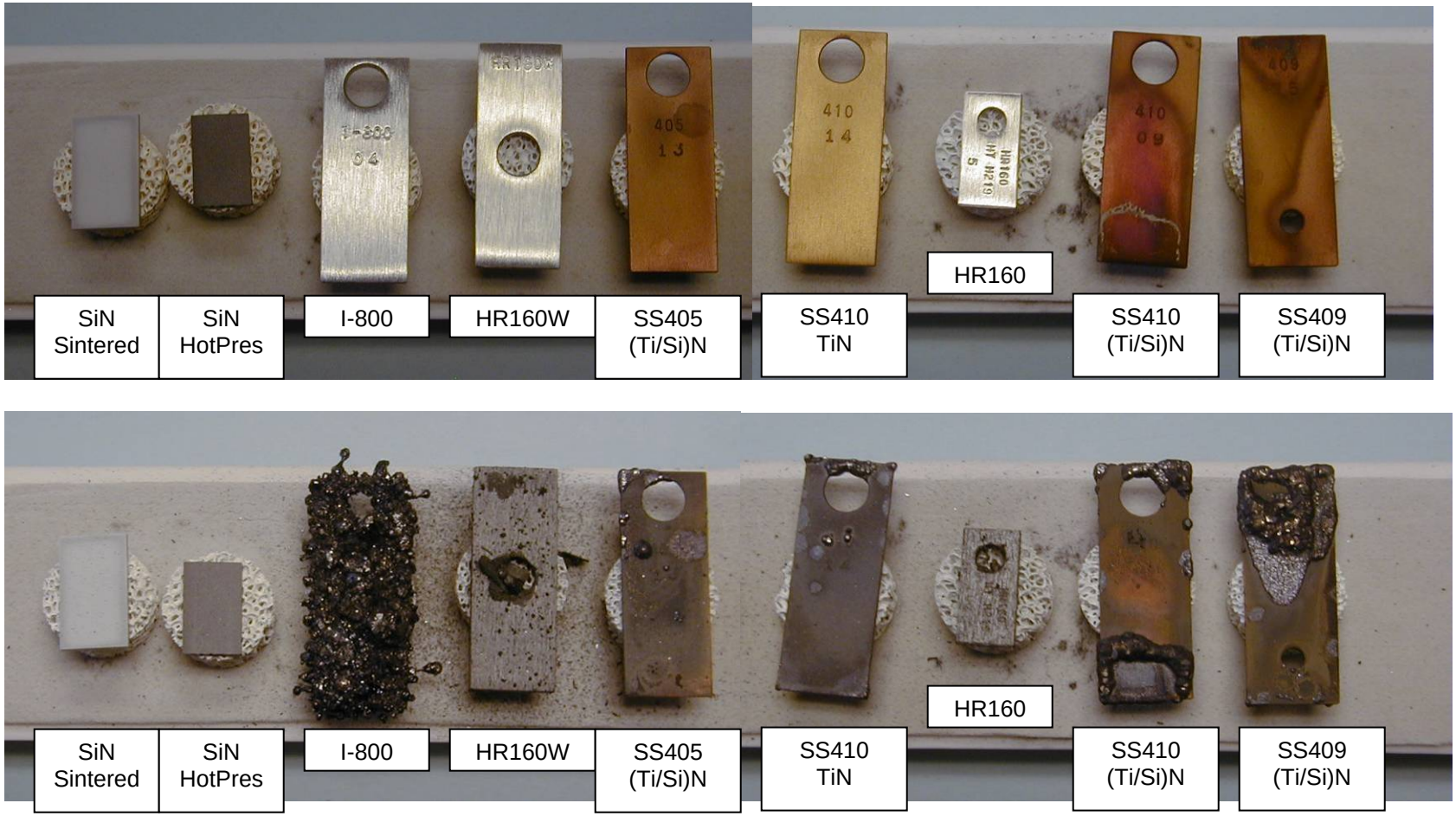

Figure 28. Samples before and after exposure for 308 h at 900°C to a simulated coal gas in Test #10.

Table 20. Substrates and coatings used in Test #10 and the results of exposure

Sample No.	Material	Coating	Run	Appearance	% Wt. Gain
1	Si_3N_4 (sintered)	None	-	No attack	0.00
2	Si_3N_4 (hot pressed)	None	-	No attack	-0.03
3	I 800	None	-	Severe attack, friable sulfide deposits; could not weigh	
4	HR-160 W	None	-	Some flakes, and corrosion at the drill hole	-1.20
5	SS405	(Ti/Si)N	89	A few localized spots of sulfide	3.22
6	SS410	TiN	90	Localized sulfide growth	3.16
7	HR-160	none	-	Looks fine	-0.35
8	SS410	(Ti/Si)N	91	Sulfide deposits along certain lines	10.58
9	SS409	(Ti/Si)N	92	Significant sulfide growth in one region	12.92
10	SS316 (p)	(TiAl)N	78	Badly corroded	19.07

This batch included two samples of silicon nitride. One of them was reaction-sintered material, and the other was hot pressed and highly dense. Neither sample showed any sign of sulfidation attack or mass loss, indicating that the formation of SiO or SiO(OH)2 was negligibly small under the tested conditions.

The third sample was a coupon of an Inconel alloy. This sample was severely corroded. There was a friable deposit (mostly FeS, as determined by XRD deposit all over the sample, and it adhered to the disc of porous alumina on which it was resting. The test also included two samples (#4 and #7) of another specialty alloy, HR-160. One of these (#4) was of the welding grade, and it developed some flakes. Both these samples lost a mall amount of their weight, possibly from the loss of CoS, but they otherwise maintained their integrity. This result is in contrast to the fate of the HR-160 coupon in the actual gasifier stream, discussed below, which underwent extensive corrosion/erosion.

The remaining four samples were various 400 grade steel coupons coated with TiN or (Ti/Si)N. The amount of corrosion varied in these samples and was mostly evidenced as deposits of FeS. The corrosion was not uniform on the sample, but seemed to be localized in certain regions. In Samples #8 and #9 the corrosion occurred where the coatings were visibly defective.

EXPOSURE TO A SIMULATED COAL GAS AT 370°C

Exposure Test #8: We tested coated alloy coupons under conditions designed to mimic the conditions in the filter unit after the high-temperature heat recovery unit (HTHRU). The filter unit is another important area where corrosion has caused unscheduled downtime, and the remedy has been the use of sintered porous metal tubes made of expensive alloys such as Inconel. The objective of our test was to determine if those coatings on 400-series steel that were not able to withstand the harsher conditions of the HTHRU, may be sufficiently resistant for use in the filter unit, at the reduced temperatures. Indeed, many of our coatings survived well; the exceptions were the coated porous samples of SS316.

We used pairs of SS405, 409, and 410 samples that had diffusion coatings of Cr and Al. Some of the coupons were sand blasted prior to coating to remove any remaining oxide layer on the surface of the coupon. A few coupons, after coating, were oxidized slowly to form a protective layer of Al_2O_3 on the surface of the coating. Also included were SS409 samples coated with TiN and TiAl)N, as well as some porous SS316 samples coated with (Ti/Ta)N and (Ti/Al)N. The samples used in Test #8 and the salient observations following the exposure test are listed in Table 21.

The top panel of Figure 28 shows the picture of the coated samples before they were exposed to simulated gasifier conditions at 370°C. The bottom panel is a photograph of the samples after exposure for a period of 300 h.

Table 21. Substrates and coatings used in Test #8 and the results of exposure

Sample No.	Material	Coating	Run	Appearance	% Wt. Gain
1	SS405	(Cr-Al)Al	72	Good, some discoloration	0.25
2	SS405	(Cr-Al)Al	72	Good, some discoloration	0.10
3	SS409	(Cr-Al)Al	76	Good, like new	0.00
4	SS409	(Cr-Al)Al	76	Good, like new	0.00
5	SS410	(Cr-Al)Al	73	Good, some discoloration	0.17
6	SS410	(Cr-Al)Al	73	Good, some discoloration	0.04
7	SS409	TiN	68	Good	0.07
8	SS316 (porous)	(TiTa)N	62	Corroded, darkened	11.86
9	SS409	(TiAl)N	77	Smooth, like new	0.03
10	SS316 (p)	(TiAl)N	78	Badly corroded	19.07

As is evident from Figure 29, all the coatings except those on the porous SS316 sample performed well. The two SS316 samples gained significant weight indicating extensive sulfidation of the coupon. All other samples also gained only minimal weight (<0.3 wt%). Examination of the weight gained (Table 1) shows some differences between these samples and points to SS409 alloy as the best substrate for these diffusion barrier coatings.

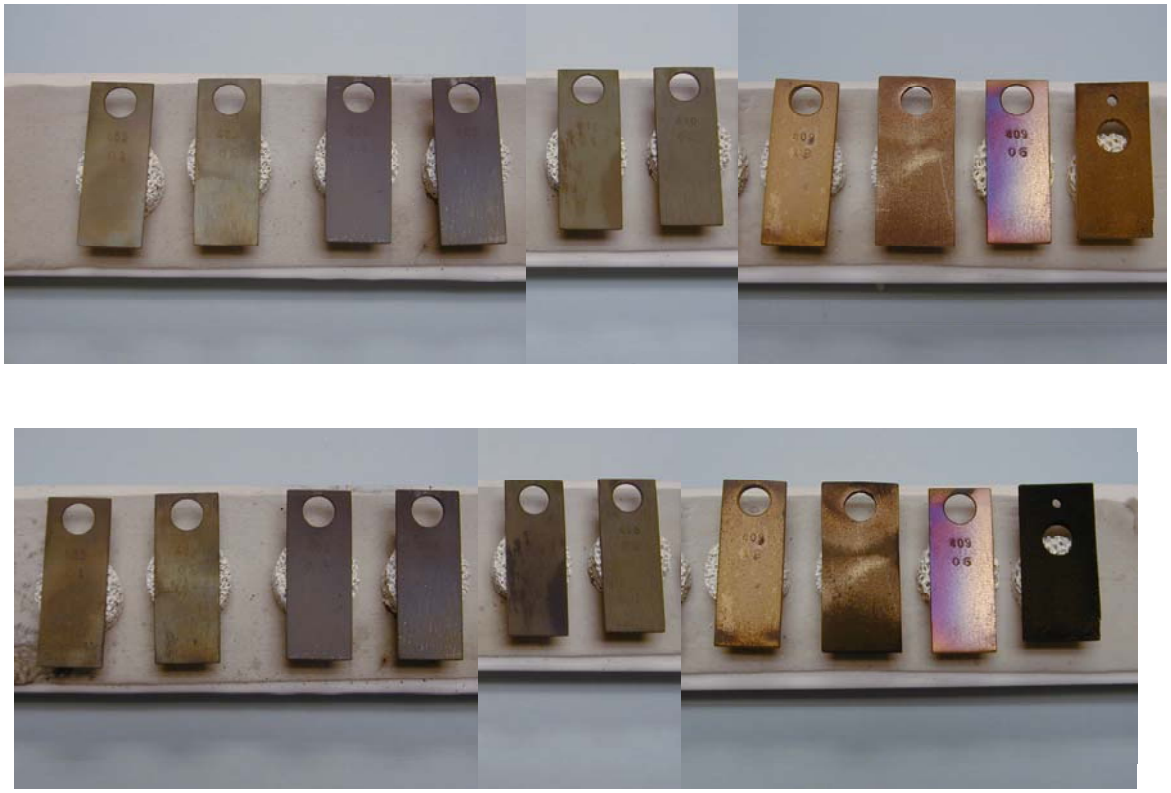

Figure 29. Samples before and after exposure to a simulated coal gas for 300 h at 370°C in Test #8.

Exposure Test #11: The purpose of this test was to see if the porous SS409 coupons that we had previously fabricated could be coated in their interior so that they would survive the conditions under the filter unit conditions. Along with the Cr/Al oxide and TiN coated porous samples, we also put in a batch of SS409 and SS410 coupons coated with various nitride coatings. Table 22 lists the samples, the specific coatings, and some general observations. The top panel of Figure 29 shows the samples before they were exposed to simulated gasifier conditions at 370°C. The bottom panel is a photograph of the samples after exposure after 300 h.

Table 22. Substrates and coatings used in Test #11 and the results of exposure

Sample No.	Material	Coating	Run	Appearance	% Wt. Gain
1	SS410	(TiSi)N	84	Virtually unchanged	1.43
2	SS409	(CrAl)Ox, porous	88	Virtually unchanged	0.23
3	SS409	TiSiN/TiAlN	92	Some bands accentuated	0.29
4	SS409	TiSiN/TiAlN, porous	93	Slightly lighter color	10.25
5	SS409	TiSiN/TiAlN	93	Virtually unchanged	0.02
6	SS410	TiSiN/TiAlN/TiAl	94	Virtually unchanged	0.20
7	SS409	TiSiN/TiAlN/TiAl	94	Virtually unchanged	0.03
8	SS409	TiSiN/W/TiAlN	95	Virtually unchanged	0.10
9	SS409	TiAlN/WTiAlN/W/TiAlN	96	Virtually unchanged	0.39
10	SS409	TiSiN/W/TiAlN	98	Virtually unchanged	-3.54
11	SS409	TiSiN/W/TiAlN	99	Virtually unchanged	0.23

All the samples looked almost exactly as before the exposure. At this relatively lower temperature, we did not expect any of the nitride coatings to show any corrosion. The only sample to gain significant weight was the TiN coated porous SS409 coupon (Sample #4). This weight gain is surprising because there was hardly any visible change. Following the exposure, cross sections of both of the porous samples were prepared and analyzed by SEM-EDX and XRF. Preliminary examination showed the presence of Ti on the interior surfaces in the depths of the porous sample, a clear indication of the ability of our fluidized bed process to deposit metals in the pores.

.

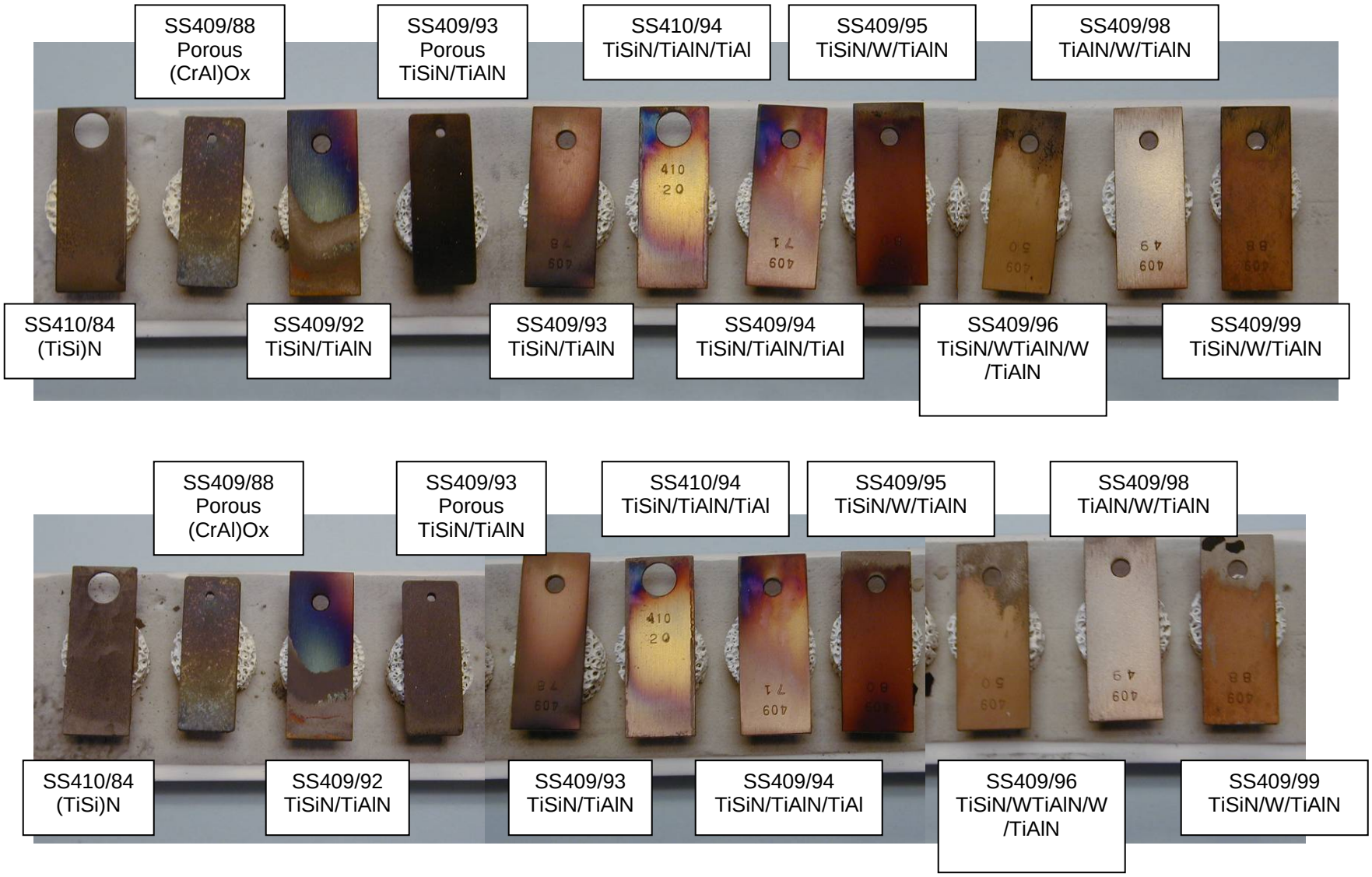

11

Figure 30. Samples before and after exposure to a simulated coal gas stream for 300 h at 937°C in Test #11.

DETAILED EXAMINATION OF COATED COUPONS BEFORE AND AFTER EXPOSURE TESTS

The exposure tests showed that the coatings of nitrides of Ti, Al, and Si may provide alloy steels significant resistance to sulfidation attack in simulated coal gas streams. In the bench scale tests, the coated coupons showed significant resistance in a gas stream containing H_2S (2%v/v) at 370°C while sulfidation attack occurred at 900°C. To understand the cause of sulfidation attack, we analyzed the coated coupons using SEM and EDX.

Composition Profile of a Nitrided Sample before Exposure Test

Figure 31 is a SEM picture of the cross-section of a SS 409 steel coated with titanium, silicon, and aluminum nitrides. As can be seen from the figure, the coating was uniform, adherent, and had a thickness around 7-8 μm. Figure 32 shows an EDX analysis of a line scan, and Figure 33 shows an elemental depth profile for Al, Si, Ti, Cr, Fe (values are normalized to 100% considering only these elements). Different zones are clearly distinguished: an external TiSiN layer followed by a TiAlN layer and a TiAl diffusion zone. The Si peak at the interface between the coating and the substrate is related to an intentionally added Si layer for a short time at the end of the TiAl diffusion step. The purpose of this addition is to provide inter-diffusion to increase adhesion and provide a thermodynamic sink to slow down the diffusion of Fe to the surface that is known to cause sulfidation under the operating conditions.

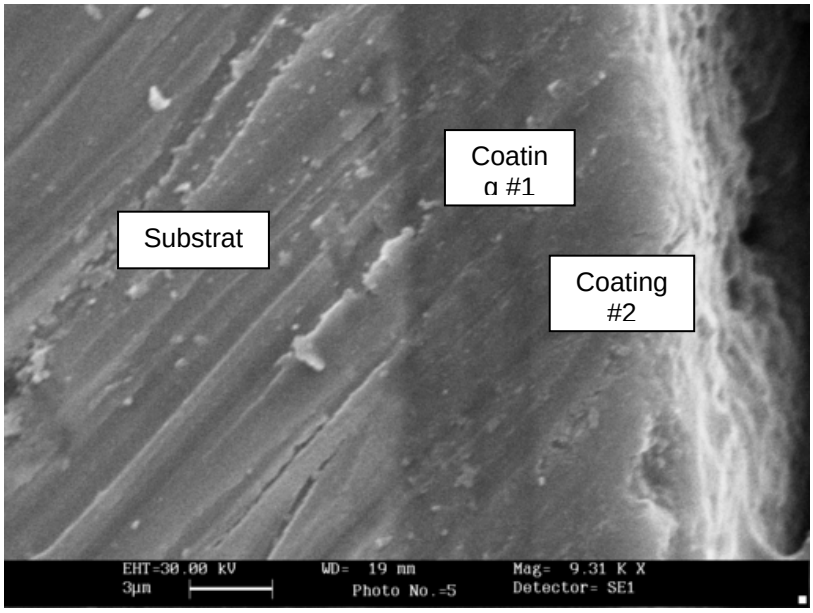

Figure 31. Cross section of a (Ti, Al, Si) nitride coating on SS 409 alloy steel.

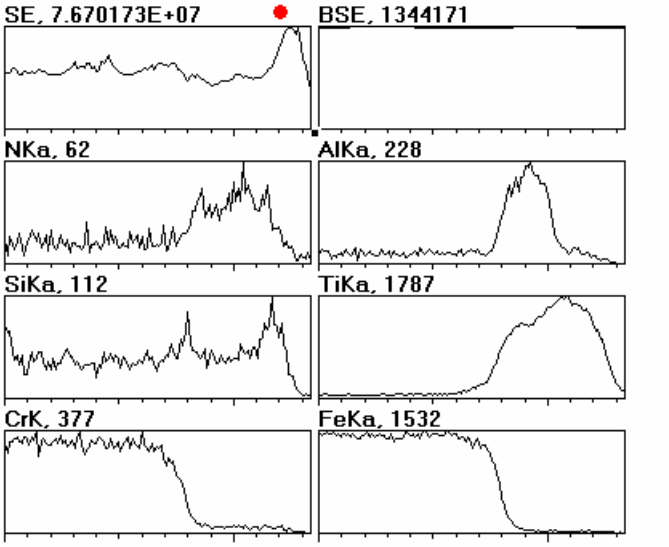

Figure 32. Elemental profile of the coating shown in Figure 31.

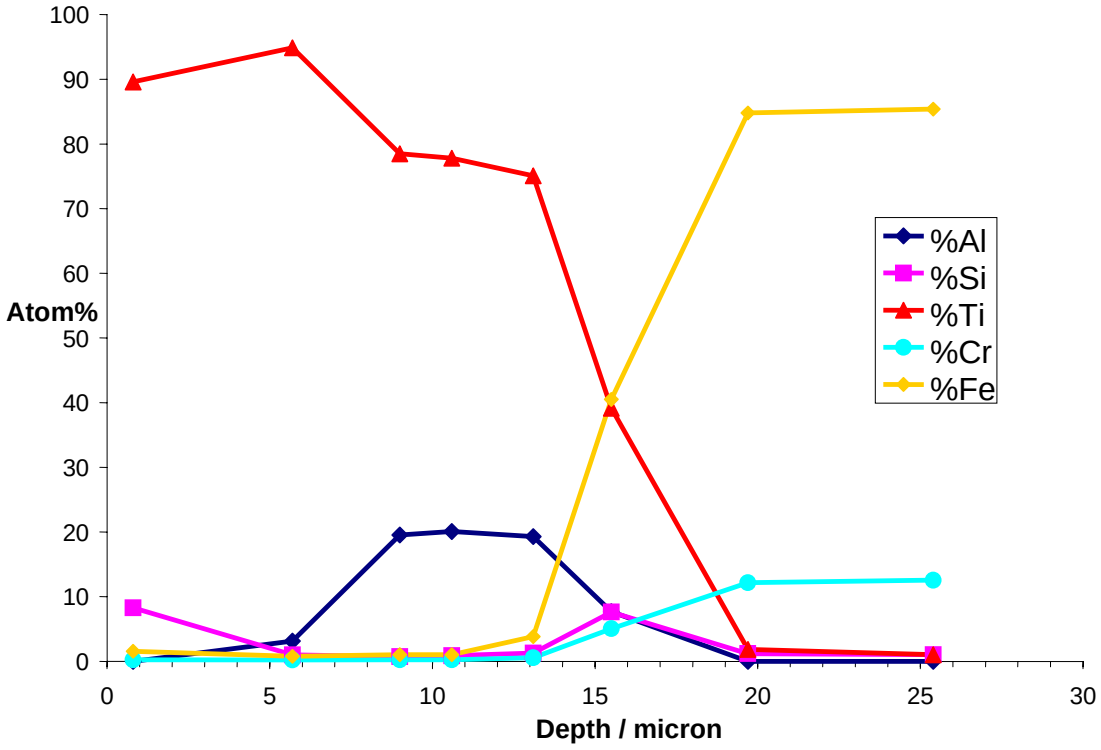

Figure 33. Depth profile of the elements in the coated specimen shown in Figure 31.

Composition Profile of a Nitrided Sample after Exposure Test

A sample of the coated alloy was exposed to a simulated coal gas stream containing H_2S at 900°C for 300 h. At the end of the exposure period, the coated sample showed significant sulfidation attack as evidenced by the formation of a scale and a weight gain of ~12%. The cross section of the coupon is shown in Figure 34. In the SEM photograph, the top section is the substrate, the middle section is the coated layer, and the bottom of the photograph shows the polymeric mounting. Figure 34 shows that, after exposure to the sulfiding gas stream, the coating layer has cracked, allowing H_2S to penetrate the coating and react with the substrate. The EDX analysis showed that the coating still contained Ti, as expected (Figure 35). However, it also shows the presence of Cr, which was not in the original coating. We believe that the Cr may have diffused along the pore surfaces to the outer boundary. The presence of Cr near the surface also indicates that the coating was adherent for some period of time, allowing the Cr to migrate through the coating layer. Alternatively, Cr may have diffused as an oxyhydroxide vapor species under the high-temperature, high-steam concentration environment. Additional studies are needed to clarify these issues.

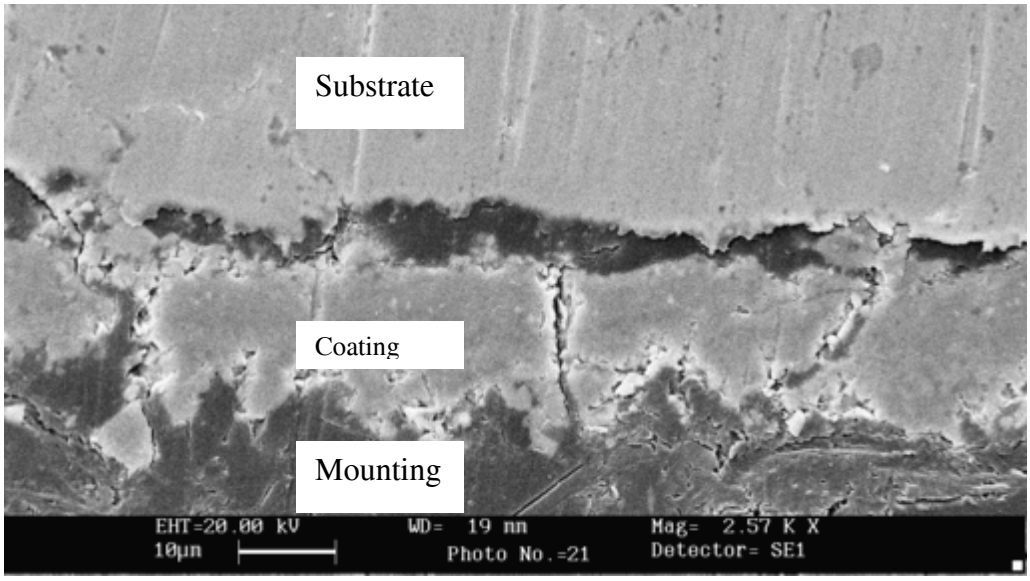

Figure 34. The cross section of a (Ti,Al,Si) nitride coated sample after exposure to a simulated coal gas at 900°C for 300 h.

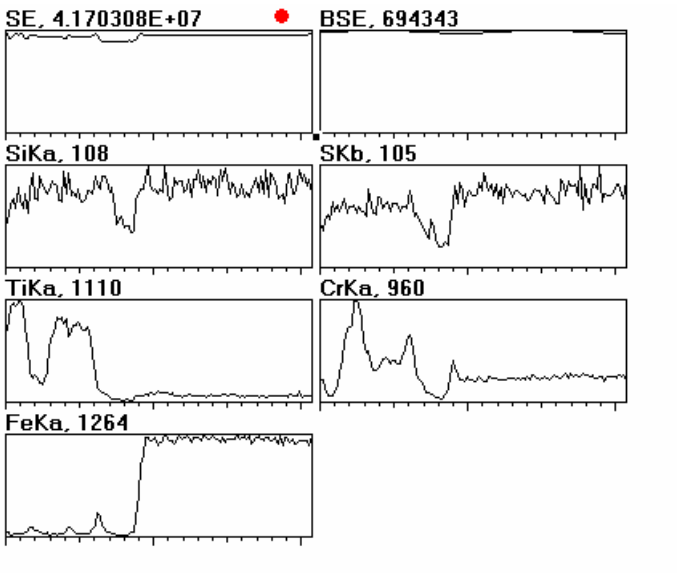

Figure 35. EDX analysis of the cross section of the sample area shown in Figure 34.

Composition Profile of a Nitrided Sample with Tungsten Barrier Layer

To eliminate the cracking of the coating and to prevent migration of the substrate elements to the outer surface of the coating, we deposited a layer of tungsten (W) on the substrate before the deposition of the (Ti,Al) nitride layer. Such layers are often used in the semiconductor fabrication as diffusion barriers. Note that we did not include silicon in this coating because Si can react with W to form tungsten silicide, which may not adhere to the substrate.

Figure 36 is a SEM photograph of the nitride coating with W diffusion barrier. In this picture, the top is the substrate, the middle is the coating, and the bottom is the specimen mount. The light, thin layer between the substrate and the coating is the W diffusion barrier. The (Ti,Al) nitride coating is homogeneous and free of cracks. The layered structure is clearly seen in the EDX analysis and the EDX elemental depth profile: the steel substrate, a diffusion layer (Ti,Al), a W layer and a TiAlN film on top. Figure 37 is the elemental profile of various elements in the vicinity of the coating. Figure 38 is the elemental profile of the coating. These profiles show that the coating layer consists of mainly Ti and Al species. Note that although the coating layer is nitrided, the N species are not shown in Figures 37 and 38 because the EDX is not sensitive to N atoms.

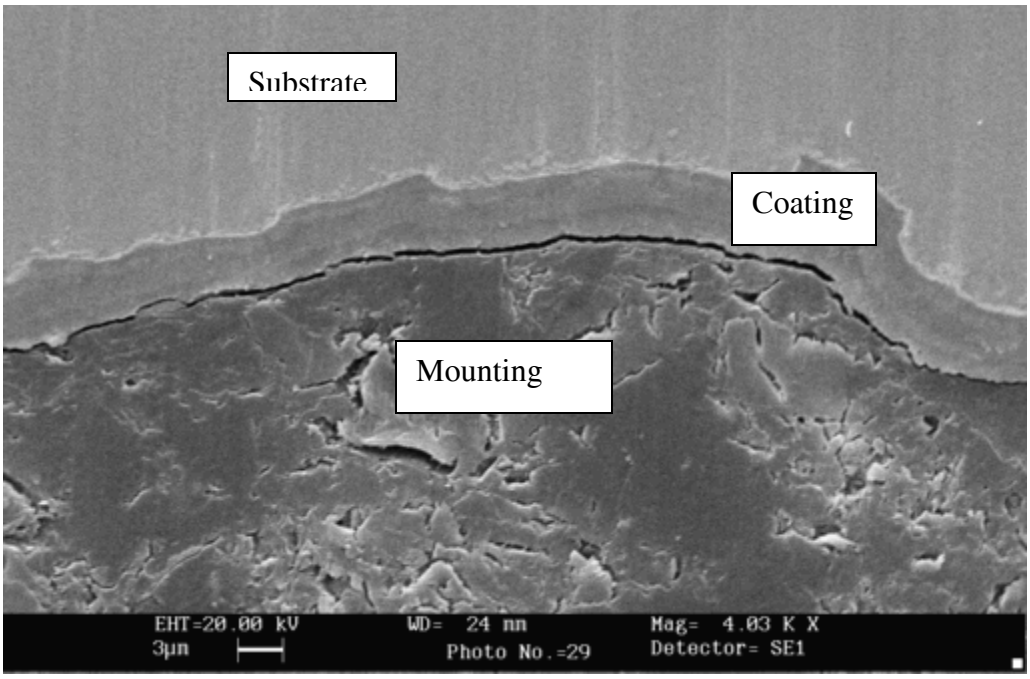

Figure 36. SEM photograph of a nitride coating on SS409 alloy with W diffusion barrier.

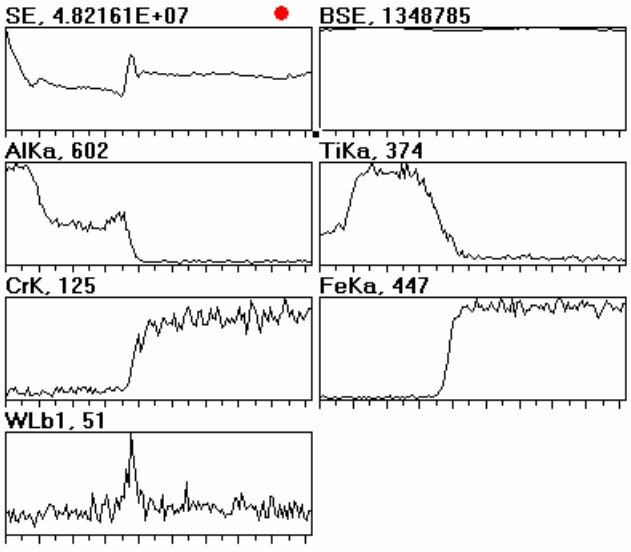

Figure 37. Elemental profile of the coating shown in Figure 36.

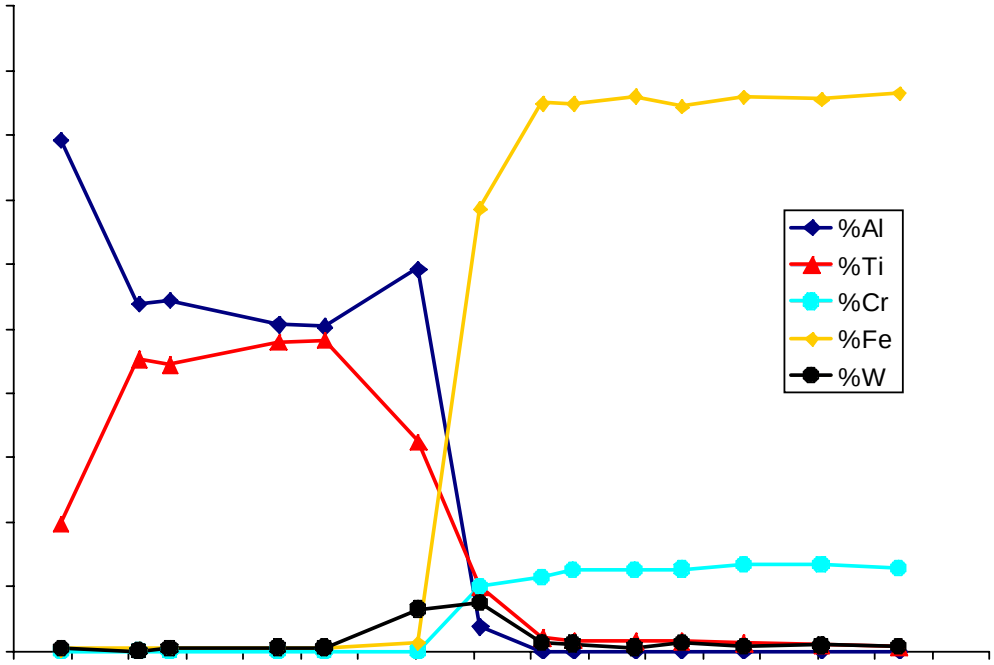

Figure 38. Profile of the elements in the coated specimen shown in Figure 36.

Characterization of Coated Porous Coupons: The uniformity of the coating inside a porous sample, similar to that of a stainless steel barrier filter, was also examined. A photograph of the cross section image, as observed by SEM, is shown in Figure 39. The photograph shows that the external part of the sample is more porous than the interior, an artifact from the sintering procedure. Figure 40 shows the SEM image of an enlarged area of the specimen (mounting polymer is the dark zone in the right). As can be seen from Figure 40, a homogeneous coating with a thickness around 2 to 3 μm was deposited. Figure 40 also depicts the result of an EDX analysis of a line-scan in that zone (analysis performed across the marked yellow line). As observed, Ti was deposited both in the external part of the sample (directly exposed to the fluidized bed) and in the internal part (exposed to one of the internal voids of the porous material). This is a good indication that infiltration of reactants to coat the internal surfaces of a filter is possible. The Al signal is remarkably higher in the external zone. This could be explained either by a lower $AlCl_3$ partial pressure in the gas phase or by a faster depletion of this reactant. As can be seen, Ti is again detected in all internal surfaces, but Al only found in the most external surface.

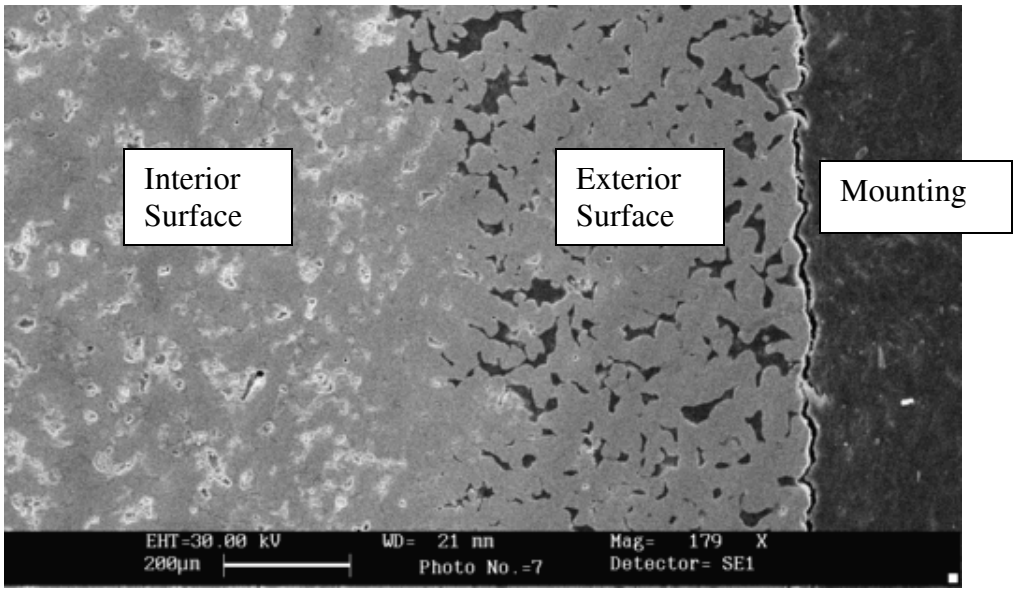

Figure 39. SEM photograph of a nitride coating on a porous SS409 alloy.

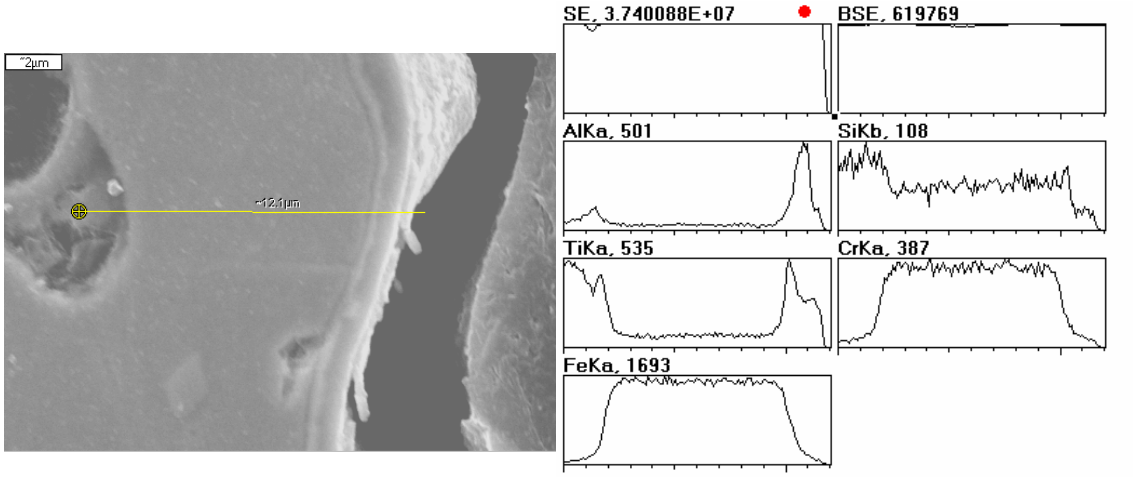

Figure 40. Magnified image of the exterior of the porous specimen and corresponding element profile.

Analysis of the Fractured Interior of a Nitrided Porous Sample

In Runs 93, 102 and 104, we coated porous SS409 samples with several combinations of Ti-based nitrides and diffusion barrier layers. Figure 41 shows a typical cross-section of the coated samples after intentionally fracturing them. This process results in less damage of the coating morphology than the traditional method of cutting, mounting and polishing. The porous structure is clearly observed. An enlarged view of an area corresponding to the bulk of the sample is presented in Figure 42. As observed, the coating is conformal and is typical in a CVD deposition process. A continuous and conformal coating is needed to provide good protection against corrosion to a sample with an irregular shape such as a filter.

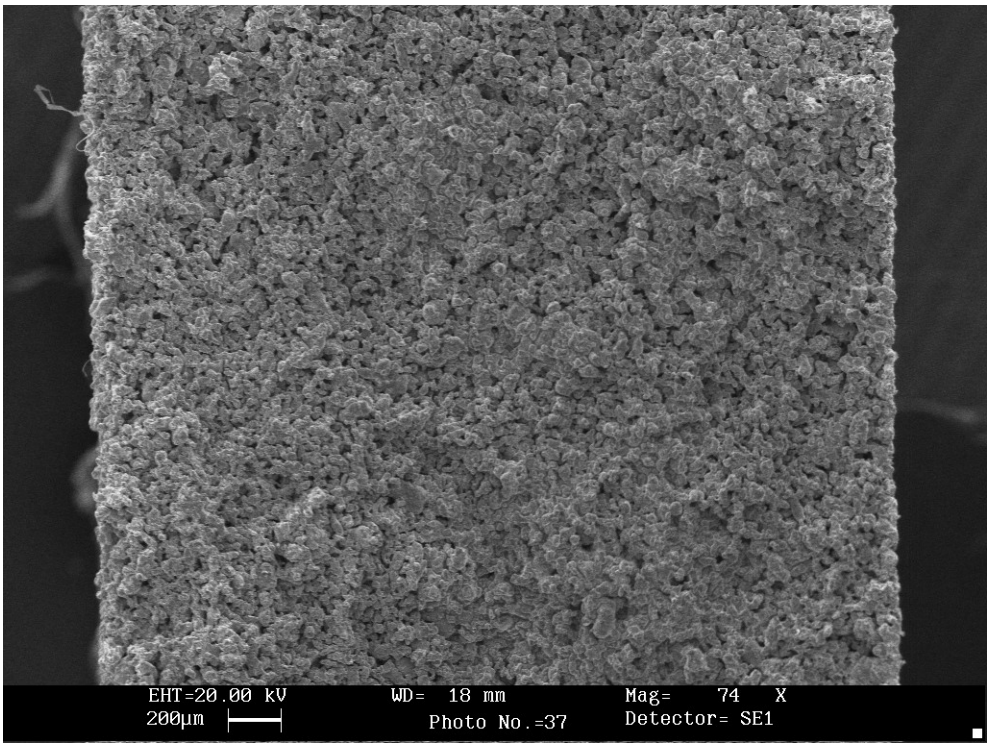

Figure 41. SEM cross-section view of a fractured sample (Run 102).

Figure 42 depicts a comparison of Ti depth profile in coupons from Runs 93, 102 and 104. In all cases, Ti concentration decreases progressively with depth, which means that the ceramic coating gets thinner as it gets inside the coupon. This was an expected feature, because $TiCl_4$ used for the deposition is consumed as the gas flows into the sample. The decrease in coating thickness with depth indicates that the bulk of the sample is prone to a corrosive attack. As can be seen in the plot of Figure 43, coating in the bulk of the sample is thicker in Runs 102 and 104 than in Run 93. As a consequence, it is expected that they suffer a lower corrosion rate in the test.

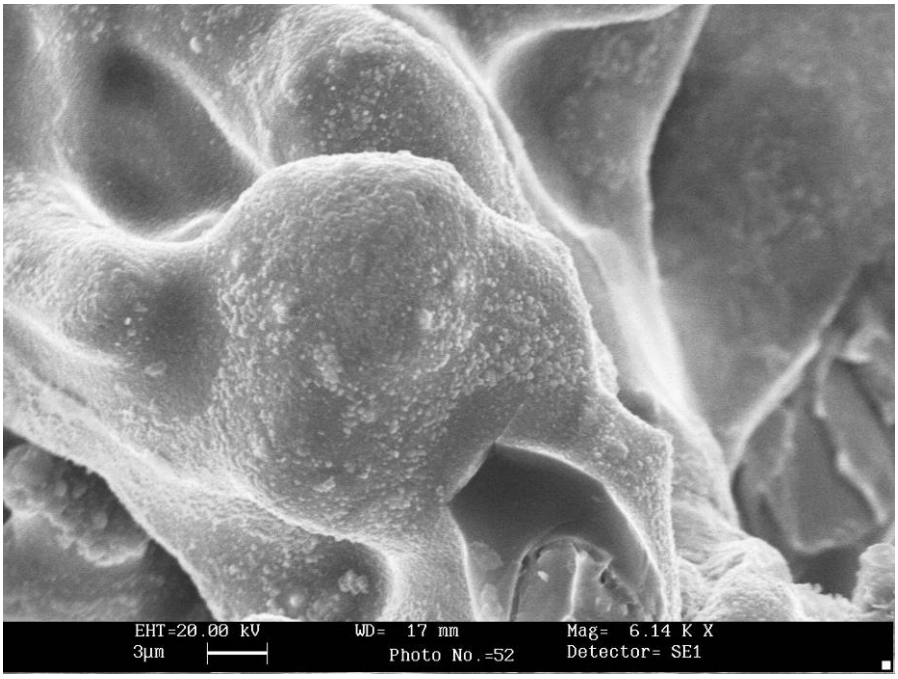

Figure 42. Enlarged view of a zone in Figure 5 (500 microns inside the bulk of the sample).

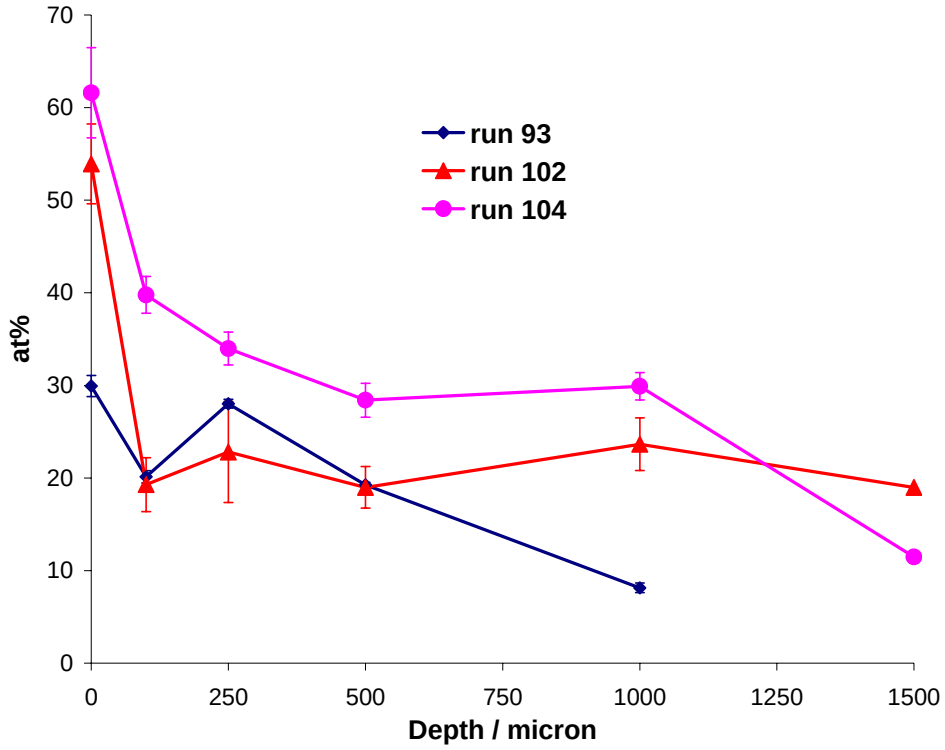

Figure 43. Evolution of Ti concentration with depth in the sample. EDX measurements were performed at different locations of the cross-section exposed after fracturing the sample.

Figure 44 shows two zones where, after fracturing the sample, a cross-section of the coating in Run 104 was exposed. In this area, a clean fracture took place and thus the thin Nb interlayer is clearly observed between the substrate and the TiAlN coating.

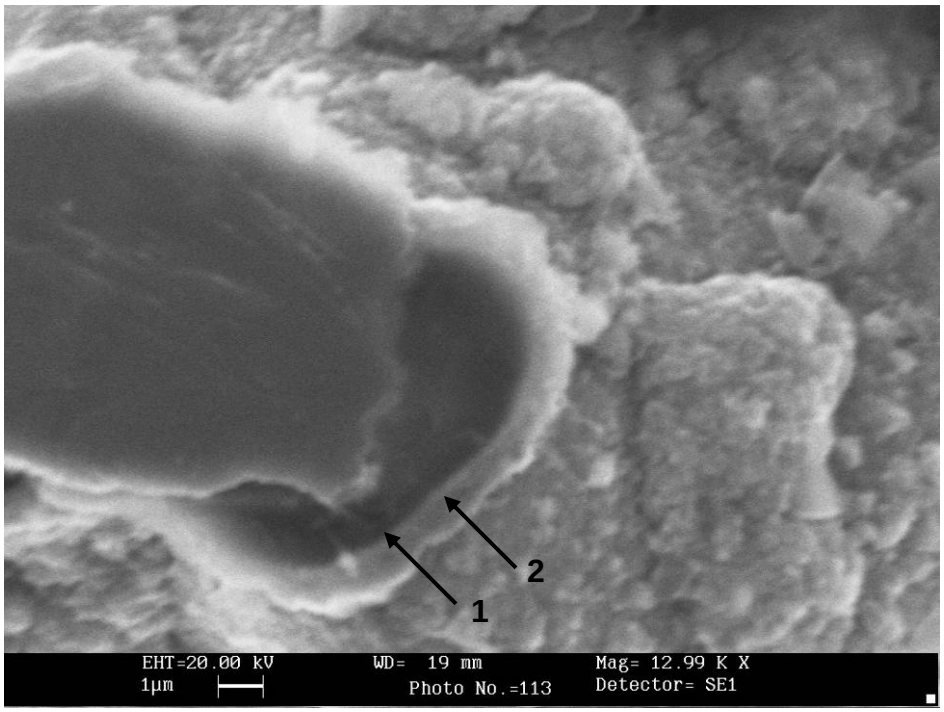

Figure 44. SEM view of a fractured zone (rUn 104, depth in the sample: 500 μm. The Nb layer (1) and the ceramic coating (2) are clearly observed.

Analysis of a Porous Nitrided Coupon after Exposure to a Simulated Coal Gas at 370°C

We examined a coated porous coupon after exposure to simulated coal gas at 370°C for 300 h. This sample from Run 93 was attacked in the corrosion test. We observed that iron sulfide scales that plugged the pores were formed in its bulk, but in the most external part of the coupon (close to the surface) the coating was protective and the porous structure was intact. As mentioned above, Runs 102 and 104 aimed for better corrosion resistance through improvement of the coatings at the bulk of the coupons. Figure 45 shows a picture of samples from Runs 102 and 104 before (left) and after (right) the corrosion test. The appearance of the samples suffered only minor changes during the test, but both suffered a weight gain: 5.1 % (Run 102) and 7.9 % (Run 104), slightly lower than what we found in Run 93 (10.3 %). However, a better estimation of the corrosion resistance requires observation of the bulk of the coupons, as discussed below.

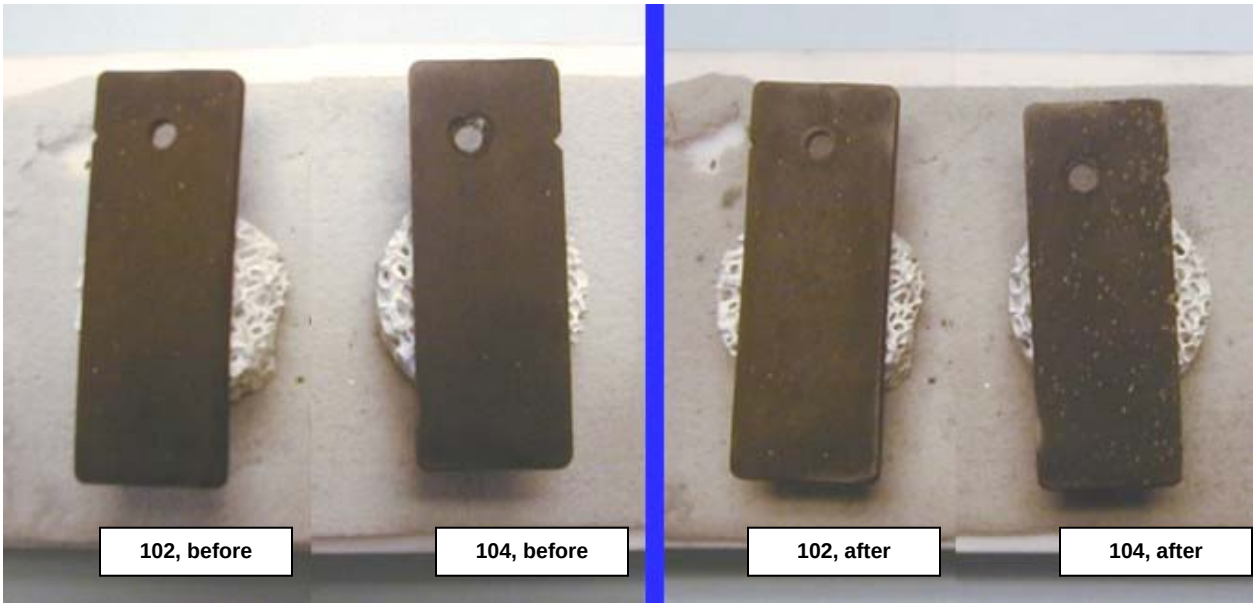

Figure 45. Samples before and after exposure for 300 h at 937°C in simulated gasifier test.

Figures 46, 47, and 48 show the cross-section views of fractured coupons from Runs 93, 102, and 104, respectively, after exposure for 300 h at 370°C. As can be seen in Run 102, we extended the zone where the coatings provided enough protection against sulfidation. It seems therefore that the protection of the full sample bulk could be achieved with longer deposition times. We observed that the sample containing a Nb-based interlayer has even higher corrosion resistance in the tested atmosphere. As shown in Figure 48, most of the sample survived the test and sulfide scales were only found in the most internal part of the coupon, as evidenced by the porosity in the interior of the specimen. Note the contrast in the morphology in the interior of the specimen in Run 93 (Figure 46) and the specimen in Run 104 (Figure 48).

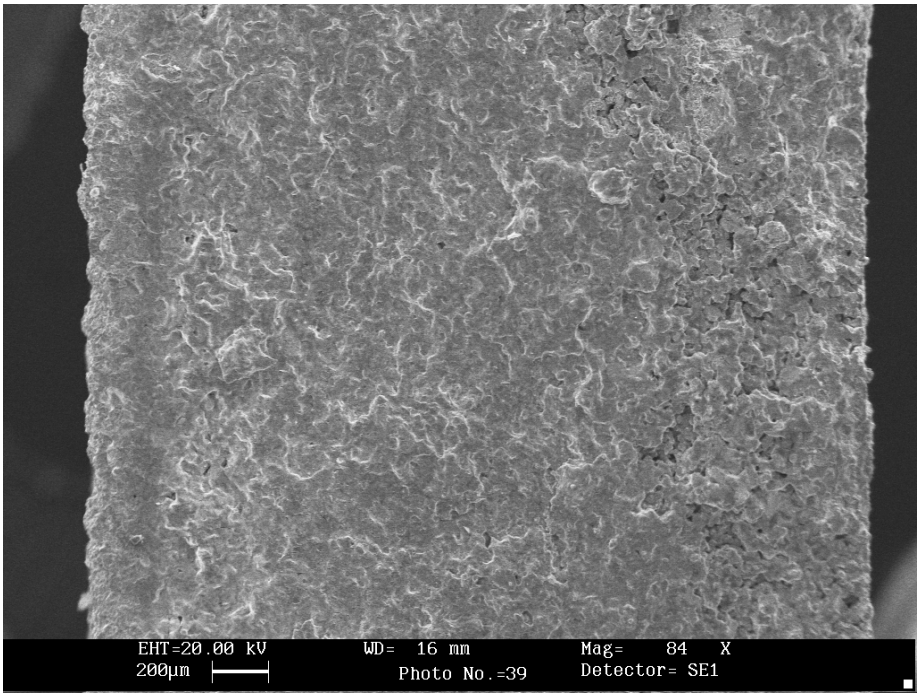

Figure 46. Cross-section of a fractured coupon from Run 93 after exposure for 300 h to the low-temperature corrosion test.

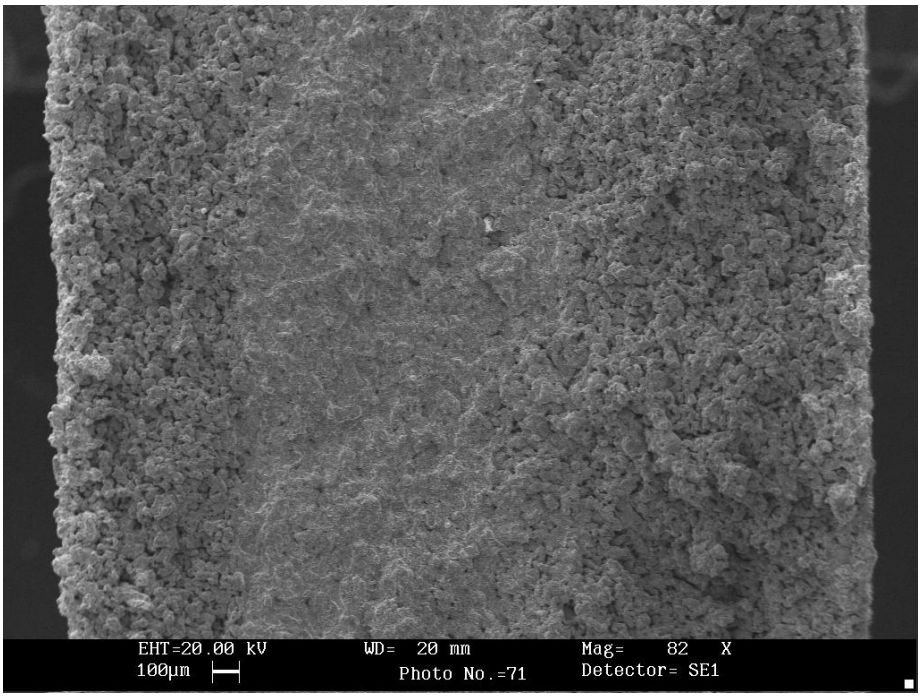

Figure 47. Cross-section of a fractured coupon from Run 102 after exposure for 300 h to the low-temperature corrosion test.

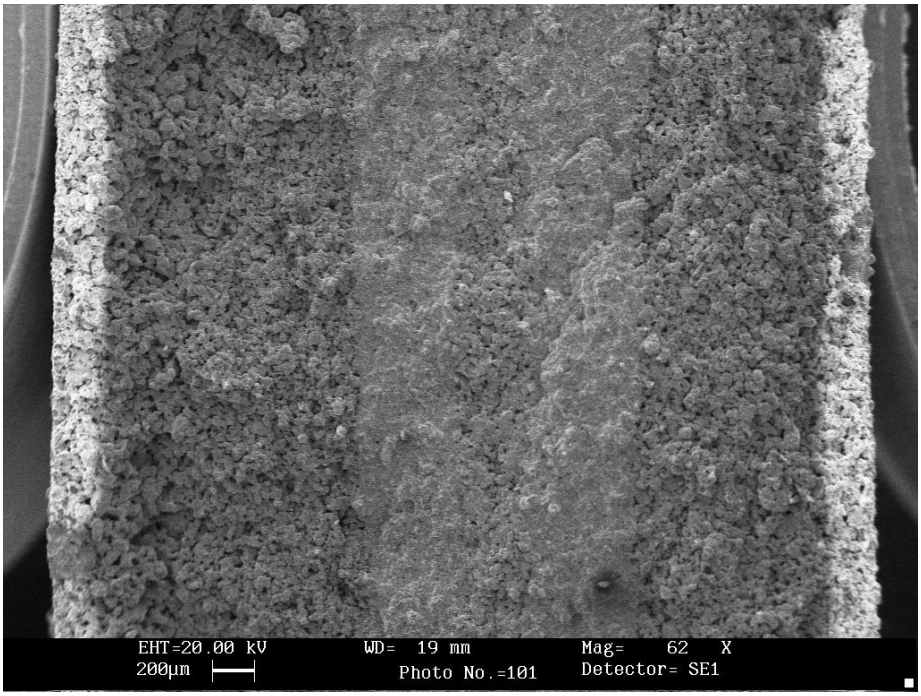

Figure 48. Cross-section of a fractured coupon from Run 104 after exposure for 300 h to the low-temperature corrosion test.

Analysis of a Porous Nitrided Coupon with a Diffusion Barrier after Exposure to a Simulated Coal Gas at 370°C

We analyzed solid coupons after a high-temperature corrosion test and found that inter-layers of metals such as Nb or W increase resistance to sulfidation attack in simulated coal stream gas. Several coated specimens containing a Nb barrier layer were prepared and the coating conditions are summarized in Table 23. As seen in Table 23, we found the highest weight gain during deposition in Run 109, indicating an overall thicker coating was deposited. This observation correlates with the lower weight gain measured during the simulated coal gas exposure, which indicates the lowest sulfidation degree of all exposed porous coupons.

Table 23. Deposition conditions (coating composition and deposition time), weight gain during both the coating process and the corrosion test.

Run	Diffusion Layer	Barrier Layer	Ceramic Film	Weight Gain % (coating)	Weight Gain % (Sulfidation test)
93	TiAl (6h)	-	TiAlSiN (7h)	2.4	10.3
102	TiAlSi (6h)	-	TiAlSiN (2.5h)	3.1	5.1
104	TiAl (8h)	Nb	TiAlN (4h)	3.5	7.9
109	TiSi (10h)	Nb	TiSiN (6h)	6.7	3.1

However, the weight gain of 3% during the sulfidation test of Run 109 coupons indicates that some sulfidation has taken place. To investigate this, we fractured the exposed sample and observed it under a scanning electron microscope. As shown in Figure 49, the sample suffered sulfidation only on one side, close to the surface. Since the gas feeding systems in our lab reactor are not optimized, it happens occasionally that one side of a coupon is less exposed to the reactants than the other. However, the most important observation in Figure 49 is that the bulk of the sample was not attacked during the corrosion test. The porous structure of the filter remained unplugged and, most important, we did not find any sulfur by EDX measurements. These results show that with optimization of the deposition conditions protective coatings can be deposited even in the bulk of the samples.

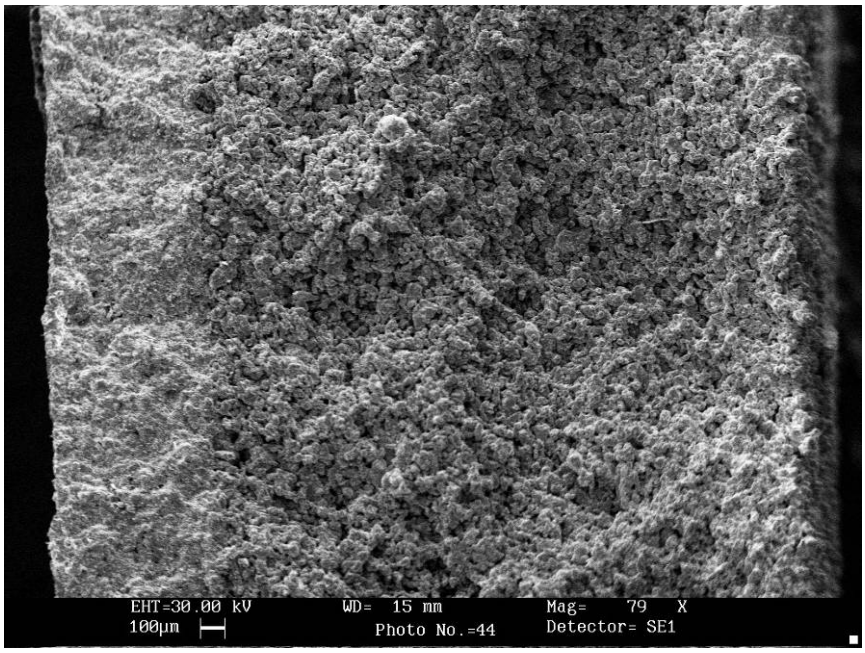

Figure 49. SEM cross-section of a fractured sample from Run 109 after exposure to simulated coal gas at 370ºC for 300 h.

Analysis of Nitrided Dense Samples with a Diffusion Barrier to a Simulated Coal Gas at 900°C

Table 24 lists the samples and the specific coatings that were deposited with nitrides of Ti, Si, and Al. The top panel of Figure 50 shows the picture of the samples before they were exposed to simulated gasifier conditions at 900°C. The bottom panel is a photograph of the samples after exposure after 300 h.

Table 24. Samples exposed in corrosion test 14.

Run	Material	Coating
94	SS409	(Ti,Si)N / (Ti,Al)N / TiAl
95	SS409	(Ti,Si)N / W / (Ti,Si)N / W / TiAl
98	SS409	(Ti,Al)N / Nb / TiAl
112	SS409	(Ti,Al)N / Nb / (TiAl)N / Nb / TiAl

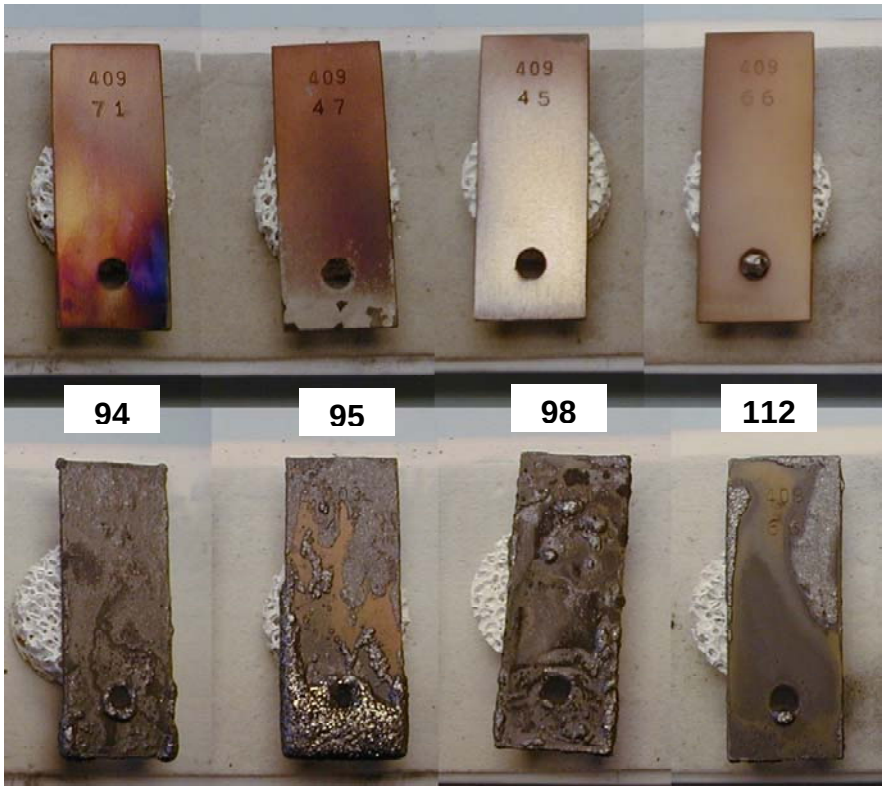

Figure 50. Samples before and after exposure for 300 h at 900°C in simulated gasifier Test 14.

As seen from the photographs, samples from Runs 94 and 98 showed general corrosion. Sample 95 was heavily attacked at the area close to the orifice (top zone during the deposition), which accidentally was at the top of the fluidized bed during that run and therefore was not coated, as seen in the top panel in Figure 50. However, the rest of the sample was mostly free of the iron sulfide blisters typical of sulfide attack. The sample from Run 112 showed only localized sulfidation attack in two areas, but the rest of the sample resisted the sulfidation. A common feature of the coatings in Runs 95 and 112 is that they have different diffusion barrier inter-layers: tungsten interlayer in Run 95 and niobium interlayer in Run 112. The main conclusion from these observations is that these inter-layers enhance the sulfidation resistance of the coupons, probably because they act as a diffusion barrier for H_2S to diffuse to the steel and for Fe to diffuse to the

surface. Some characterization of samples after exposure to the corrosion test will be presented below. Special attention was paid to sample 112, which showed the highest corrosion resistance at 900°C for several hundred hours.

We performed EDX measurements on the areas where the sulfide deposits grew during the exposure test (see Figure 50). Results presented in Table 25 show that these deposits are composed mainly of iron sulfides with several compositions. Figure 51 shows the X-ray diffraction pattern of crystals grown around the orifice of the sample from Run 95 during the corrosion test. The main peaks match the diffraction pattern of hexagonal pyrrhotite, an iron sulfide with variable stoichiometry. From all these results, it is clear that the corrosion mechanism involves the formation of iron sulfide crystals with several stoichiometries that depend on the availability of iron atoms at each area.

Table 25. EDX results of iron sulfide deposits on several samples

Run	Coupon area	at% Fe	at% S	at% Cr
94	All areas	83	17	-
95	Deposits around the orifice	58	42	-
	Deposits in other zones	70	30	-
98	Deposits, right zone in the photo	39	53	8
112	Deposits, top right in the photo	75	25	-

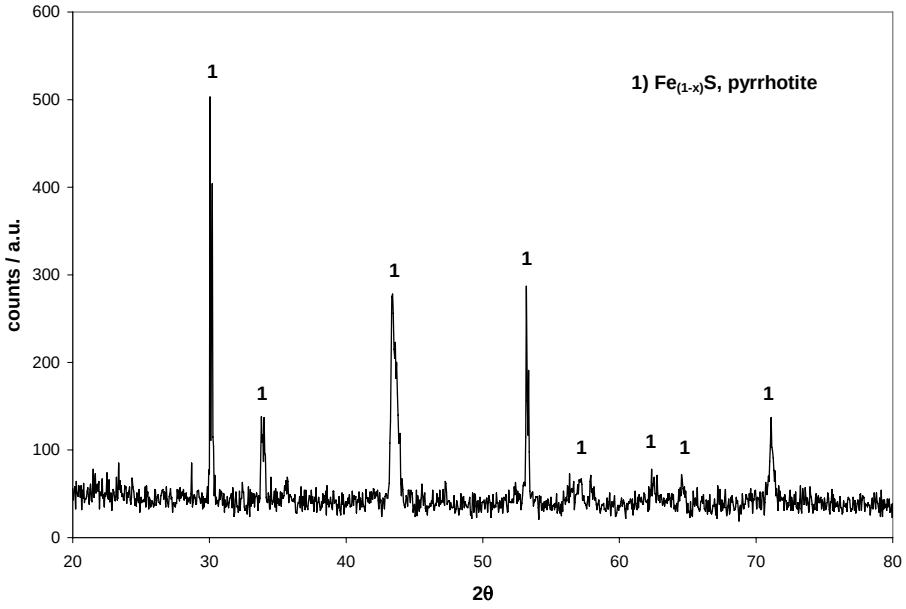

Figure 51. X-ray diffraction pattern of the crystals that grew around the orifice of the sample from Run 95 during exposure to simulated coal gas at 900ºC for 300 h.

To gain a better understanding of the protection mechanism provided by the coatings in Runs 95 and 112, we examined the areas that exhibited resistance. Figure 52 shows micrographs at two different magnifications of the zone in coupon from Run 112 that survived the corrosion test. Both the reddish areas and the gray areas observed in Figure 50 show the same morphology: dense crystals are observed covering the surface. The surface composition on that areas found by means of EDX analyses was 77-87 at% Ti, 6-14 at% Cr, 4-8 at% Fe and 0-3 at% Al (note that O was not considered for quantification). The reddish area had 3 at% Al, whereas we did not find Al in the gray area. As observed in the EDX spectrum presented in Figure 53, sulfur was not detected in any of these two zones, thus showing that the coatings provided good protection against sulfidation.

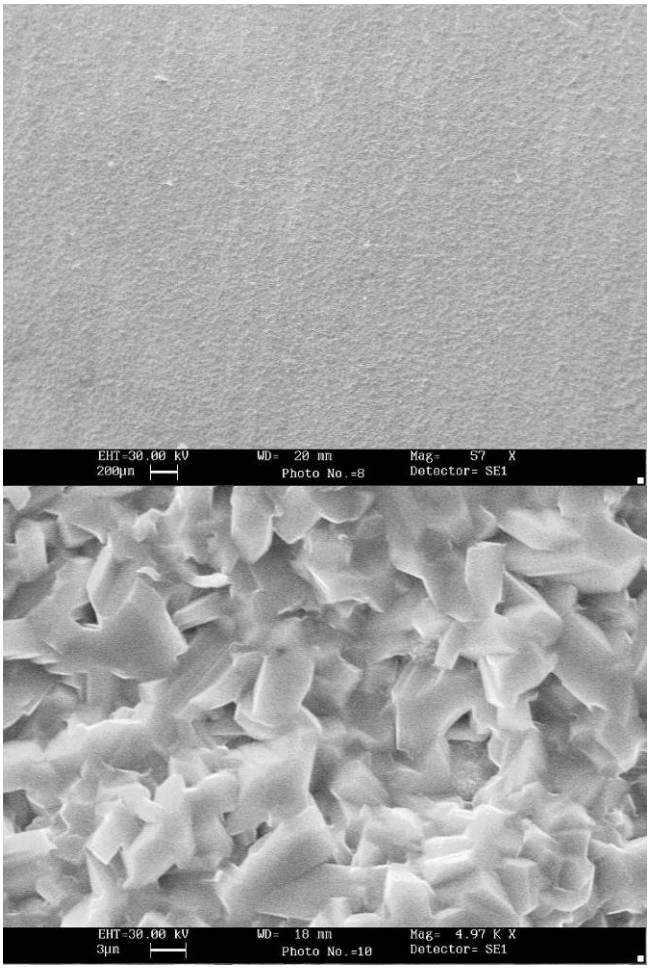

Figure 52. SEM top views at different magnifications of the zone that survived the corrosion test (scale bars are 200 μm in the top micrograph and 3 μm in the bottom micrograph).

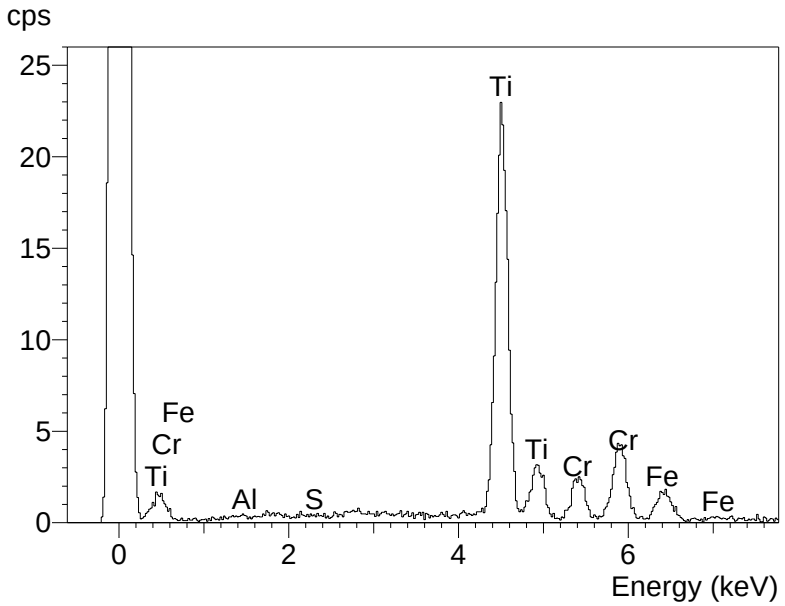

Figure 53. EDX spectrum acquired in the zone showed in Figure 52 (bottom micrograph).

We performed some XRD measurements to determine the phases present in the coating after exposure to the coal gas. Figure 54 shows the diffraction pattern of the part of the coupon from Run 112 that was not attacked after exposure to the simulated coal gas at 900°C. The main peaks in the spectrum correspond to rutile, a phase of titanium dioxide (TiO_2). This result shows that the oxygen activity as a result of the water vapor in the system is high enough to fully oxidize TiN. The resulting oxide coating must be dense, free of cracks, and therefore protective against sulfidation. Two chromium oxide phases are observed in the XRD spectrum: CrO and Cr_2O_3. It is well known that chromium oxide scales provide corrosion protection in many environments, so the formation of these phases provides an added protection to the steel substrate. Note that the only observed peak corresponding to substrate steel has a very low intensity, indicating that the overlaying coating is relatively thick.

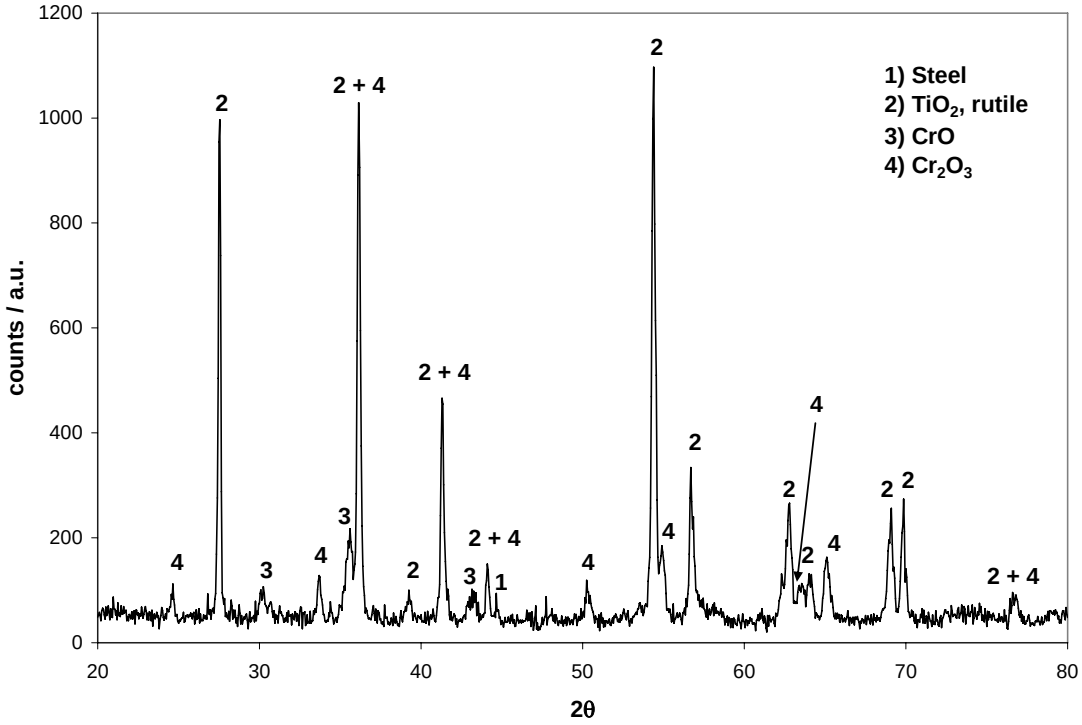

Figure 54. X-ray diffraction pattern of the zone from coupon 112 that survived sulfidation during exposure to simulated coal gas at 900ºC for 300 h.

In order to study the coating morphology after exposure to coal simulated gas at high temperature, the coupon was intentionally fractured. A cross-sectional SEM view is presented in Figure 55. EDX measurements showed that the zone labeled as 1 in the micrograph corresponds to the titanium dioxide scale observed also in top SEM views (Figure 52) and detected by means of XRD measurements (Figure 54). Interestingly, the zone labeled as 2 had a high Cr content (77.8 at%), some Ti (13.0 at%) and Fe (9.2 at%). It is probably in this area that the mixture of chromium oxides, as detected by XRD, was formed. The zone labeled as 3 is the base 409 stainless steel. We conclude from these characterizations that a protective titanium and chromium oxide scales were formed in the areas that survived the sulfidation during exposure to simulated coal gas at 900ºC.

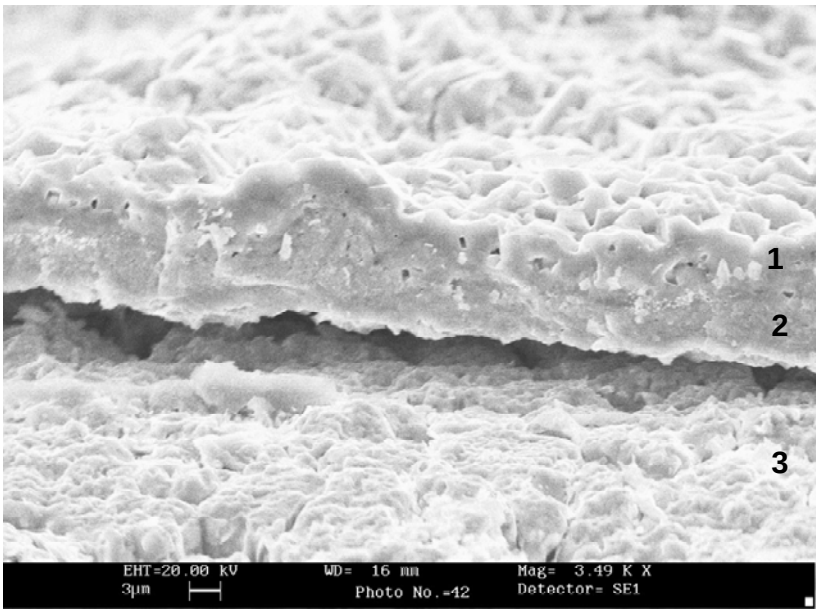

Figure 55. Cross-section micrograph of the exposed coupon from Run 112 after fracturing.

Analysis of Coupons with Multilayer Coatings before Exposure to a Simulated Coal Gas at 900°C

The results discussed in the previous section show that coatings containing a combination of several ceramic/metal layers are effective in protecting SS 409 alloy coupons during exposure to simulated coal gas at 900ºC. We carried out several experiments to deposit four ceramic layers and four metal inter-layers, as shown in Table 26.

Characterization of similar coatings with a few nitrided layers has been discussed earlier. Coatings deposited in Runs 119 and 120 (with Nb and Ta inter-layers) showed good adhesion. Cross-sectional views of a coupon from Run 120 after mounting and polishing (Figure 56) and after fracturing (Figure 57) revealed that the desired layered structure was achieved. As observed in Figure 56, the coating was conformal and showed good adhesion to the substrate (note that the sample was mounted under pressure). Figure 57 shows that the individual layers are dense and have a fine-grained structure.

Table 26. Coupons with multilayer coatings

Run	Material	Coating
119	SS409	4 x [(Ti,Al)N / Nb] / TiAl
120	SS409	4 x [(Ti,Al)N / Ta] / TiAl
121	SS409	4 x [(Ti,Al)N / Zr] / TiAl
122	SS409	4 x [(Ti,Al)N / W] / TiAl

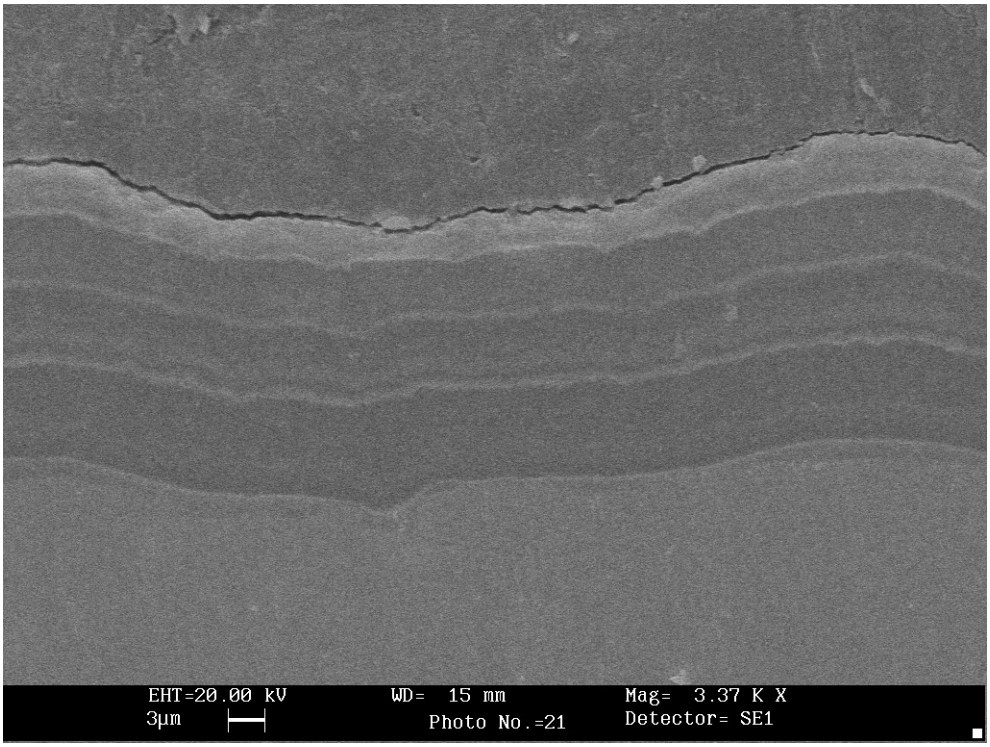

Figure 56. SEM cross-section of a sample from Run 120 showing the substrate (bottom), the multilayer coating and the mounting polymer (top).

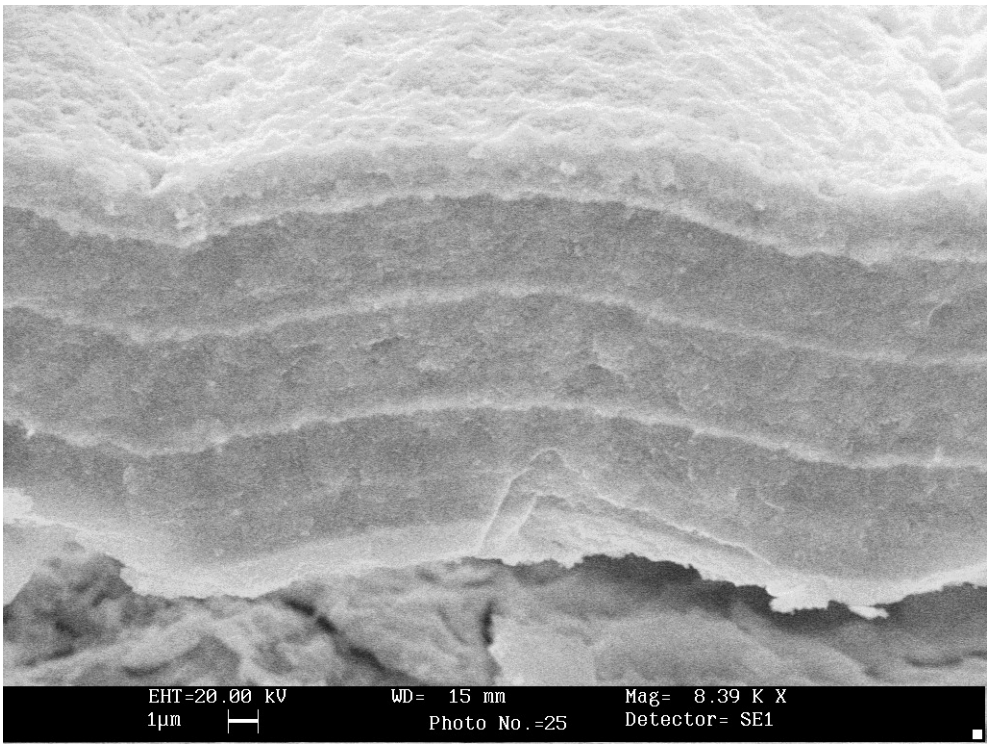

Figure 57. SEM cross-section of the fractured sample showing a closer view of the coating.

Analysis of Coupons with Multilayer Coatings after Exposure to a Simulated Coal Gas at 900°C

Coupons coated with the multilayers described in the previous section were exposed to simulated coal gas at 900ºC. Figure 58 shows a picture of the samples before and after the corrosion test. As can be seen, the coupon from Run 119 (Nb interlayers) showed good sulfidation resistance under the tested conditions. The weight change that we measured was only of 1.2% (typical weight gains in similar coupons were in the range 5-10% if they showed partial corrosion resistance, and above 10% if they were severely attacked). As observed in the picture, minor corrosion was observed only in two zones at the edge of the coupon, due to normal vertical inhomogeneities in the laboratory reactor. Examination of the corroded areas in other samples revealed that the sulfide scales formed had the same composition and morphology found in previous corrosion tests.

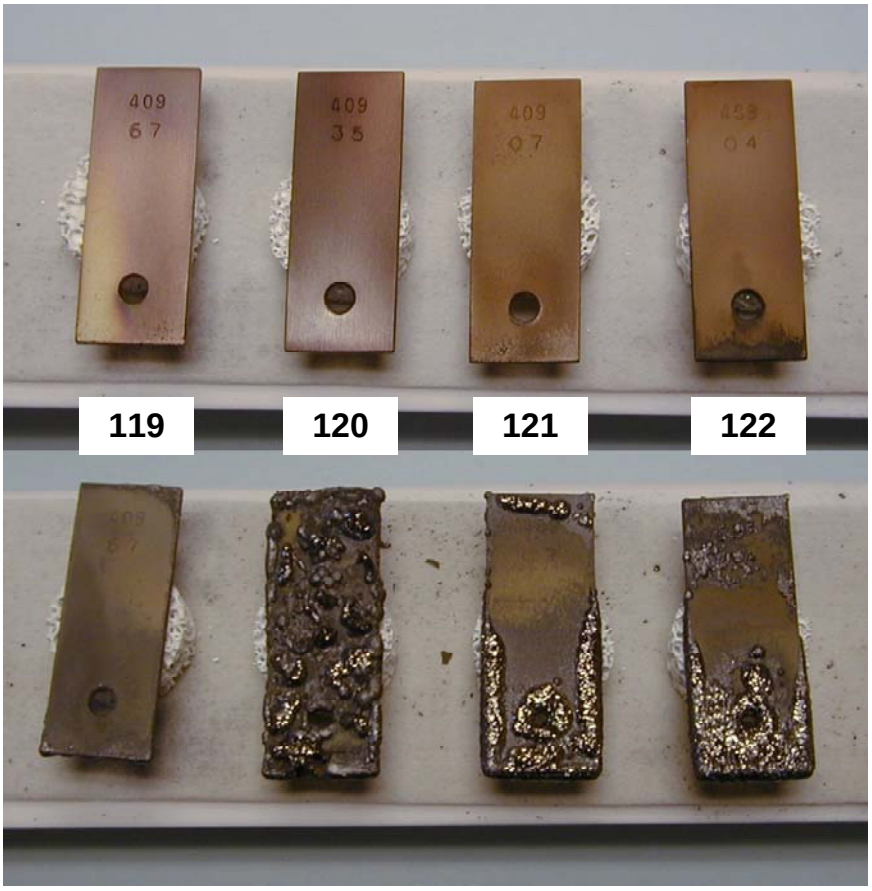

Figure 58. Samples before and after exposure for 300 h at 900°C in simulated gasifier Test 15.

A top SEM observation of the coupon from Run 119 after exposure to simulated coal gas (Figure 59) showed that it has the same surface morphology as found in coupon areas that survived during exposure in the previous corrosion test, namely, a homogeneous microcrystalline coating. EDX analyses in several areas revealed the following surface composition: 1-2 at% Al, 92-95 at% Ti, 2-4 at% Cr, 0-2 at% Fe and 1 at% Nb. We did not detect any S by means of EDX measurements, indicating that no sulfidation has occurred. The XRD analysis of the surface showed only the presence of oxides of titanium and chromium with extremely low levels of iron (Figure 60).

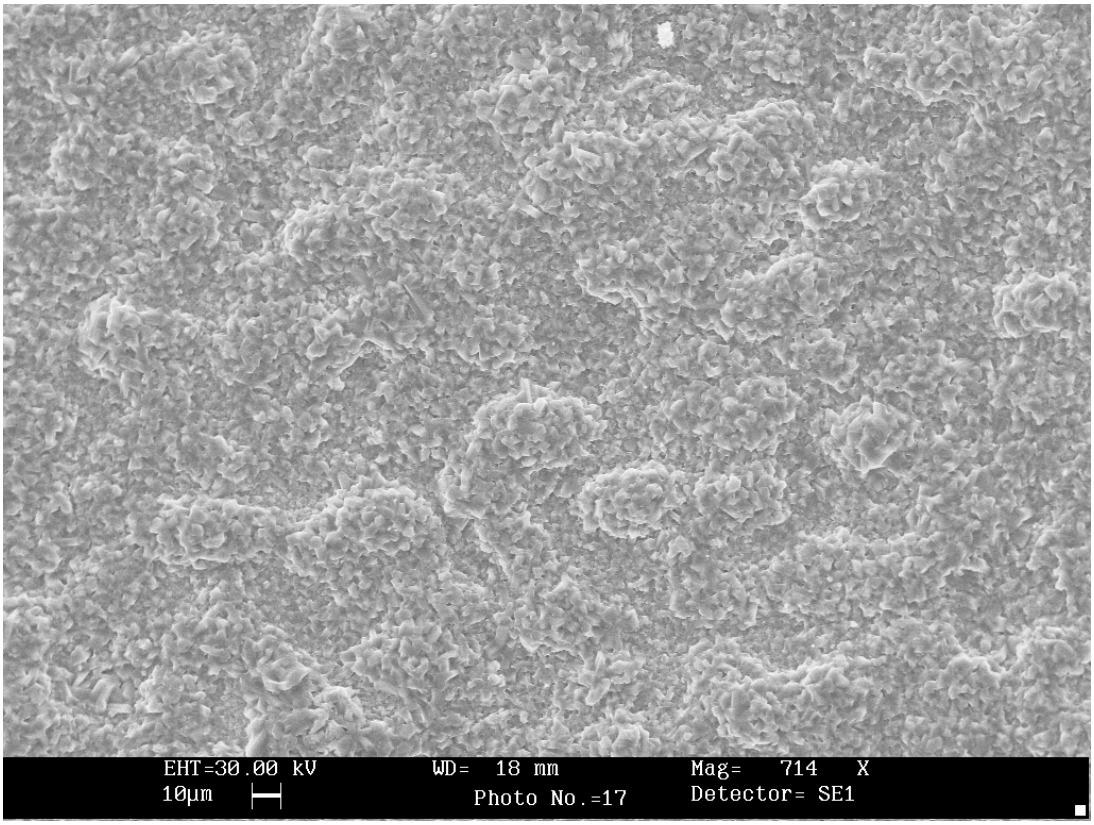

Figure 59. SEM top view of the coupon from Run 119 after exposure to simulated coal gas at 900ºC for 300 h (scale is 10 µm).

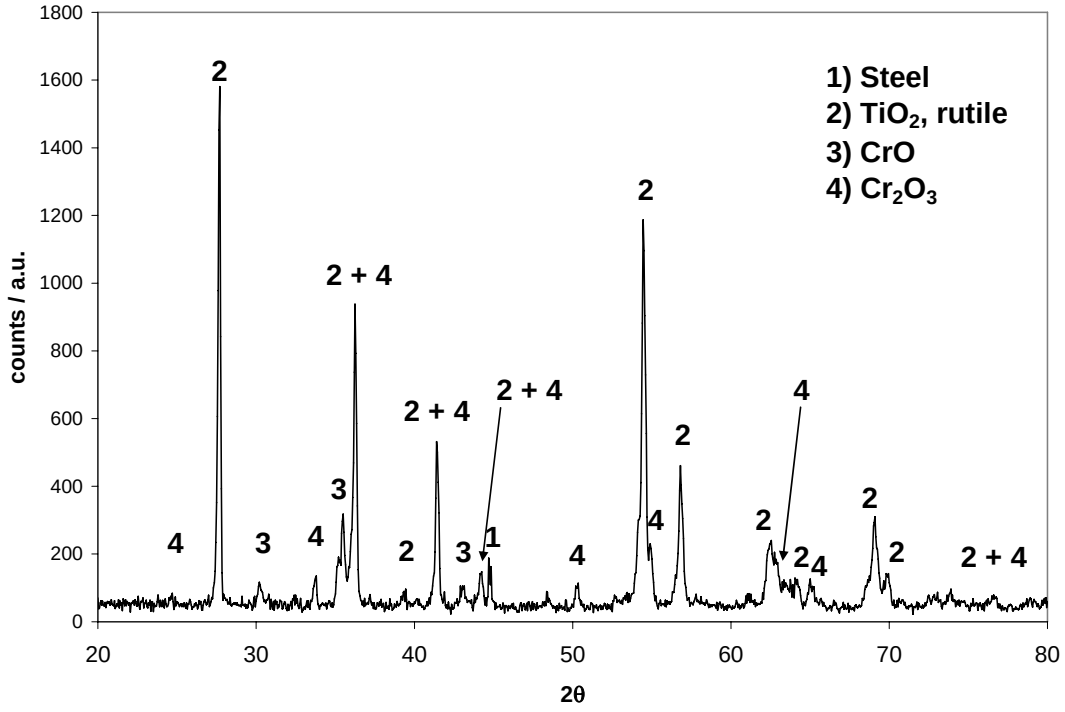

Figure 60. X-ray diffraction pattern, coupon from Run 119 after exposure to simulated coal gas at 900ºC for 300 h.

Figure 61 is the SEM cross-sectional views at two magnifications of the exposed coupon from Run 119 after intentionally fracturing it. The titanium dioxide (TiO_2) crystals that form the external coating layer are clearly seen. Although there is some porosity as a result of elemental diffusion and oxide formation, after exposure to the corrosion test the coating is still relatively dense. The results of a line EDX analysis carried out across the coating are presented in Figure 62.

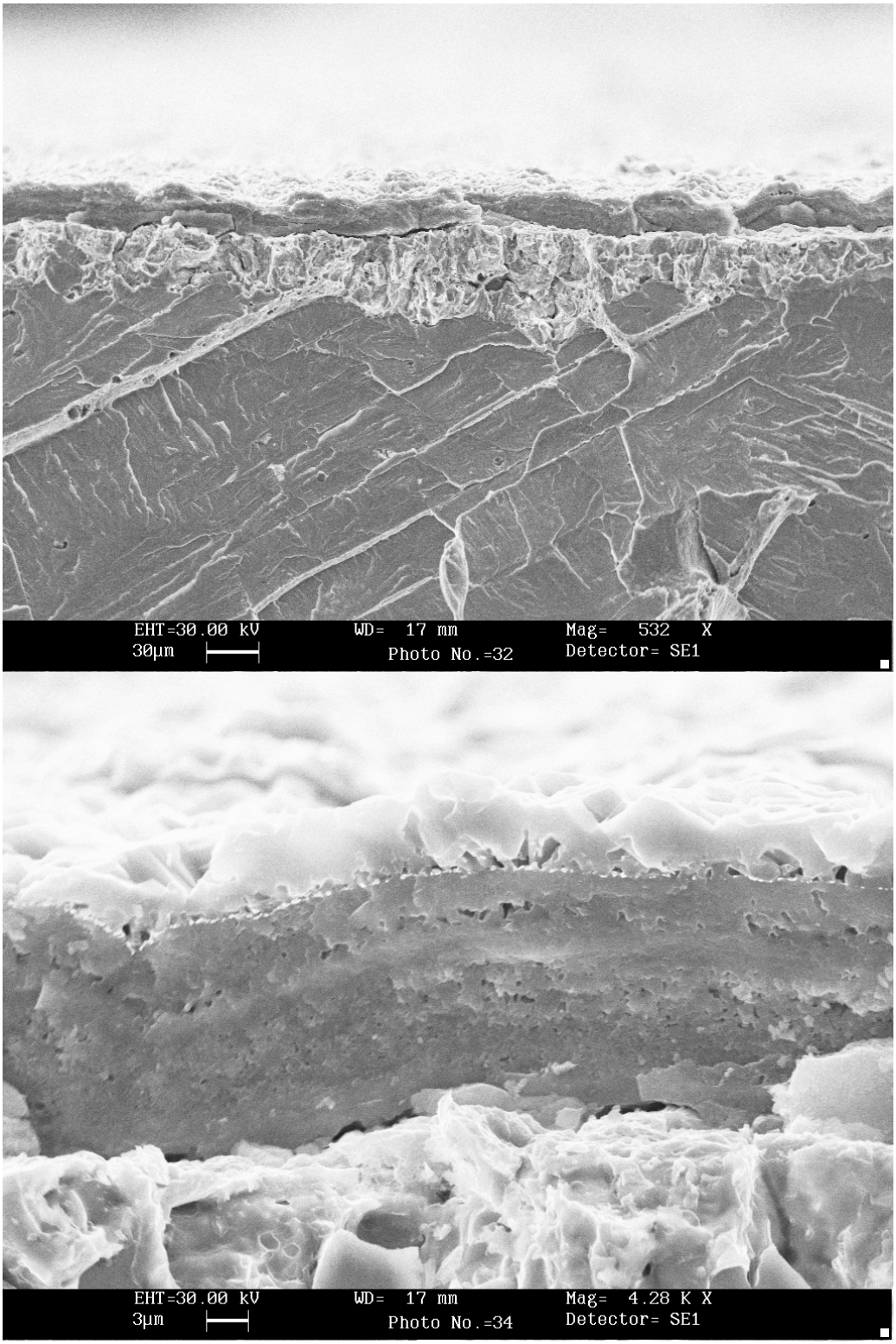

Figure 61. Cross-section micrographs at two different magnifications of the exposed coupon from Run 119 after fracturing (scale bars are 30 μm in top micrograph and 3 μm in bottom micrograph).

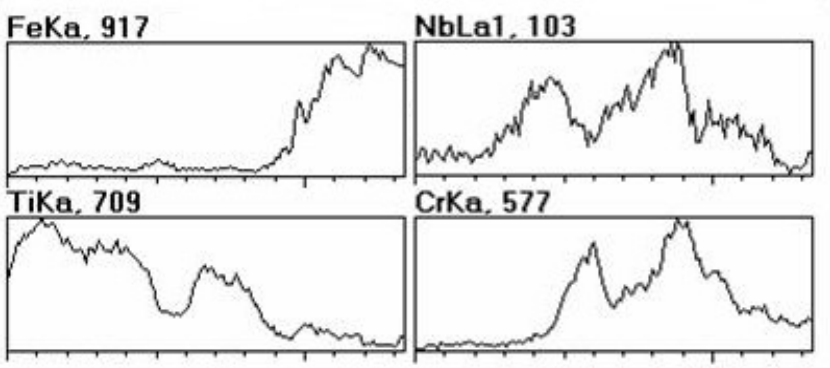

Figure 62. Elemental EDX line analysis across the coating shown in the bottom micrograph in Figure 61 (Origin in x-axis corresponds to coating surface).

From left to right in each plot, the Ti-based coating and some Nb- and Cr-rich layers are clearly seen. In the Fe plot it is clearly seen that outward diffusion of this element was blocked by the coating. Since Fe diffusion is known to be the key process leading to corrosion of steels by sulfidation in the tested environment, this result shows that a multilayer coating formed by combination of Ti-based nitride films with Nb interlayers is a good candidate for protecting components of coal gasification plants.

EXPOSURE TO AN OPERATING GASIFIER ENVIRONMENT

We conducted several long-term exposure tests at the WREL facility in Terre Haute, IN. The samples were inserted and withdrawn and the gasifier shut down for scheduled maintenance. Table 27 lists the first batch that was sent for the gasifier test in June 2004. However, because of certain difficulties with the gasifier operation, the samples were never exposed to coal gas. Those samples were exposed to about 100 h of start-up attempts with natural gas.

Table 27. Samples sent for gasifier exposure tests (June 2004)

Coupon #	Size (mm)	Marking	Alloy	Coating	Run No.
1	31 x 27 x 3.5	None	Porous 316	TiN, TaN	47
2	50 x 25 x 3.5	None	Porous 316	Cr	41
3	55 x 25 x 3.5	None	Porous 316	Si/TiN	50
4	14 x 52 x 9.7	None	409	Cr	49
5	51 x 19 x 3.5	405-11	405	Cr	49
6	51 x 19 x 3.5	304, A4074 A0765	304	Cr	42
7	51 x 19 x 3.5	410, HTT 478 B0154	410	Cr	48
8	51 x 19 x 3.5	410-09	410	Si/TiN	50

Subsequent plant shutdown and labor disputes delayed the start of the next run. In July 2005, the plant was to be restarted, and that presented another opportunity to test samples in a real gasifier. During that period, we had improved our coating procedures and also observed that oxidized Cr/Al-Al and TiN coatings seemed to be quite effective. We chose samples of coated and uncoated alloys (listed in Table 28) for the test, and sent them to Conoco/Phillips. These samples will likely be retrieved when the plant is next shut down for scheduled maintenance.

Table 28. Samples for gasifier exposure tests (April 29, 2005)

Coupon	Alloy	Marking	Coating	Run No.	Size (mm)
1	HR160	05	None	-	41.7x19.6x3.2
2	I 800	08	None	-	51.2x19.4x3.7
3	SS 410	05	None	-	51.2x19.6x3.0
4	SS 304 L	02	None	-	51.2x19.5x3.0
5	SS 409	12	Cr-Al/Al/Ox	59	51.5x19.5x3.9
6	SS 409	16	Cr-Al/Al/Ox	70	51.3x19.5x3.8
7	SS 409	17	Cr-Al/Al/Ox	70	51.4x19.5x3.8
8	SS 405	15	TiN	66	51.2x19.6x3.6
9	SS 405	16	TiN	66	51.2x19.5x3.4
10	SS 409	18	TiN	68	51.5x19.5x3.8
11	SS 409	20	TiN	68	51.4x19.5x3.9
12	SS 316 porous	-	TiN	62	52.8x24.8x3.3

1. Sample 5 has already survived 500+ hours in simulated gasifier environment in the lab.
2. Sample 12 will not survive the high-temperature conditions. It is to be exposed to only colder gases after the HTRU, perhaps in a slip stream.

Figure 63 shows a picture of the samples before and after exposure. The unlabeled samples were those that Conoco/Phillips had put in for their own work. The samples were subjected to 1,100 h of the high-temperature synthesis gas environment. All the samples were severely damaged, with many of them even falling off the coupon tree and getting lost in the gasifier. One of the samples (#5) SS409 coated with Cr/Al oxide had already survived over 500 hours in simulated coal gas stream with no apparent degradation. Only the Haynes alloy (#1) remained on the sample holder, but even this sample showed extensive sulfidation attack. Other samples that seemed to have survived to some extent were Inconel 800 (#2), austenitic stainless steel SS304 (#4), and two SS409 samples coated with TiN (#10 and #11). Note that the Inconel 800 coupon was severely sulfided even in the laboratory test. The severity of damage in all these samples suggests that the environment in the gasifier is much harsher than that provided in the laboratory test. To a large extent this may be due to the erosion by particles that is not provided

in the lab setup. However, the specific problem of tube sheet corrosion is not exacerbated by erosion due to ash particles, and so the coupon tree setup may represent a vastly more severe test.

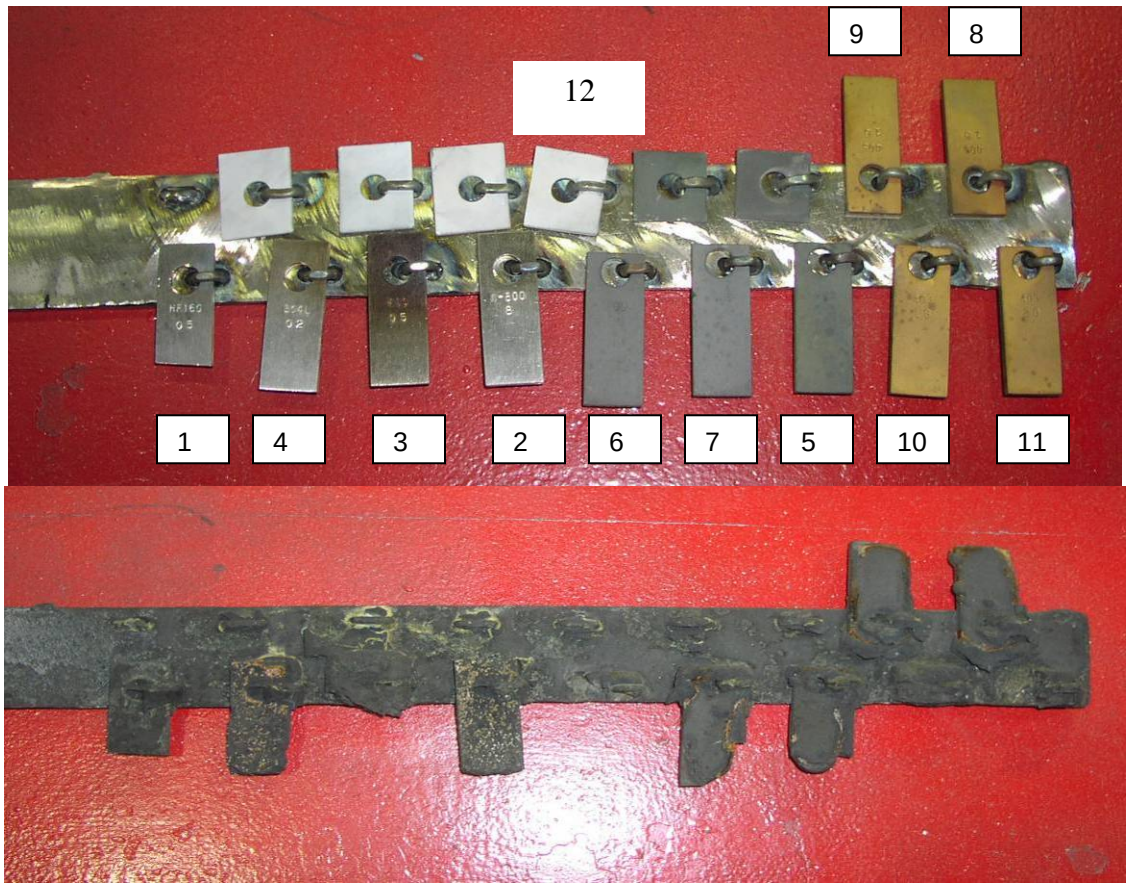

Figure 63. Samples before and after exposure to the hot gas stream in the Wabash River Plant during May-Sep, 2005 (1,100 hours, petcoke syngas)

A second batch of samples (Table 29) was submitted to Conoco/Phillips for testing in their gasifier in October 2005. Figure 64 shows photographs of the tree with the samples before and after exposure in the high-temperature, abrasive synthetic gas stream for 3,814 h. During removal of the coupon tree, the coupon designated as 410-01 was inadvertently broken off. This was the only coupon to have remained intact. A second detached coupon that can be seen in the photo was recovered during an earlier vessel inspection, as it had already broken off.

Table 29. Samples for gasifier exposure tests (October 17, 2005)

Coupon	Alloy	Coating	Run No.	Weight (g)	Size (mm)
1	SS 409	Cr/Al/Al-Ox	76	11.4886	51.1X19.3X1.74
2	SS 410	Cr/Al/Al-Ox	73	9.9638	51.2X19.4X1.5
3	SS 409	Ti/Al Nitride	77	11.3632	51.1X19.5X1.7
4	SS 409	Ti/Al Nitride	77	11.1244	51.2X19.4X1.7
5	SS 410	Ti/Al Nitride	79	9.9997	51.2X19.4X1.5
6	SS 405	Ti/Al Nitride	80	7.8017	51.0X19.4X1.3
7	SS 409	Ti/Ta Nitride	81	11.3005	51.0X19.3X1.7
8	SS 409	Ti/Ta/Al Nitride	82	11.3563	51.1X19.4X1.7
9	SS 409	Ti/Al Nitride	85	11.5160	51.1X19.4X1.7
10	SS 410	Ti/Si Nitride	86	9.9388	51.1X19.4X1.5
11	SS 405	Ti/Si Nitride	87	7.7653	51.0X19.4X1.3
12	SS 409	Ti/Si Nitride	87	11.4653	51.1X19.3X1.7
13	SS 410	Ti/Si Nitride	87	9.8130	51.1X19.5X1.5

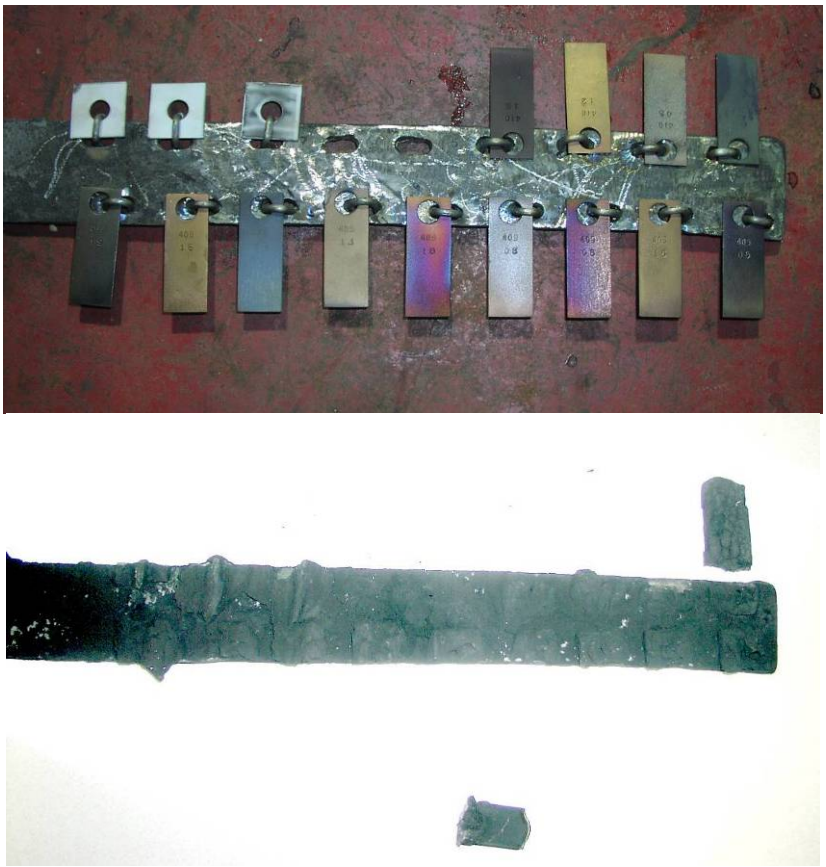

Figure 64. Samples before and after exposure to the hot gas stream in the Wabash River Plant during May-Sep, 2005 (3,814 h)

Characterization of Porous Coupons after the Long-Term Exposure

Porous coupons from Runs 62 and 88 were exposed at 370ºC for 2,140 h at the Wabash River Gasifier plant. These coupons contained coatings of Cr/Al (Run 88) or nitrided Ti/Ta (Run 62). After exposure, the samples retained their structural integrity allowing detailed examination. In the exposed sample from Run 62, we could not observe internal porous structure, due to the growth of sulfide scales in the interior of the sample (Figure 65). Table 30 shows results of EDX measurements carried out at the marked points in the micrograph, which show high S contents in many areas, and we observed the presence of sulfide islands. We did not detect the presence of Ti or Ta.

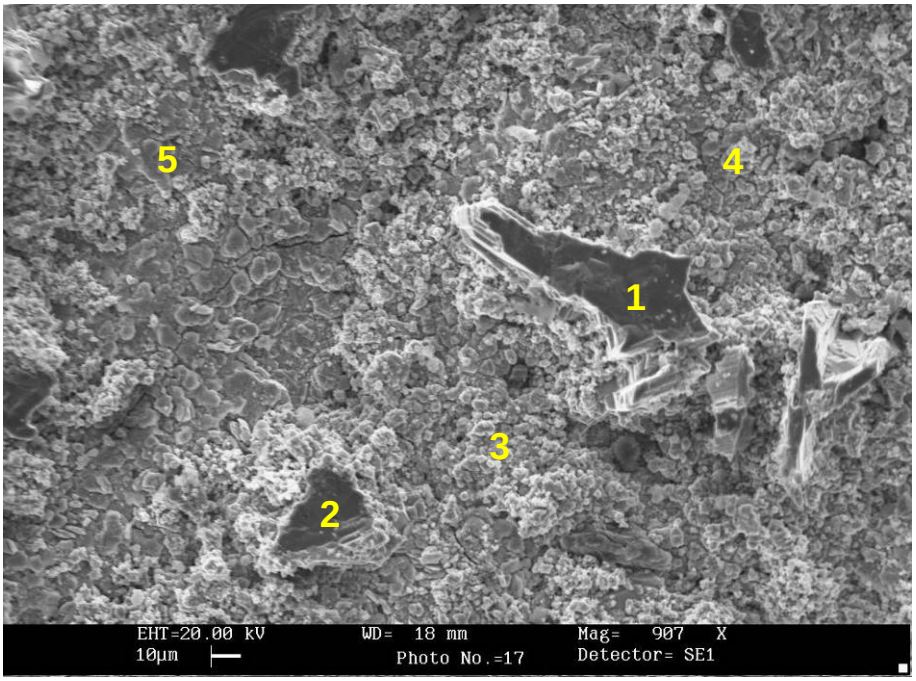

Figure 65. SEM of the top of sample from Run 62.

Table 30. EDX analyses at points marked in Figure 65

Point	Atom% Si	Atom% S	Atom% Fe	Atom% Ni
1	-	45.5	14.6	39.5
2	-	45.8	23.2	30.7
3	-	31.3	37.1	30.8
4	-	22.9	38.7	37.3
5	6.47	33.2	34.0	26.4

A cross-section of the sample, after cutting, mounting and polishing, is shown in Figure 66. The insets in the micrograph are EDX mapping for S, Cr, Fe, Ni. As can be seen, Cr and S maps are complementary, Fe is detected in all zones, and Ni is especially concentrated at the surface. This elemental distribution confirms that the scales formed after exposure are mainly Ni and Fe sulfides. This observation indicates that TiTaN-coated 316 alloy steel did not survive the corrosion test.

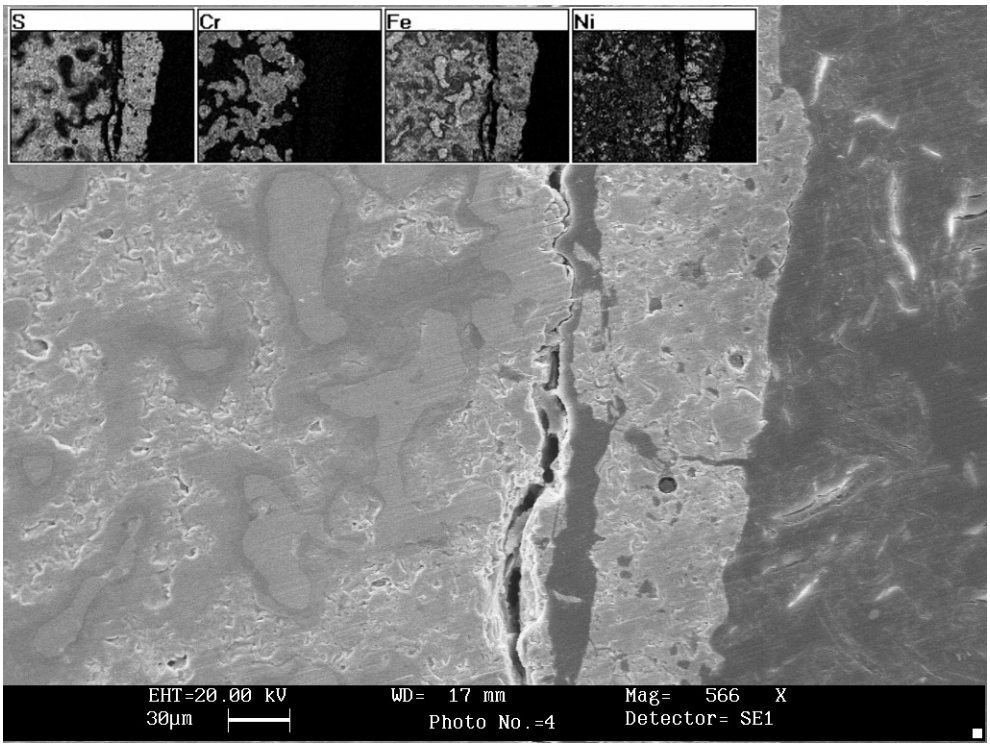

Figure 66. SEM cross-section view and map of EDX analyses for S, Cr, Fe and Ni.

Figure 67 shows the SEM photograph of the surface of a coupon from Run 88 after exposure to the gasifier plant environment. The morphology of the sample did not change after exposure; the porous structure generated by sintering alloy steel powder remains unchanged. Results regarding EDX surface analyses done in three different zones of the coupon are presented in Table 31. They show a high surface concentration of Al and a low concentration of S. According to these results, an alumina layer was formed that covered the steel and prevented the formation of iron sulfide.

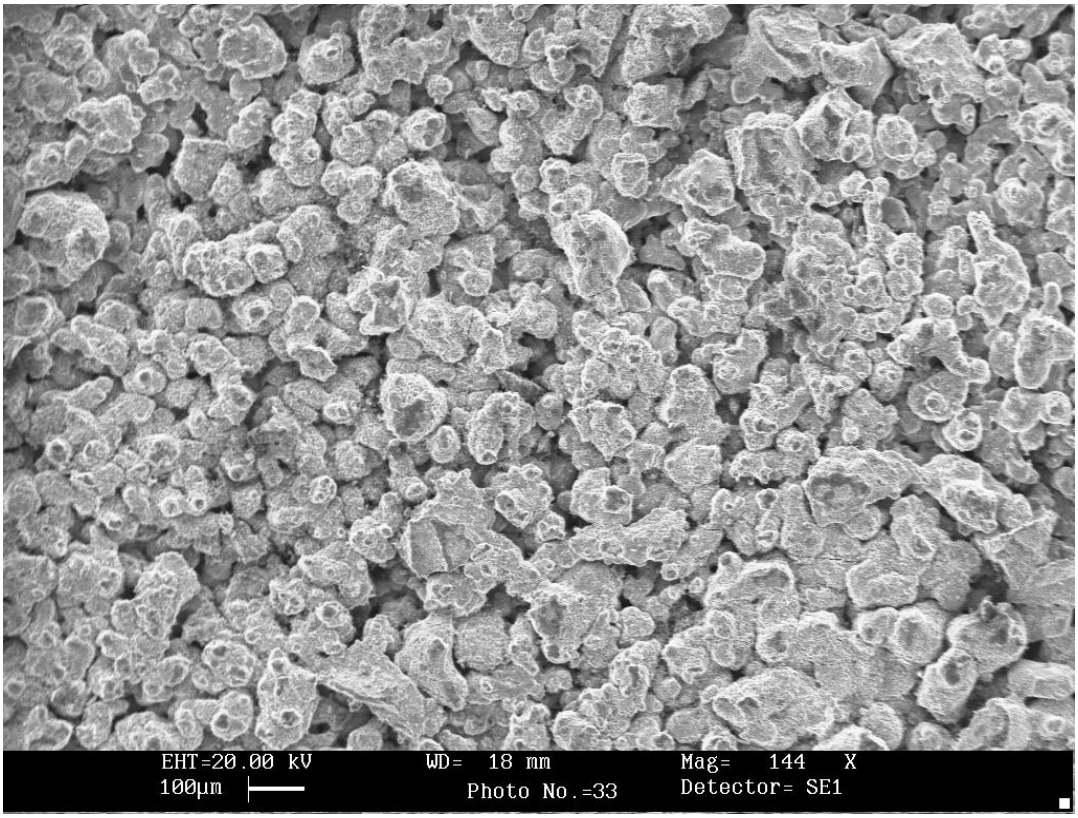

Figure 67. SEM of the surface of the porous coupon from Run 88 after exposure in the gasifier.

Table 31. EDX results of the coupon from Run 88 after exposure in the Gasifier

	Atom% Al	Atom % Si	Atom % S	Atom % Cr	Atom % Fe
zone 1	55.5	3.7	4.3	12.4	24.2
zone 2	58.7	3.5	2.6	4.7	30.7
zone 3	53.9	1.7	0.6	14.4	29.1

Figure 68 shows a cross-section view of the porous sample as observed in the SEM. We observed clearly that the external part of the coupon (approximately the first 100 µm) is different than in the bulk. To investigate the differences, insets in the same figure show EDX maps for Fe, Cr, Al, S and Ti, in this order. As observed, the external part is rich in Al. But beneath the external area, a solid was found inside the voids of the filter, composed of S and Fe. This observation suggests that an alumina layer was formed in the external portion that was protective against sulfidation, but such protection did not occur in the bulk of the sample. We believe that Al was not deposited in the interior portion of the sample. During coating deposition, $AlCl_3(g)$ reacts in contact with the coupon and it is depleted as the gas infiltrates into the bulk of the sample. As a consequence, Al deposition is more efficient in the external parts of the coupon. In the outer zone, a protective alumina layer can be formed.

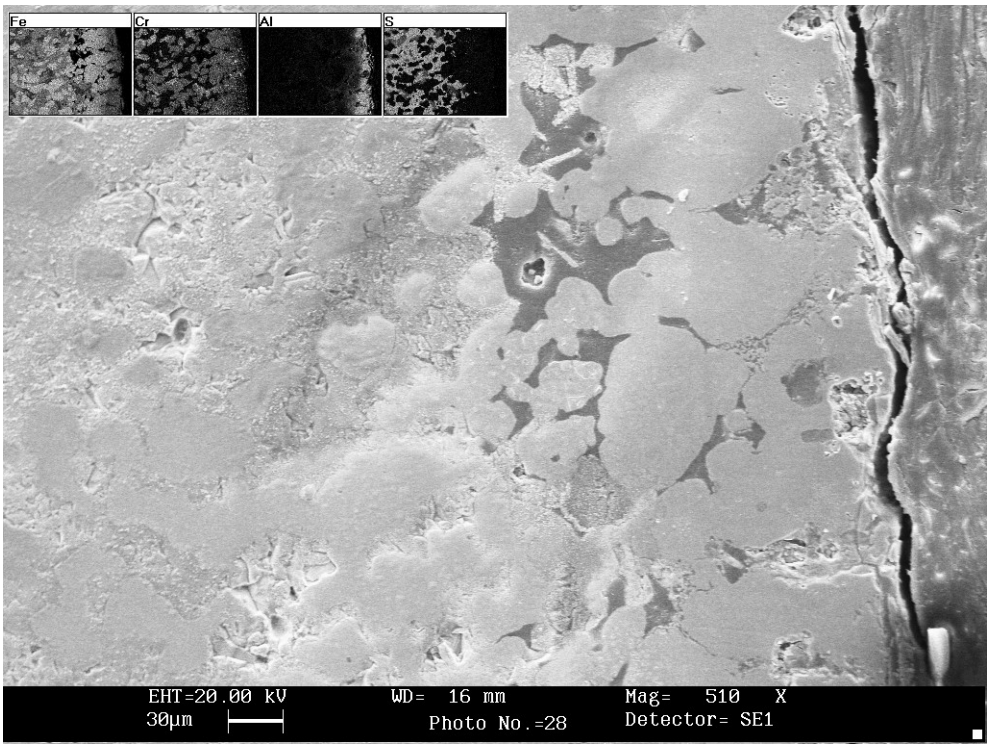

Figure 68. SEM cross section, porous coupon from run 88, and EDX map for Fe, Cr, Al and S.

In summary, the results from the gasifier exposure tests show that the conditions inside the gasifier are aggressive. At 900°C, the coated coupons did not survive the test conditions, although they no significant sulfidation was observed in the simulated, bench-scale exposure tests. The difference between tests with simulated and actual gasifier conditions may be due to (1) increased length of duration and (2) higher temperature at the actual gasifier. Under these conditions, the Cr and Al surface coatings may have diffused into the bulk of the coupons thereby decreasing their enhancement at the surface. Such depletion would have reduced the resistance to attack by H_2S and allowed iron sulfide formation.

The gasifier exposure tests at 370°C showed Cr/Al coatings provided sufficient corrosion resistance to low alloy steel substrates such as SS409 alloy. Most of the exterior of the tested coupons showed little sulfide attack. Although a certain level of sulfidation occurred at the interior of the coupon due to non-uniformity of the coating, improving the coating process can produce acceptable filters made of low alloy steel.

CONCLUSIONS AND RECOMMENDATIONS

Based on this study, the following conclusions are derived:

1. The fluidized-bed chemical vapor deposition technique is ideally suited to deposit diffusion coatings of Cr and Al for protection against sulfidation corrosion in coal gasification gas streams. The technique can be used also to deposit adherent multilayer coatings containing Si, Ti, Al, and Nb with subsequent nitridation of these elements to increase the corrosion resistance.

2. Bench-scale exposure tests at 900°C with a simulated coal gas stream containing 1.7% H_2S showed that the low alloy steels such SS405 and SS409 coated with ~20%Cr and Al each can be resistant to sulfidation attack for 500 h.

3. Multilayer coatings containing Ti and Si nitrides along with a diffusion barrier containing Nb were deposited on SS410 and they were found also to be resistant to sulfidation attack in the bench scale tests at 900°C.

4. Exposure to an actual coal gasifier gas stream at the Wabash River gasifier facility for 1000 h in the temperature range 900° to 950°C indicated that the diffusion coatings containing Cr and Al diffused further into the substrate decreasing the protective ability of these elements against attack by H_2S.

5. The FBR-CVD technique was also capable of depositing diffusion coatings containing Cr and Al onto porous steel substrates such as those used as an ash particulate filter. As with the dense substrates, the technique can be used also to deposit multilayer coatings containing nitrides of Ti, Al, and Si with diffusion barrier elements such as W and Nb in porous substrates.

6. Bench-scale exposure tests with a simulated coal gas containing 1.7% H_2S at 370°C showed that porous SS 409 alloy coupons can be resistant to sulfidation attack when coated with Cr/Al or nitrides containing Ti, Si, and Al.

7. Exposure test at the Wabash River gasifier facility at 370°C for 2100 h showed that only a minor sulfidation attack occurred inside the porous SS409 alloy coupons that contained Cr and Al diffusion coatings. This attack can be prevented by improving the coating process to deposit uniform coatings at the interior of the porous structure. The coupons coated with the multilayer nitride coatings were attacked by H_2S in this long-term test.

Based on the results of this study, the following recommendations are made:

1. Additional studies need to be initiated to optimize the FBR-CVD process to deposit diffusion coatings of the corrosion resistant elements such as Cr, Al, and Ti inside porous metal filters to increase their corrosion resistance.

2. Long-term exposure tests using an actual gas stream from an operating gasifier need to be conducted to determine the suitability of the coatings for use in the gasifier environment.

BIBLIOGRAPHY

Bradshaw, R. W., R. E. Stoltz, and D. R. Adolphson, 1977. Report SAND 77-8277, Sandia National Laboratory, Livermore, CA.

Humphreys, A. and A. O. Schaefer (1983). A program to discover materials suitable for service under hostile conditions in equipment for the gasification of coal and other solid fuels. Annual Reports 1975 to 1982. The Metal Properties Council, New York.

Lai, G. Y., 1990. High-temperature corrosion of engineering alloys, ASM International, Materials Park, OH.

Lippert, T. E., E. E. Smeltzer, J. H. Meyer, and C. A. Hughes. 1989. Performance Evaluation of Ceramic Cross-Flow Filters at New York University PFBC. *Proceedings of the Sixth Annual Coal-Fueled Heat Engines and Gas Stream Cleanup Contractors Review Meeting*, 304-312. DOE/METC-89/6101. NTIS/DE89000952. Springfield, Va.: National Technical Information Service.

Lippert, T. E., D. M. Bachovchin, E. E. Smeltzer, M. A. Alvin, J. H. Meyer, and C. A. Hughes. 1991. Subpilot-Scale Gasifier Evaluation of Cross-Flow Filters. *Proceedings of the Eleventh Annual Gasification and Gas Stream Cleanup Contractors Review Meeting*, 396-405. DOE/METC-91/6123. NTIS/DE92001102. Springfield, Va.: National Technical Information Service.

Natesan, K., 1993. Applications of Coatings in Coal-Fired Energy Systems, Surface and Coatings **56**, 185-187.

Natesan, K., 2001. Corrosion resistance of iron aluminides, Report by Argonne National Laboratory under contract No. W31-109-Eng-38.

Perkins, R. W., W. C. Coons and S. J. Vonk, 1982. Materials Problems in Fluidized-Bed Combustion and Coal Gasification Systems: Further Studies of Corrosion Chemistry in Low Oxygen Activity Atmospheres. Report No.: EPRI-CS-2452 (DE82905772)

Quann, R. J., M. Neville, and A. F. Sarofim. 1990. Combustion Generated Particles. Combustion Sci. and Technol. **74**, 245-266.

Verma, S. K., 1982. Corrosion behavior of selected alloys in laboratory and pilot plant environments, 7th Annual Conference on Materials for Coal Conversion and Utilization, Gaithersburg, MD, November 1982.

Viswanathan, R., R. Romanosky, U. Rao, R. Purget, and H. Johnson, 2003. Boiler Materials for USC Plant, EPRI Preprint.